Contents

ASM Sc. J.
Volume 4(2), 2010

RESEARCH ARTICLES

Continued on the inside of the back cover.

ISSN 1823-6782
9 771823 678004

MOSTI

AKADEMI SAINS MALAYSIA

ASM Science Journal 4(2) 2010

ASM JOURNAL Science

In Pursuit of Excellence in Science

Vol. 4, No. 2, December 2010 • ISSN : 1823-6782

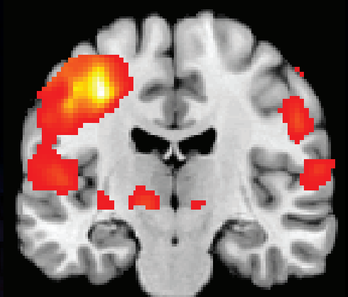

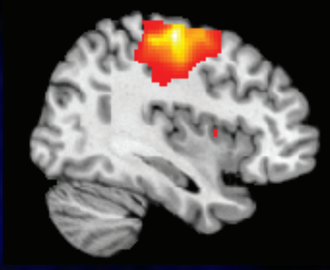

cover 4(2).indd 1 1/20/2011 12:09:03 PM

Price (2 Issues)

Malaysia: RM100 (*Individual*)
RM200 (*Institution*)

Other Countries: USD50 (*Individual*)
USD100 (*Institution*)

Publication.indd 221 5/2/2010 1:32:27 AM

ASM Science
JOURNAL

INTERNATIONAL ADVISORY BOARD

Ahmed Zewail
Richard R. Ernst
John Sheppard Mackenzie
M.S. Swaminathan

EDITORIAL BOARD

Editor-in-Chief/Chairman: Md. Ikram Mohd Said

Abdul Latiff Mohamad
Chia Swee Ping
Ibrahim Komoo
Lam Sai Kit
Lee Chnoong Kheng
Looi Lai Meng
Mashkuri Yaacob
Mazlan Othman
Mohd Ali Hashim
Francis Ng
Radin Umar Radin Sohadi

Cover:

Researchers from the National University of Malaysia and the Masterskill University College of Health Sciences Malaysia have discovered that during unilateral finger tapping, the contralateral primary motor (M1) would act as the input center which in turn triggered the propagation of signals to supplementary motor area (SMA) in the same hemisphere and to M1 and SMA in the opposite hemisphere.

The two brain images were taken from Figure 2 (page 167) depicting statistical parametric maps obtained from random-effects analysis showing brain activation—in the article *Intrinsic Couplings between the Primary Motor Area and Supplementary Motor Areas during Unilateral Finger Tapping Task* (pages158–172).

The lower image in the cover is the expression of receptor-interacting protein 140 in a developing zebrafish embryo (72 hpf, lateral view)—Figure 7 (page 130) of article entitled *Expression of Receptor-interacting Protein (RIP 140) in Zebrafish Tissues and Embryonic Stages* (pages 123–132).

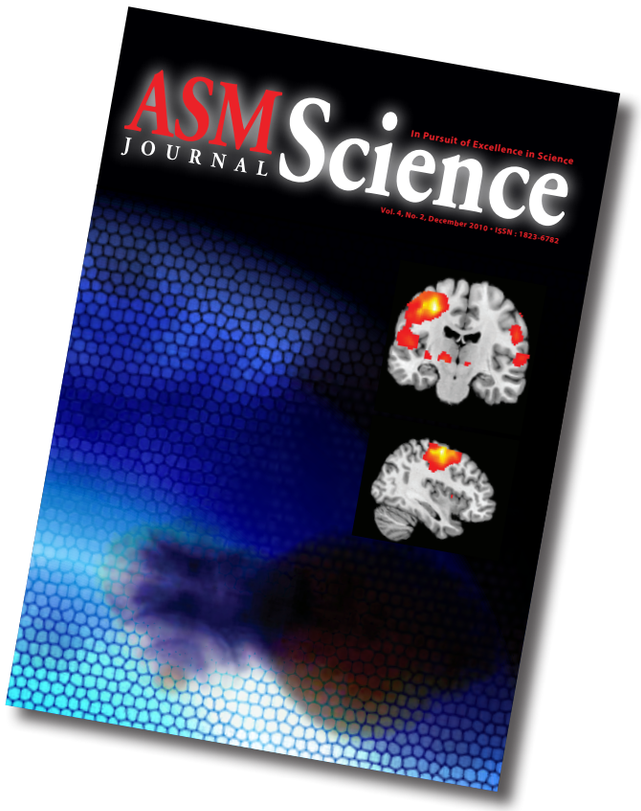

© Academy of Sciences Malaysia

All rights reserved. No part of this publication may be reproduced in any form or by any means without permission in writing from the Academy of Sciences Malaysia

The Editorial Board, in accepting contributions for publications, accepts no responsibility for the views expressed by authors

Published by the Academy of Sciences Malaysia

The Academy of Sciences Malaysia (ASM)

The Academy of Sciences Malaysia (ASM) was established, under the *Academy of Sciences Act 1994* which came into force on 1 February 1995, with the ultimate aim to pursue excellence in science. Thus the mission enshrined is to pursue, encourage and enhance excellence in the field of science, engineering and technology for the development of the nation and the benefit of mankind.

The functions of the Academy are as follows:

- To promote and foster the development of science, engineering and technology
- To provide a forum for the interchange of ideas among scientists, engineers and technologists
- To promote national awareness, understanding and appreciation of the role of science, engineering and technology in human progress
- To promote creativity among scientists, engineers and technologists
- To promote national self-reliance in the field of science, engineering and technology
- To act as a forum for maintaining awareness on the part of the Government of the significance of the role of science, engineering and technology in the development process of the nation and for bringing national development needs to the attention of the scientists, engineers and technologists
- To analyse particular national problems and identify where science, engineering and technology can contribute to their solution and accordingly to make recommendations to the Government
- To keep in touch with developments in science, engineering and technology and identify those developments which are relevant to national needs to bring such developments to the attention of the Government
- To prepare reports, papers or other documents relating to the national science, engineering and technology policy and make the necessary recommendations to the Government
- To initiate and sponsor multi-disciplinary studies related to and necessary for the better understanding of the social and economic implications of science, engineering and technology
- To encourage research and development and education and training of the appropriate scientific, engineering and technical man power
- To establish and maintain relations between the Academy and overseas bodies having the same or almost similar objectives in science, engineering and technology as the Academy
- To advise on matters related to science, engineering and technology as may be requested by the Government from time to time; and
- To carry out such other actions that are consistent with the *1994 Academy of Sciences Act* as may be required in order to facilitate the advancement of science, engineering and technology in Malaysia, and the well being and status of the Academy.

The Academy is governed by a Council. Various Working Committees and Task Forces are charged with developing strategies, plans and programmes in line with the Academy's objectives and functions.

The functions of the Council are:

- To formulate policy relating to the functions of the Academy
- To administer the affairs of the Academy
- To appoint such officers or servants of the Academy as are necessary for the due administration of the Academy
- To supervise and control its officers and servants
- To administer the Fund; and
- To convene general meetings of the Academy to decide on matters which under this Act are required to be decided by the Academy.

The Academy has Fellows and Honorary Fellows. The Fellows comprise Foundation Fellows and Elected Fellows. The Academy Fellows are selected from the ranks of eminent Malaysian scientists, engineers and technocrats in the fields of medical sciences, engineering sciences, biological sciences, mathematical and physical sciences, chemical sciences, information technology and science and technology development and industry.

The Future

Creativity and innovation are recognised the world over as the key measure of the competitiveness of a nation. Within the context of K-Economy and the framework of National Innovation System (NIS), ASM will continue to spearhead efforts that will take innovation and creativity to new heights in the fields of sciences, engineering and technology and work towards making Malaysia an intellectual force to be reckoned with.


C
M
Y
CM
MY
CY
CMY
K

Contents

ASM Sc. J.
Volume 4(2), 2010

RESEARCH ARTICLES

content.indd 1 1/20/2011 12:39:36 PM

REVIEW

SCIENCE FORUM

ANNOUNCEMENTS

content.indd 2 1/20/2011 12:39:36 PM

ASM Sci. J., **4(2)**, 103–112

Application of Statistical Experimental Designs for Optimization of Medium Composition in Biodegradation of Procion Red MX-8B

O. Khadijah[1]*, K.K. Lee[1] and M.F.F. Abdullah[1]

Two sequential statistical experimental designs were used to screen and investigate the dependence of the amount of biodegradation of Procion Red MX-8B (PR-MX8B) on the fermentation variables. Fourteen factors were screened using the Plackett-Burman design. Among these factors, the most significant variables which included yeast extract, corn steep solids and starch influencing PR-MX8B decolourisation were statistically elucidated for optimization. The optimum concentrations of 5.00 g/l yeast extract, 2.99 g/l starch and 1.89 g/l corn steep solids were predicted by applying the Box-Behnken design to the second order polynomial model fitted to the results obtained. The best predicted optimal conditions verified experimentally yielded 72.11% while the predicted value from the polynomial model was 79.17%. The experimental values were in good agreement with the predicted values with a 90.81% degree of accuracy.

Key words: azo dyes; decolourisation; microbial consortium; medium optimization; Plackett-Burman design; Box-Behnken design; nutrient components

Colour elimination in wastewater is today the principal problem concerning the textile industries. The inefficiency in dyeing processes has resulted in 10%–15% of unused dyestuff entering the wastewater directly (Easton 1995). The major classes of synthetic dyes used include azo, anthraquinone and triarylmethane dyes. Azo dyes represent the largest group of all synthetic dyes and represent 70% of all organic dyes used by the textile industry (Zollinger 2003). On discharge to the environment, these azo dyes will eventually be reduced, in anoxic or anaerobic environments to aromatic amines. In the absence of oxygen to convert these products, they can cause toxic effects to the environment.

At present, the conventional biological wastewater treatment to eliminate colour is inefficient due to the low biodegradability of the dyes, while physical and chemical treatment processes are costly and have little adaptability to a wide range of dyes (Hao *et al*. 2000; Robinson et al. 2001). Micro-organisms have become a viable alternative to remediate the colour problem associated with reactive azo dyes due to their genetic diversity and metabolic versatility (Hao *et al.* 2000; Nigam *et al.* 1996a). Many studies on the decolorizing capability of micro-organisms especially fungi and bacteria have been reported and reviewed (Chang & Lin 2000; Kandelbauer & Guetbitz, 2005; Novotný *et al.* 2001).

Process improvements in the productivity of fermentation processes are generally ascribed to the development of superior strains via mutation. However, other parameters such as the nutritional and physical environments to which the organisms are exposed to also significantly alter product yield. Classical medium optimization involves a single-dimensional search and does not examine the interactions between different parameters. More often, this method does not guarantee the determination of optimal conditions. Methods which utilize a full factorial search that would examine every possible combination of independent variables at appropriate levels can be used, but are laborious and time-consuming especially for a large number of variables. Alternatively, statistical methods based on fractional factorial searches are more practical approaches. Medium optimization using statistical designs was recently used for decolourisation studies (Annadurai *et al*. 2000; El-Sersy 2007).

In the present study, the improvement of processes focused on medium optimization and parameters which included the nutrients, pH and inoculum size. Two experimental designs were sequentially applied as tools for optimizing bacterial consortium decolourisation processes. The Plackett-Burman design was applied to screen the relative importance of various factors on the decolourisation of a mixture of azo dyes. In the following steps, the Box-Behnken design was applied for further optimization of the most significant variables. The results for batch study carried out on degradation of the reactive dye are presented.

[1]Faculty of Applied Sciences, Universiti Teknologi MARA, 40450 Shah Alam, Selangor, Malaysia
*Corresponding author (e-mail: khadijah@salam.uitm.edu.my)

paper 1.indd 103 1/20/2011 11:14:12 AM

DESIGN OF EXPERIMENTS

Identification of Important Nutrient Components – The Plackett-Burman design

The Plackett-Burman experimental design (Plackett & Burman 1946) was used to screen and evaluate the relative importance of various nutrient and culture parameters for the decolourisation of Primazin Red MX-8B (PRMX-8B) by the bacterial consortium. This design, is a two-level fractional factorial design for studying $k = N - 1$ variables in N runs, where N is a multiple of four (Montgomery 1997). A total of 14 components (variables, $k = 14$) were selected for the study with each variable represented at two levels, (+) for high level and (–) for low level together with four dummy variables in 20 trials as shown in Tables 1 and 2, respectively.

The number of positive and negative signs per trial were (k + 1)/2 and (k–1)/2, respectively. Each column contained an equal number of positive signs. Each row represented a trial and each column represented an independent (assigned) or dummy (unassigned) variable. The effect of each variable was determined by the following Equation 1:

$$E_{(\chi_i)} = \frac{2\left(\sum M_{i+} - M_{i-}\right)}{N} \quad (1)$$

where $E_{(\chi i)}$ is the concentration effect of the tested variables, Mi+ and Mi– are the percentage of decolourisation from the trials where the variable (χ_i) measured was present at low and high values, respectively; and N is the number of trials, 20.

Experimental error was estimated by calculating the variance among the dummy variables as in Equation 2 below:

$$V_{eff} = \frac{\sum (E_d)^2}{n} \quad (2)$$

where V_{eff} is the variance of the concentration effect, E_d is the concentration effect of the dummy variable and n is the number of dummy variables.

The standard error (*S.E.*) of the concentration effect was the square root of the variance of an effect and the significance level (P-value) of each concentration effect was determined using student's *t*-test as in Equation 3:

$$V_{eff} = \frac{\sum (E_d)^2}{n} \quad (3)$$

where $E_{(\chi i)}$ is the effect of variable.

This model does not describe interactions among variables and was used to screen and evaluate the important variables that influenced the response. All experiments were carried out in triplicate and the averages of the percentage dye decolourisation were taken as response. The variables were screened at the confidence level of 99% based on their effect. If the variable displayed a significance level at or above 99% confidence level and its effect was positive, it indicated that the variable was effective in decolorizing the dyes and a high level value (+) was required in the following optimization studies. However, if the effect was negative, a low level value (–) was required (Gohel et al. 2007).

Table 1. Variables showing medium components and conditions used in the Plackett-Burman design.

Variables	Medium components	High level (+)	Low level (–)
X_1	Yeast extract	5.0 g/l	0.5 g/l
X_2	Peptone	5.0 g/l	0.5 g/l
X_3	Corn steep solids	5.0 g/l	0.5 g/l
X_4	Ammonium sulfate	5.0 g/l	0.5 g/l
X_5	Urea	5.0 g/l	0.5 g/l
X_6	Sodium nitrate	5.0 g/l	0.5 g/l
X_7	Nutrient broth	5.0 g/l	0.5 g/l
X_8	Glucose	5.0 g/l	0.5 g/l
X_9	Maltose	5.0 g/l	0.5 g/l
X_{10}	Mannitol	5.0 g/l	0.5 g/l
X_{11}	Starch	5.0 g/l	0.5 g/l
X_{12}	Sodium acetate	5.0 g/l	0.5 g/l
X_{13}	pH	9.0	5.0
X_{14}	Inoculum size	10% v/v	5% v/v

paper 1.indd 104 1/20/2011 11:14:12 AM

Table 2. Plackett-Burman design matrix where X_1, X_2,....X_{14} are independent variables and D_1, D_2, D_3, D4 and D_5 are dummy variables.

Trial	Variables																		
	X_1	X_2	X_3	X_4	X_5	X_6	X_7	X_8	X_9	X_{10}	X_{11}	X_{12}	X_{13}	X_{14}	D_1	D_2	D_3	D_4	D_5
1	+	–	+	+	–	–	–	–	+	–	+	–	+	+	+	+	–	–	+
2	+	+	–	+	+	–	–	–	–	+	–	+	–	+	+	+	+	–	–
3	–	+	+	–	+	+	–	–	–	–	+	–	+	–	+	+	+	+	–
4	–	–	+	+	–	+	+	–	–	–	–	+	–	+	–	+	+	+	+
5	+	–	–	+	+	–	+	+	–	–	–	–	+	–	+	–	+	+	+
6	+	+	–	–	+	+	–	+	+	–	–	–	–	+	–	+	–	+	+
7	+	+	+	–	–	+	+	–	+	+	–	–	–	–	+	–	+	–	+
8	+	+	+	+	–	–	+	+	–	+	+	–	–	–	–	+	–	+	–
9	–	+	+	+	+	–	–	+	+	–	+	+	–	–	–	–	+	–	+
10	+	–	+	+	+	+	–	–	+	+	–	+	+	–	–	–	–	+	–
11	–	+	–	+	+	+	+	–	–	+	+	–	+	+	–	–	–	–	+
12	+	–	+	–	+	+	+	+	–	–	+	+	–	+	+	–	–	–	–
13	–	+	–	+	–	+	+	+	+	–	–	+	+	–	+	+	–	–	–
14	–	–	+	–	+	–	+	+	+	+	–	–	+	+	–	+	+	–	–
15	–	–	–	+	–	+	–	+	+	+	+	–	–	+	+	–	+	+	–
16	–	–	–	–	+	–	+	–	+	+	+	+	–	–	+	+	–	+	+
17	+	–	–	–	–	+	–	+	–	+	+	+	+	–	–	+	+	–	+
18	+	+	–	–	–	–	+	–	+	–	+	+	+	+	–	–	+	+	–
19	–	+	+	–	–	–	–	+	–	+	–	+	+	+	+	–	–	+	+
20	–	–	–	–	–	–	–	–	–	–	–	–	–	–	–	–	–	–	–

Optimisation of Selected Components – The Box-Behnken Design

For optimisation of the media, response surface methodology (RSM) was used. RSM is a collection of mathematical and statistical techniques that is useful for the modelling and analysis of problems in which a response of interest is influenced by a set of controlled experimental variables. The objective of RSM is to optimise this response (Montgomery 1997). In general the optimisation design experiments involve three major steps; firstly, performing the statistically designed experiments, followed by estimating the coefficients in the proposed mathematical model and finally predicting the response and checking the adequacy of the model (Annadurai *et al*. 2000). The response surface is usually represented graphically and the shape of a response surface is often visualized in the form of contour plots. Each contour corresponds to a particular height of the response surface (Montgomery 1997).

For this study, a class of three-level complete factorial designs for the estimation of the parameters in a second order model developed by Box-Behnken was chosen. These designs are formed by combining 2^k factorials with incomplete block designs. The variables were selected at three levels: –1, 0, +1, and the response Y is given by a second order polynomial as in Equation 4:

$$Y = \beta_0 + \sum_{j=1}^{k} \beta_i X_i + \sum \beta_{ii} \; X_i^2 + \sum_{j=1,i<j}^{k-1} \sum_{j=2}^{k} \beta_{ij} X_i X_j + \varepsilon \quad (4)$$

where X_1, X_2, …. , X_3 are the input variables which influence the response Y ; β_0 β_i (i = 1, 2, 3, …. ,) β_{iij} (i = 1, 2, 3, …. , k ; j = 1, 2, 3, …. , k) are known parameters and ε is a random error.

The effect of the concentration of yeast extract (g/l), soluble starch (g/l) and corn steep solids (g/l) on dye decolourisation were selected as the critical variables and designated as X_1, X_2, and X_3, respectively. Other variables with less significant or negative effects were omitted in the optimisation experiments. This was decided after initial experiments with the addition of these variables at their minimum levels did not show any difference from the results obtained when the variables were not added. The low, middle and high level of each variable was designated as –1, 0, and +1 with values of 0.50 g/l, 2.75 g/l and 5.00 g/l respectively. The actual design of the experiments is tabulated in Table 3. Decolourisation was subjected to analysis of variance (ANOVA), appropriate to the design experiments.

The mathematical correlation between the decolourisation of the dyes (Y) with the three variables was approximated by the quadratic model in Equation 5:

$$Y = \beta_0 + \beta_1 X_1 + \beta_2 X_2 + \beta_3 X_3 + \beta_{11} X_{12} + \beta_{22} X_2^2 + \beta_{33} X_3^2 + \beta_{12} X_1 X_2 + \beta_{13} X_1 X_3 + \beta_{23} X_2 X_3 \quad (5)$$

where Y = predicted response (% decolourisation), β_0 = constant, X_1 = yeast extract (g/l), X_2 = soluble starch

paper 1.indd 105 1/20/2011 11:14:13 AM

(mg/l), X_3 = corn steep solids (mg/l), β_1, β_2, and β_3 = linear coefficients, β_{12}, β_{13}, and β_{23} = cross product coefficients.

Analysis of the design experiments were carried out using statistical software package Design Expert (Stat-Ease Inc. Statistics Made Easy, Minneapolis, MN ver. 6, 1999). A total of 17 trials with five replicates at the centre point were employed to fit a second-order response surface. All experiments were done in triplicates and the mean response values were used in the computation.

Verification and Confirmation of the Proposed RSM Model

Five out of the ten optimal conditions computed from the optimization experiments were verified experimentally and compared with the calculated data from the model. Similar general media was used with addition of yeast extract, starch and corn steep solids as indicated by the proposed model. A triplicate set of experiments were conducted and the average of the three datasets was used to attain the optimized point. The observed percentage decolourisation was then compared to the predicted one as generated by the software.

MATERIALS AND METHODS

Micro-organisms and Culture Conditions

The selected bacterial consortium consist of three isolates identified as *Chryseobacterium* and *Flavobacterium* genus and was prepared by inoculating the individual strains grown overnight on nutrient agar plates in an Erlenmeyer flask containing 100 ml nutrient broth (NB). The culture media was shaken at 150 r.p.m. at room temperature and left for 24 h.

Media and Components

Nutrient broth, yeast extract (YE), peptone, nutrient agar (NA), soluble starch, yeast extract peptone dextrose (YEPD) and yeast nitrogen base (YNB) were purchased from Difco and corn steep solids was purchased from Sigma laboratory supplies. Media for the decolourisation experiments contained (g/l): NaCl (2.0), $MgSO_4.7H_2O$ (0.4), $CaCl_2.2H_2O$ (0.5), $MgCl_2.6H_2O$ (0.7), K_2HPO_4 (0.3), and KH_2PO_4 (0.3). The other variables were added and adjusted accordingly as listed in Table 1, 2 and 3.

Chemicals

All the general chemicals used were purchased from Sigma (USA), Merck (Germany) and BDH (England). Commercial test kits for the determination of some of the environmental parameters were purchased from HACH Company (USA). Depending upon the use, all chemicals were of Analar, HPLC or equivalent grade. PR-MX8B, a reactive azo dye was obtained from the Textile Technology Laboratory, Faculty of Applied Sciences, Universiti Teknologi MARA, Shah Alam, Selangor.

Decolourisation Assay

Decolourisation of the individual dyes was determined at their respective maximum absorption wavelength in the culture supernatants using a spectrophotometer. A sample of culture broth was withdrawn daily and about 1 ml was centrifuged at 10 000 r.p.m. for 15 min (Eppendorf Centrifuge 5415), before its optical density was measured.

Table 3. The actual Box-Behnken design for the three independent variables.

Trial	Yeast extract (g/l)	Soluble Starch (g/l)	Corn steep solids (g/l)
1	–1	–1	0
2	1	–1	0
3	–1	1	0
4	1	1	0
5	–1	0	0
6	1	0	–1
7	0	0	–1
8	0	0	1
9	0	–1	1
10	0	1	–1
11	0	–1	–1
12	0	1	1
13	0	0	0
14	0	0	0
15	0	0	0
16	0	0	0
17	0	0	0

paper 1.indd 106 1/20/2011 11:14:13 AM

The optical densities (OD) measured were then converted to the dye concentrations using the respective standard curves. The efficiency of colour removal was expressed as the percentage ratio of the decolorized dye concentration to that of initial one based on the following Equation 6 (Chen *et al*. 2003),

$$\text{Colour removal (\%)} = \frac{\text{Dye (i)} - \text{Dye (r)} \times 100\%}{\text{Dye (i)}} \qquad (6)$$

where Dye (i) = initial dye concentration (mg/l), Dye (r) = residual dye concentration (mg/l).

RESULTS AND DISCUSSION

Screening of Variables Required for Decolourisation of PR-MX8B by Plackett-Burman Design

The results of the Plackett-Burman design experiments are shown in Table 4. The table shows the magnitude of effect, its standard error (*S.E.*), the *t*-test ($t_{(5)}$) and its associated *P*-value and percentage confidence level. The t-test estimates the probability of finding an observed effect on decolourisation (the measured output) if $P < 0.01$ i.e. confidence level >99%. A positive effect value, E (X_i) indicates that the growth factor i exert a beneficial effect on decolourisation when present at a high amount, and vice versa.

Of the various organic and inorganic nitrogen sources tested, yeast extract had the most significant positive effect on the decolourisation of all dyes. This result was in accordance to findings in other studies (Chen *et al*. 2003; Khehra *et al.* 2005; Moosvi *et al.* 2007). Yeast extract has been widely reported as the most effective carbon-nitrogen source (Nigam *et al*. 1996; Kapdan *et al*. 2000), where complete decolourisation of several dyes was obtained in 24 h. In addition to yeast extract, peptone and corn steep solids also showed significant positive effects on decolourisation. Contrasting results however, were obtained by several researchers with regards to the peptone effect on decolourisation. A positive effect of peptone was reported in stimulating biodecolourisation of Reactive Brilliant Blue KN-R (Nam & Renganathan 2000), while for Remazol Violet 5R, poor decolourisation was observed in its presence (Moosvi *et al*. 2007). The positive effect of corn steep solids on decolourisation was an advantage in terms of cost since corn steep solids were much cheaper compared to yeast extract and peptone. The addition of organic nitrogen sources were considered essential medium supplements for the regeneration of nicotinamide adenine dinucleotide (NADH) that act as electron donor for the reduction of azo dyes by microorganisms (Nam & Renganathan 2000).

The decolourisation of dyes by bacteria has been reported to have been attained in synthetic media containing various extra carbon sources (Nigam *et al*. 1996a; 1996b). Of all the carbon sources tested, starch and glucose gave the most significant positive effects on dye decolourisation. A similar observation was obtained based on decolourisation of Reactive Turquoise Blue (RTB) and it was suggested that glucose is a readily biodegradable carbon and energy source and sufficient glucose promotes microbial proliferation, thus producing more bacterial cells capable of removing RTB (Fu *et al*. 2002). However, contrasting results where the addition of glucose reduced the decolourisation efficiency of various dyes had also been observed and in addition, lactose and sucrose had caused nearly complete decolourisation of the dyes (Kapdan *et al*. 2000). These observations suggest that the suitability of the carbon sources varied according to the consortium since different types of micro-organisms required different nutrients to support growth.

Table 4. Statistical analysis of the effect of medium components on decolourisation of PR-MX8B based on Plackett-Burman design results.

Variables	Medium component	Effect	*S.E.*	$t_{(5)}$	*P*-value	Confidence level (%)
X_1	Yeast extract	11.55	0.9168	12.60	6×10^{-5}	99.99
X_2	Peptone	6.45	0.9168	7.035	0.0009	99.91
X_3	Corn steep solids	7.25	0.9168	7.906	0.0001	99.94
X_4	Ammonium sulfate	1.35	0.9168	1.473	0.2009	79.91
X_5	Urea	–1.55	0.9168	1.691	0.1517	84.83
X_6	Sodium nitrate	–3.45	0.9168	3.763	0.00232	46.29
X_7	Nutrient broth	–0.65	0.9168	0.709	0.5100	49.00
X_8	Glucose	–0.95	0.9168	1.036	0.3476	65.24
X_9	Maltose	1.05	0.9168	1.145	0.3039	69.61
X_{10}	Mannitol	–0.85	0.9168	0.9272	0.3964	60.36
X_{11}	Starch	6.65	0.9168	7.254	0.0008	99.92
X_{12}	Sodium acetate	0.65	0.9168	0.709	0.5100	48.99
X_{13}	pH	0.65	0.9168	0.709	0.5100	49.00
X_{14}	Inoculum size	8.75	0.9168	9.544	0.0002	99.98

paper 1.indd 107 1/20/2011 11:14:13 AM

The effects of other components such as the pH and inoculum size on the majority of the dyes were found to be not statistically significant (confidence level < 99%), although some dyes displayed improved decolourisation with increase in inoculum size and decrease in pH. pH within the range of 6–8 was favourable for efficient decolourisation (Çetin & Dönmez 2006) and pH 7 was identified as the optimum pH for fast and efficient decolourisation of Reactive Red 22 (Chang & Kuo 2000) and Reactive Violet 5R (Moosvi *et al.* 2007). Thus, for further optimization experiments, yeast extract, corn steep solids and starch were chosen as part of the general culture medium. These substrates were chosen on the basis of the calculated *t*-values and also after the decolourisation efficiency and economical factors were considered. In addition, the initial pH of the medium was maintained at 7 and the culture was inoculated with 10% inoculum size since smooth efficient decolourisation was obtained with 10% inoculum size (Assadi *et al.* 2001).

Optimisation of Screened Medium Components for Decolourisation of PR-MX8B

In order to approach the optimum response region for decolourisation efficiency, the significant independent variables (yeast extract, X_1; starch, X_2; and corn steep solids, X_3) were further explored, each at three levels. A second order quadratic model was used to explain the mathematical relationship between the controllable variables and the response since the estimated response seemed to have a functional relationship only on a local region or near the centre points of the model. Contour plots were then obtained when the data were fed into the design expert software and analyzed by it. Each contour plot represented the effect of two medium components at their studied concentration range and at a fixed concentration of the third medium component. The value of the third medium component was varied for that situation with the software and the optimum value was obtained. For the PR-MX8B, the final mathematical expression in terms of coded variables relating to the percentage decolourisation of the dyes with the above variables like X_1, X_2 and X_3 is given in the following Equation 7, where Y is the predicted response.

$$Y = 53.41 + 18.24\,X_1 - 0.56\,X_2 + 4.82\,X_3 + 7.80\,X^2_1 - 3.22\,X^2_2 - 2.51\,X^2_3 + 0.64\,X_1X_2 - 5.86\,X_1X_3 + 0.40\,X_2X_3 \quad (7)$$

The percentage decolourisation of DM from the model at each experimental point is summarized in Table 5 together with the experimental and theoretical predicted values. The summary of the analysis of variance (ANOVA) is shown in Table 6. Based on the analysis, the multiple correlation coefficient, R^2 for biodecolourisation of the dye obtained is 0.9976 while the coefficient of determination (Adj. R^2) is 0.9945. These values relatively indicate that the experimental data obtained fitted well with the predicted model. The model *F*-value of 325.10 implies the model is significant and the lack of fit F-value of 5.90 implies the lack of fit was not significant relative to the pure error.

Surface plots representing the experimental results are shown in Figures 1 to 3, respectively. From Figure 1 the maximum predicted percentage dye decolourisation

Table 5. Experimental and theoretical values for percent decolourisation of PR-MX8B.

Trial	Actual value (%)	Predicted value (%)
1	41.11	41.19
2	75.02	76.13
3	39.90	38.81
4	76.40	76.30
5	29.88	29.96
6	78.90	77.98
7	50.20	51.13
8	75.99	75.91
9	44.54	44.35
10	41.43	42.46
11	53.95	52.93
12	52.45	52.63
13	54.05	53.91
14	54.21	53.91
15	54.41	53.91
16	54.01	53.91
17	52.88	53.91

paper 1.indd 108 1/20/2011 11:14:13 AM

Table 6. Regression analysis for the decolourisation of PR-MX8B (quadratic response surface model fitting).

Source	Sum of squares	Degree of freedom	Mean square	*F* value	Prob > *F*
Model	3244.40	9	360.49	325.10	<0.0001
Residual	7.76	7	1.11		
Lack of fit	6.33	3	2.11	5.90	0.0596
Pure error	1.43	4	0.36		
Correlation total	3252.17	16			

Coefficient of correlation (R^2) = 0.9976; coefficient of determination (Adj R^2) = 0.9945

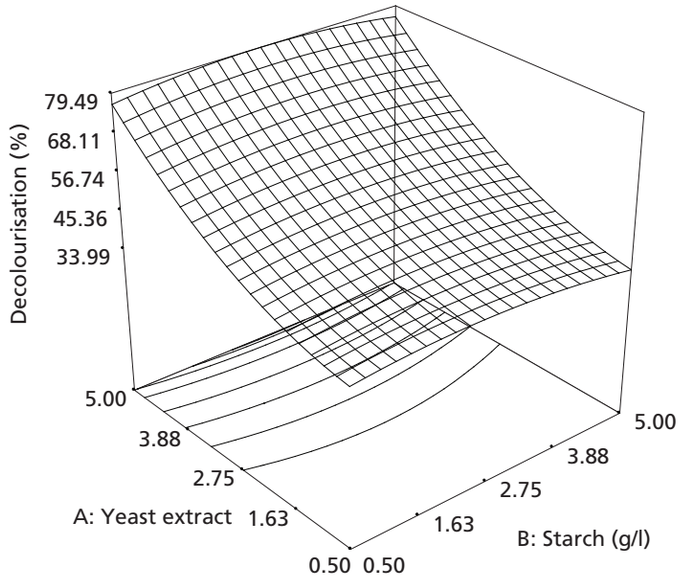

Figure 1. Surface plot showing the effect of starch and yeast extract on percentage decolourisation of PR-MX8B.

between 0.50 g/l to 5.00 g/l of yeast extract and starch is 79.17%. The optimisation level of dye decolourisation was 79.17% at 5.00 g/l yeast extracts and 2.99 g/l starch. Yeast extract has been widely reported as the most effective carbon-nitrogen source where complete decolourisation of several dyes was obtained in 24 h (Nigam *et al*. 1996a; Kapdan *et al*. 2000). Efficient decolourisation was also observed based on decolourisation of RTB, and it was suggested that sufficient carbon source promotes microbial proliferation, thus producing more bacterial cells capable of decolorizing the dye (Fu *et al*. 2002). An increase in yeast extract and starch concentrations resulted in increased decolourisation, but addition of too much yeast extract was costly while increased amount of starch would contribute to higher COD.

The effect of yeast extract and corn steep solids can be clearly seen in Figure 2. Optimum level of dye decolourisation was 79.17% at 5.00 g/l yeast extract and 1.89 g/l corn steep solids. With increasing corn steep solids concentration there was no effect on dye decolourisation. However, sufficient levels of corn steep solids, with a gradual increase in yeast extract concentration resulted in maximum dye decolourisation. The positive effect of corn steep solids on decolourisation was an advantage in terms of cost since corn steep solids were much cheaper compared to yeast extract.

The maximum percentage of dye decolourisation was found to occur with increasing starch (0.500 g/l to 2.75 g/l) and corn steep solids (0.50 g/l to 2.99 g/l) at 5.00 g/l yeast extract as shown in Figure 3. An optimum level of starch of 2.99 g/l with corn steep solid concentration of 1.89 g/l showed a maximum percentage dye decolourisation of 79.17%. With further increase of starch and corn steep solids, dye decolourisation was decreased. Overall, the analysis of the surface plots in the optimization experiments results indicated that the presence of yeast extract in the culture medium was essential for decolourisation of the dye; with increasing amount of

paper 1.indd 109 1/20/2011 11:14:14 AM

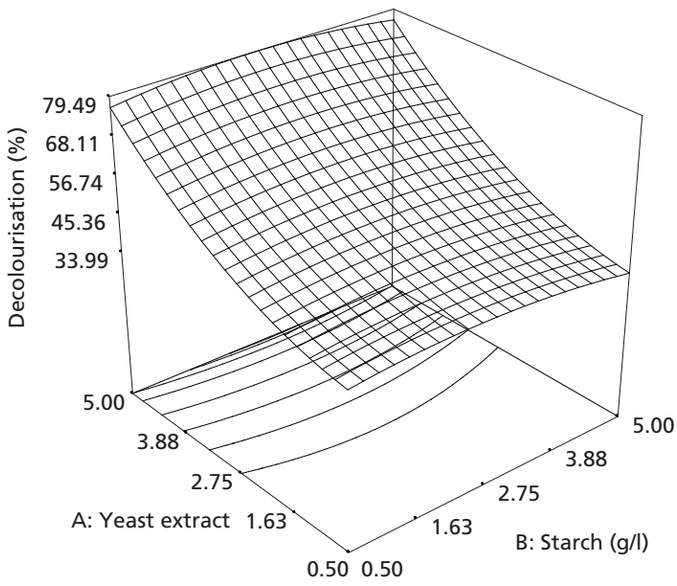

Figure 2. Surface plot showing the effect of yeast extract corn steep solids on percentage decolourisation of PR-MX8B.

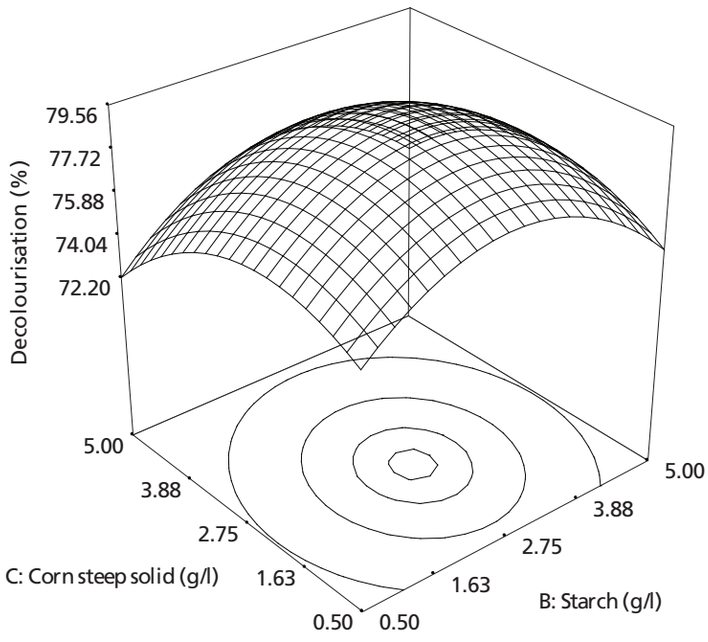

Figure 3. Surface plot showing the effect of corn steep solids and starch on percentage decolourisation of PR-MX8B.

Table 7. Theoretical and actual values for percentage decolourisation of PR-MX8B based on the proposed optimised media combinations.

Proposed solutions	Yeast extract (g/l)	Starch (g/l)	Corn steep solids (g/l)	% Decolourisation	
				Predicted value	Actual value[a]
I	4.98	3.11	3.02	51.06	40.11 ± 1.12
II	5.00	0.78	2.96	79.00	70.10 ± 2.71
III	4.97	2.92	1.75	78.91	69.68 ± 3.55
IV	4.99	3.02	2.84	78.47	68.97 ± 1.85
V	5.00	2.99	1.89	79.17	72.11 ± 0.50

[a]Note: Results represent an average of three independent experiments

yeast extract (from 0.5 g/l – 5 g/l), there was an increase in dye decolourisation. Several studies have reported similar findings (Chen *et al*. 2003; Asad *et al*. 2007) and in addition it was also found that the decolourisation increased only slightly in the range of 5 g/l – 10 g/l of yeast extract (Chen *et al.* 2003).

Verification of the Model

The optimal conditions obtained from the optimization experiments were verified experimentally and compared to those of calculated data from the model. Five out of 10 proposed calculated optimal culture compositions for the yeast extract, starch and corn steep solids were selected at random and the results are shown in Table 7. In general, the experimental percentage decolourisations were lower than those of the predicted values. Those are common observations as found by other experimental design studies (El-Sersy 2007; Abdel-Fattah & Olama 2002). The highest estimated percentage decolourisation was 72.11 obtained from the proposed solution V (5.00 g/l yeast extract; 2.99 g/l starch; 1.89 g/l corn steep solids) while the predicted value from the polynomial model was 79.17%. The result of the verification experiment revealed a 90.81% degree of accuracy for the model.

CONCLUSION

The two-factorial Plackett-Burman design chosen for the study allowed the investigation of 14 independent variables at two different levels. Based on the analysis, three critical variables: yeast extract; starch and corn steep solids were identified and tested further in the optimisation experiments. In the optimization process, analysis of the Box-Behnken results showed that 5.00 g/l yeast extract, 2.99 g/l starch and 1. 89 g/l corn solids were the best combination for treating PR-MX8B. In conclusion, the result indicated that the methodology of Plackett-Burman and Box-Behnken designs had proved efficient and the use of these techniques had helped to identify the important medium components which had significant effects on dye and textile wastewater decolourisation. Further studies are being conducted on applying the techniques in a bioreactor.

ACKNOWLEDGEMENT

The author would like to thank Universiti Teknologi MARA, Shah Alam, Selangor, Malaysia for funding the research.

Date of submission: November 2008
Date of acceptance: May 2010

REFERENCES

Abdel-Fattah, YR & Olama, ZA 2002, 'L-asparaginase production by *pseudomonas aeruginosa* in solid-state culture: evaluation and optimization of culture conditions using factorial designs', Process Biochemistry, vol. 38, pp. 115–122.

Annadurai, G, Sivakumar, T & Babu, SR 2000, 'Photocatalytic decolourisation of congo red over ZnO powder using Box-Behnken design of experiments', *Bioprocess Engineering*, vol. 23, pp. 167–173.

Asad, S, Amoozegar, MA, Pourbabaee, AA, Sarbolouki, MN & Dastgheib, SMM 2007, 'Decolorization of textile azo dyes by newly isolated halophilic and halotolerant bacteria', *Bioresource Technology*, vol. 11, pp. 2082–2088.

Assadi, MM, Rostami, K, Shahvali, M & Azin, MA 2001, 'Decolorization of textile wastewater by *Phanerochaete chrysosporium', Desalination*, vol. 141, pp. 331–336.

Çetin, D & Dönmez, G 2006, 'Decolorization of reactive dyes by mixed cultures isolated from textile effluent under anaerobic conditions', *Enzyme Microbial Technol*. vol. 30, pp. 926–930.

Chang, J & Kuo, T 2000, 'Kinetics of bacterial decolorization of azo dye with *Escherichia coli* NO3', *Biores Technology*, vol. 75, pp. 107–111.

Chang, JS & Lin, YC 2003, 'Fed batch bioreactor strategies for microbial decolorization of azo dye using *Pseudomonas luteola* strain', *Biotechnol Progress*, vol. 16, pp. 979–985.

Chen, K, Wu, J, Liou, D & Hwang, SJ 2003, 'Decolorization of the textile dyes by newly isolated bacterial strains', *J. of Biotechnology*. vol.101, pp. 57–68.

Dong, X, Zhou, J & Ying, L 2003, 'Peptone-induced biodecolourisation of Reactive Brilliant Blue (KN-R) by

paper 1.indd 111 1/20/2011 11:14:15 AM

Rhodocyclus gelatinosus XL-1', *Process Biochemistry,* vol. 39, pp. 89–94.

Easton, J 1995, 'The dye maker's view', in *Colour in dyehouse effluent*, ed P Cooper, Society of Dyers and Colourists, Bradford.

El-Sersy, NA 2007, 'Bioremediation of Methylene Blue by Bacillus thuringiensis 4 G1: application of statistical designs and surface plots for optimization', *Biotechnology*, vol. 6, no.1, pp. 34–39.

Fu, L, Wen, X & Qian, Y 2002, 'Removal of copper-phthalocyanine dye from wastewater by acclimated sludge under anaerobic or aerobic conditions', *Process Biochemistry*, vol. 37, pp. 1151–1156.

Gohel, V, Chaudhary, T, Vyas, P & Chhatpar, HS 2006, 'Statistical screening of medium components for the production of chitanase by the marine isolate *Phantoea dispersa*', *Biochem Eng J.*, vol. 28, pp. 50–56.

Hao, OJ, Kim, H, Chiang, P 2000, 'Decolorization of wastewater', *Crit. Rev. Environ. Sci. Technol.*, vol. 30, no. 4, pp. 449–5051.

Kandelbauer, A & Guebitz, GM 2005, 'Bioremediation for the decolorization of textile dyes — a Review', in *Environmental chemistry — green chemistry and pollutants in ecosystem*, eds E Lichtfouse, J Schwarzbauer and D Robert, Berlin: Springer Berlin Heidelberg.

Kapdan, IK, Kargi, F, McMullan, G & Marchant, R 2000, 'Effect of environmental conditions on biological decolorization of textile dyestuff by *C. versicolor', Enzyme & Microbial Technol.*, vol. 26, pp. 381–387.

Khehra, MS, Saini, HS, Sharma, DK, Chadha, BS & Chimni, SS 2005, 'Decolorization of various azo dyes by bacterial consortium', *Dyes & Pigments*, vol. 67, pp. 55–61.

Montgomery, DC 1997, *Design and analysis of experiments*, 3rd edn, John Wiley & Sons Inc., New York.

Moosvi, S, Kher, X & Madamwar, D 2007, 'Isolation, characterization of textile dyes by a mixed bacterial consortium JW-2', Dyes & Pigments, vol. 74, pp. 723–729.

Nam, S & Renganathan, V 2000, 'Non-enzymatic reduction of azo dyes by NADH', *Chemosphere*, vol. 40, pp. 351–357.

Nigam, P, Banat, IM, Singh, D & Marchant, R 1996a, 'Microbial process for the decolorization of textile effluent containing azo, diazo and reactive dyes', *Process Biochemistry*, vol. 31, no. 5, pp. 435–442.

Nigam, P, Mc Mullan, G, Banat, I, Marchant, R 1996b, 'Decolourisation of effluent from the textile industry by a microbial consortium', *Biotechnol. Letter*, vol. 18, pp. 117–120.

Novotný, C, Rawal, B, Bhatt, M, Patel, M *et al*. 2001, 'Capacity of *Irpex lacteus* and *Pleurotus ostreatus* for decolorization of chemically different dyes', *J of Biotechnology*, vol. 89, pp. 113–121.

Plackett, RL & Burman, JP 1946, 'The design of optimum multifactorial experiments', *Biometrika*, vol. 37, pp. 305–325.

Robinson, T, McMullan, G, Marchant, R & Nigam, P 2001, 'Remediation of dyes in textile effluent: a critical review on current treatment technologies with a proposed alternative', *Biores Technology*, vol. 77, pp. 247–255.

Zollinger, H 2003, Colour chemistry — synthesis, properties and application of organic dyes and pigments, 3rd edn, Wiley-VCH, Zurich.

paper 1.indd 112 1/20/2011 11:14:15 AM

ASM Sci. J., **4(2)**, 113–122

Physicochemical Properties of Margarines Enriched with Medium- and Long-chain Triacylglycerol

N. Arifin[1,5], L.Z. Cheong[1], S.P. Koh[1], K. Long[2]*, C.P. Tan[3], M.S.A. Yusoff[4] and O.M. Lai[1,6]

Several binary and ternary medium- and long-chain triacylglycerol (MLCT)-enriched margarine formulations were examined for their solid fat content, heating profile, polymorphism and textural properties. MLCT feedstock was produced through enzymatic esterification of capric and stearic acids with glycerol. The binary formulations were produced by mixing MLCT feedstock blend (40%–90%) and palm olein (10%–60%) with 10% increments (w/w). Solid fat profiles of commercial margarines were used as a reference to determine the suitability of the formulations for margarine production. The solid fat content of the binary formulations of MO 82 and MO 91 (M, MLCT, O, palm olein) were similar to the commercial margarines at 25°C which met the basic requirement for efficient dough consistency. Ternary formulations using reduced MLCT feedstock blend proportion (from 80%–90% to 60%–70%) were also developed. The reduction of MLCT feedstock blend was done as it had the highest production cost (3USD/kg) in comparison to palm olein (0.77USD/kg) and palm stearin (0.7USD/kg). The proportions of 5%–15% of palm stearin were substituted with palm olein in MO 64 and MO 73 (M, MLCT; O, palm olein) formulations with 5% increment (w/w). As a result, MOS 702010 and MOS 603010 (M, MLCT; O, palm olein; S, palm stearin) margarine formulations showed similar SFC % to the commercial margarines at 25ºC. These formulations were subsequently chosen to produce margarines. The onset melting and complete melting points of MLCT-enriched margarine formulations were high (51.04ºC –57.93ºC) due to the presence of a high amount of long chain saturated fatty acids. Most of the formulations showed β´- crystals. MOS 702010 was selected as the best formulation due to values for textural parameters comparable ($P<0.05$) with commercial margarine.

Key words: medium- and long-chain triacylglycerol (MLCT); margarines; solid fat content; heating profiles; polymorphism; textural properties; formulation; palm olein; palm stearin

Historically, margarine was invented by a French chemist, Mege Mouries to substitute butter (Chrysam 1985). It is similar in taste and appearance to butter but possesses several distinct differences. In terms of microstructure, margarine is water in an oil emulsion consisting of edible oils and an aqueous phase. The emulsion contains dispersed water droplets of typically 2-4 µm diameter (Moran 1993). Margarine is a very important ingredient for the baking industry because it comprises 10%–50% of most baked products. Excess consumption of these products is normally associated with health problems such as obesity (List 2004). However, fat-containing diets cannot be restricted due to some functionalities of fat in our body. Fat also plays an important role in texture and flavour development in food. The consumption of food having low calories is suggested for consumers with lifestyle-related diseases (Sandrou & Arvanitoyannis 2000).

Medium- and long-chain triacylglycerols (MLCT) are tailor-made lipids that contains medium-chain fatty acids (MCFA) and long chain fatty acids (LCFA) on the same glycerol backbone (Kasai *et al.* 2003). Medium chain fatty acids give low caloric availability by fast burning and make them good candidates for efficient dietary treatment in obesity. Consumption of MLCT containing 10%–18% of MCFA has been reported to reduce body weight accumulation over short and long periods (Shinohara *et al.* 2005; Kasai *et al.* 2003; Matsuo *et al.* 2001). Nosaka *et al.* (2003a; 2003b) reported that consumption of MLCT-enriched margarine led to a significant decrease

[1]Dept. of Bioprocess Technology, Faculty of Biotechnology and Biomolecular Sciences, Universiti Putra Malaysia, 43400 Serdang, Selangor, Malaysia
[2]Malaysian Agricultural Research and Development Institute, P.O. Box 12301, 50774 Kuala Lumpur, Malaysia
[3]Dept. of Food Technology, Faculty of Food Science and Technology, Universiti Putra Malaysia, 43400 Serdang, Selangor, Malaysia
[4]Golden Hope Research Centre, P.O. Box 207, 47200 Banting, Selangor, Malaysia
[5]Faculty of Science and Technology, Universiti Sains Islam Malaysia, 71800 Bandar Baru Nilai, Negeri Sembilan, Malaysia
[6]Institute of Biosciences, Universiti Putra Malaysia, 43400 Serdang, Selangor, Malaysia
*Corresponding author (e-mail: amai@mardi.my)

paper 2.indd 113 1/20/2011 11:18:04 AM

in body fat accumulation as compared to LCT-enriched margarine. Clinically, MLCT has no adverse effect on body fat reduction when ingested excessively (Matulka *et al.* 2006).

Recently, the production of structured lipids involving the incorporation of medium- and long-chain fatty acids in the same molecule structure has received a lot of attention (Koh *et. al.* 2008; Lai *et al*. 2005; Yankah & Akoh 2000; Zainal & Yusoff 1999; Seriburi & Akoh 1998). Some examples of commercial structured lipids are Caprenin™ (Procter & Gamble Co., Cinnati, OH) and Healthy Resseta™ (Nisshin Oillio Group, Ltd). Caprenin™ is a modified lipid containing caprylic, capric and behenic fatty acids esterified randomly to a glycerol backbone and used as a cocoa butter replacement. On the other hand, Healthy Resseta™ has been approved as FOSHU (Food for Specified Health Use) by the Ministry of Health, Labor and Welfare of Japan in December 2002 for use as cooking oil (Aoyama *et al*. 2007).

The aim of this study was to determine the suitability of various MLCT-enriched formulations for margarine production. In this present study, binary and ternary formulations of MLCT-enriched margarine were developed by mixing MLCT feedstock blend, palm olein and palm stearin. The physicochemical properties of these formulations such as solid fat content, heating profiles and polymorphism were determined. The solid fat profiles of commercial margarines were used as a guideline to choose the suitable formulations for margarine production. Textural analysis was also performed on the selected MLCT-enriched margarines.

MATERIAL AND METHODS

Materials

MLCT feedstock were produced through Lipozyme RM IM lipase-catalyzed esterification of capric and stearic acids with glycerol. Further details on the production of MLCT feedstock were described in "Production and Purification of MLCT feedstock". The palm stearin IV44 was obtained from Golden Jomalina Food Industries Sdn. Bhd. (Teluk Panglima Garang, Selangor). Palm olein IV60 and commercial margarines, Planta (Unilever Malaysia Holding Sdn Bhd, Malaysia) and Daisy (Lam Soon (M) Berhad, Malaysia) were bought from Carrefour Hypermarket (Putrajaya, Wilayah Persekutuan). The commercial margarines were palm-based products. Commercial immobilized lipase from Rhizomucor meihei (Lipozyme RM IM) was obtained from Novozymes A/S (Bagsvaerd, Denmark). All chemicals and solvents used were either of analytical or high-performance liquid chromatography (HPLC) grades, respectively.

Production and Purification of MLCT Feedstock

The production of MLCT feedstock was conducted in a 10 l stirred tank bioreactor equipped with a vacuum pump and two vertically aligned three-bladed impellers in the feed tank (Paramount Impact Sdn. Bhd., Sri Kembangan, Selangor) as described in Arifin *et al*. (2009). Optimized parameters of MLCT feedstock production were obtained using response surface methodology (RSM) (unpublished data). The optimized parameters used for MLCT feedstock production were: reaction temperature, 65ºC; reaction time, 14 h; enzyme load, 8% (w/w) and fatty acids/glycerol molar ratio, 3:1. At the end of the reaction time, the products were removed and filtered out using a muslin cloth from the bottom of the vessel. The products were then purified using a short path distillator (SPD). The conditions of short path distillation used for MLCT feedstock purification followed Arifin *et al.* (2009). Other settings used were: feed rate, 5 kg/h; evaporator vacuum, 0.001 and heat exchanger temperature, 80ºC. Palm olein was mixed with unrefined MLCT feedstock in a 1:1 ratio to reduce the melting point of the latter fat. This was done due to the quick solidification of MLCT feedstock in the feeding tank, subsequently disabling the process being carried out.

Sample Preparation

The fats and oil composition for MLCT-enriched formulations are shown in Table 1. Six binary formulations of MLCT feedstock blend (40%–90%) and palm olein (10%–60%) (w/w) were produced with increments of 10% (w/w) for each formulation. Ternary formulations were developed by substituting 5%, 10% and 15% of palm olein with palm stearin in MO 73 and MO 64. MLCT feedstock blend, palm olein and palm stearin were heated at 80ºC for 30 min in an oven to remove crystal structures. The liquefied fats and oil were then mixed according to their proportions with a total weight of 50 g of fats and oil (w/w) in the sample bottles. All the formulations were kept at room temperature (25ºC) prior to analysis.

Fatty Acid Composition (FAC)

The fatty acid composition (FAC) of MLCT feedstock, palm olein, and palm stearin was determined by *AOCS (1997) Official Methods Ce 1-62*. FAC of the samples was determined after converting free and glyceride fatty acids to their corresponding fatty acid methyl esters (FAME) and analyzing the FAME by gas chromatography (Hewlett-Packard, Wilmington, DE, USA equipped with a flame-ionization detector). FAME's were prepared by transesterification of fat (50 µl) with isopropanol (950 µl) and sodium methoxide (0.5 N, 50 µl). The conditions of FAC analysis were: column oven, 170ºC (isothermal); carrier gas, helium 99.9%; carrier gas flow, 1 ml/min and running time, 13 min.

paper 2.indd 114 1/20/2011 11:18:04 AM

Table 1. Composition of binary and ternary MLCT-enriched margarine formulations.

Formulations [a]	Composition (Proportion w/w)		
	MLCT feedstock (M)	Palm olein (O)	Palm stearin (S)
MO 46	40	60	–
MO 55	50	50	–
MO 64	60	40	–
MO 73	70	30	–
MO 82	80	20	–
MO 91	90	10	–
MOS 603505	60	35	5
MOS 603010	60	30	10
MOS 602515	60	25	15
MOS 702505	70	25	5
MOS 702010	70	20	10
MOS 701515	70	15	15

[a] Indicates the MLCT feedstock, palm olein and palm stearin ratio.
Abbreviations: M, medium and long-chain triacylglycerol (MLCT) feedstock; O, palm olein; S, palm stearin

Solid Fat Content (SFC)

Solid fat content was measured by Bruker PC/20 series pulsed Nuclear Magnetic Resonance (pNMR) Analyzer (Minispec, Bruker, Karlsruhe, Germany) as described in AOCS official method Cd 10-57 (AOCS 1997). The samples were heated at 80ºC for 30 min to destroy the history of the crystal. During this study, the samples were evaluated at 5ºC intervals from temperatures of 0ºC to 60ºC.

Heating Profiles

Heating profiles of MLCT-enriched margarine formulations were measured using Pyris Diamond DSC equipped with an intra-cooler 2P (Perkin Elmer, Norwalk, CT, USA) according to the Official Method Cj 1-94 of AOCS (1997). An empty aluminum pan was used as a reference, and 7 mg – 9 mg samples were weighed. The samples were heated to 80ºC for 10 min to destroy their crystal memory. A crystallization curve was obtained by cooling to –60ºC at 5ºC/min and holding the temperature for 10 min. The samples were then heated to 80ºC to determine the heating profiles at heating rates of 5ºC/min. Although both cooling and heating profiles were done, only heating curves will be discussed here.

Fourier Transform Infrared Spectroscopy

Fourier Transform Infrared Spectroscopy (FT-IR) is a rapid technique that measures vibrations of bonds within functional groups. The polymorphism of MLCT-enriched margarine formulations was determined according to Piska *et al.* (2006) using FT-IR spectroscopy. The sample was first melted at 80ºC to erase the crystallization history and then the liquid sample was compressed between two KBr windows. IR spectra were collected by using a Perkin Elmer FT-IR Spectrum 2000 Spectrometer (Norwalk, CT). The sample was measured using wavelengths between 900 cm^{-1} and 600 cm^{-1}.

Production of Margarine

Margarines were produced according to the modified method of Li *et al.* (1999). The fat phase comprised 80% fats and oils, and 0.003% colouring and flavouring while the water phase consisted of 14% hot water, 1% skimmed milk and 2% salt. The two phases were prepared separately in two different 1000 ml beakers. The formulations selected for margarine production were MOS 602010 and MOS 702010. The two mixtures of 560 g of fat phase and 119 g of water phase were mixed in a 1000 ml beaker and blended for one min using a food blender (Cornell, Kuala Lumpur). The margarine containing beaker was then put in the vessel and chilled with ice at the bottom and surrounding the beaker. The mixture was stirred using a spatula until crystals were completely formed. The beaker was removed from the vessel and stored at room temperature for four h. The fat crystals were kneaded with the mixer for approximately one min at speed two and kept at 25ºC. The margarine (approx. 60 g) was then transferred into a cup of identical shape and size and kept at room temperature (25ºC) for textural analysis.

Textural Profile Analysis (TPA)

TPA was conducted for commercial and MLCT-enriched margarines using TA.XT2i Texture Analyzer (Stable Micro Systems, Godalming, Surrey, UK), with a 5 kg load cell as described in MAR2/45C TA.XT Plus Application Study Method (2006). A forty-five degree conical probe (P/45C) was employed and conditions of analysis were: pre-test speed, 2.0 mm/s; test speed, 1.0 mm/s; post-test speed, 10 mm/s; strain, 10%; data acquisition rate, 200 p.p.s., and trigger type, 5 g. The hardness and adhesiveness of the

paper 2.indd 115 1/20/2011 11:18:04 AM

margarines were estimated by maximum force (g) and the negative area of the texture profiles (g/sec).

Statistical Analysis

Statistical Analysis System software (SAS, Cary, NC) was used to perform statistical analysis (SAS 2000). Analysis of variance (ANOVA) with Duncan's multiple range test was performed to determine the significance of difference at $P<0.05$.

RESULTS AND DISCUSSION

Solid Fat Content (SFC)

Figure 1 shows the solid fat profiles of Planta (Unilever, Malaysia), Daisy (Lam Soon, Malaysia) and MLCT-enriched binary margarine formulations. The solid fat profile was used to assist in the proper choice of MLCT-enriched formulations to produce margarine. Formulations of MO 82 and MO 91 showed a similar SFC% to those of commercial margarines at 25°C with respect to the desired consistency for use in bakery and other cooking purposes. The solid fat of binary margarine formulations completely melted at 55ºC, excluding the formulation of MO 46 which melted at 50ºC. The domination of unsaturated fatty acids (USFA) which comprised oleic and linoleic acids (40.8%) as showed in Table 2 in the MO 46 formulation might contribute to the lower melting temperature. The solid fats of both commercial margarines liquefied completely at a temperature of 45ºC.

In the MLCT-enriched margarine binary formulations, the amounts of solid fat increased as the percentage of MLCT feedstock blend increased. This was associated to the high proportion of long chain saturated fatty acids (LCSFA) which consisted of myristic, palmitic and stearic acids in the binary formulations (Table 2). These results were in agreement with that of Karabulut *et al.* (2004). They reported that high contents of saturated fatty acids contributed to high SFC. There were differences in the SFC slope observed for binary formulations (Figure 1). Litwinenko and co-researchers (2002) reported that the changes in the slopes of their fat blends were due to the contributions of the various TAG fractions comprising of low and high melting fats and oils in the raw materials. The curves of MO 64, MO 73, MO 82 and MO 91 formulations were remarkably decreased at temperatures between 0ºC and 25ºC. A small region of slope was then observed at temperatures 25ºC to 55ºC showing gradual decrement in SFC %. There were changes in slope at temperatures ranging from 5ºC to 15ºC for MO 46 and MO 55 formulations. The slopes then decreased steadily to the melting temperatures.

Amongst MLCT feedstock blend (3 USD/kg), palm olein (0.77 USD/kg) and palm stearin (0.70 USD/kg), production of the former fat was considered as the most expensive. Developing the ternary formulations was therefore an attempt to reduce the proportion of MLCT feedstock blend (from 80%–90% to 60%–70%) in the margarine formulations. Margarine formulations of MO 64 and MO 73 were selected to produce the ternary formulations. These formulations were chosen as they

Table 2. The percentage of fatty acid distribution of binary and ternary MLCT-enriched margarine formulations[a].

Formulations [b]	Fatty acid distribution (%)		
	MCFA	LCSFA	USFA
MO 46	11.4 ± 0.03	47.8 ± 0.14	40.8 ± 0.09
MO 55	15.1 ± 0.02	48.7 ± 0.05	36.2 ± 0.06
MO 64	16.1 ± 0.16	51.1 ± 0.05	32.8 ± 0.10
MO 73	17.9 ± 0.02	52.4 ± 0.07	29.7 ± 0.08
MO 82	19.4 ± 0.07	53.5 ± 0.07	27.1± 0.10
MO 91	21.4 ± 0.04	55.1 ± 0.08	23.5 ± 0.03
MOS 603505	16.0 ± 0.03	52.5 ± 0.12	31.5 ± 0.01
MOS 603010	16.2 ± 0.05	53.4 ± 0.05	30.4 ± 0.13
MOS 602515	16.8 ± 0.02	54.0 ± 0.01	29.3 ± 0.13
MOS 702505	17.6 ± 0.10	54.8 ± 0.08	28.6 ± 0.06
MOS 702010	18.0 ± 0.12	54.1 ± 0.16	27.9 ± 0.04
MOS 701515	17.8 ±0.06	53.5 ± 0.11	27.6 ± 0.10

[a] Each value in the table represents the mean ± standard deviation of duplicate analyses.
[b] The fats and oil composition for each formulation are shown in Table 1.
Abbreviation: MCFA, medium chain fatty acid; LCSFA, long chain saturated fatty acids; USFA, unsaturated fatty acids; M, medium- and long chain triacylglycerols (MLCT); S, palm stearin; O, palm olein.

paper 2.indd 116 1/20/2011 11:18:04 AM

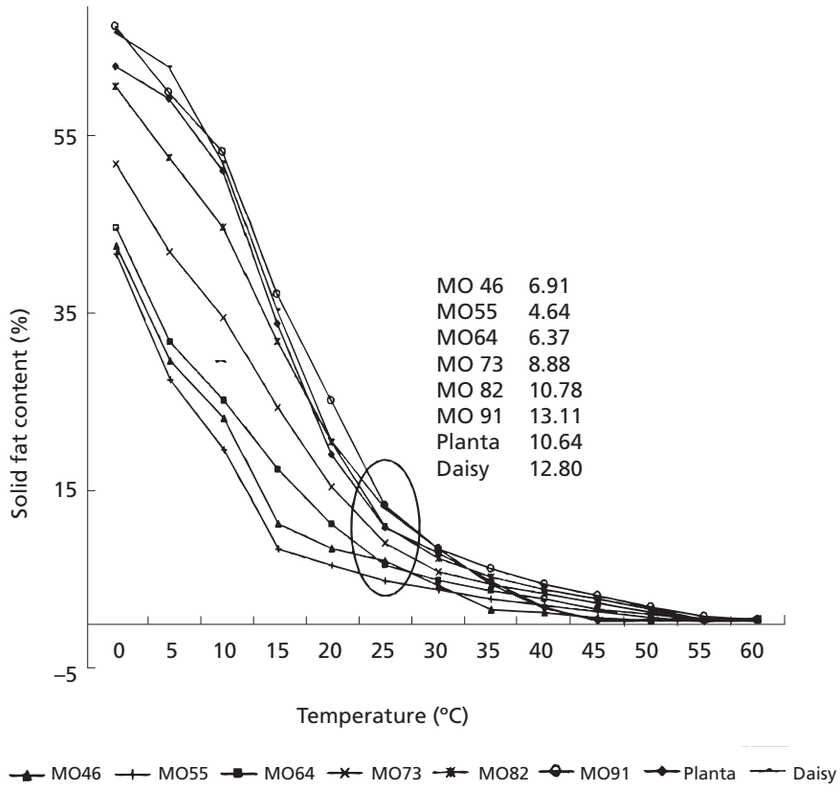

(M, medium- and long-chain triacylglycerols (MLCT); S, palm stearin; O, palm olein.)
Figure 1. Solid fat profiles of commercial and binary MLCT-enriched margarine formulations.

had the most similar SFC to the commercial margarines at 25ºC, and also due to the limitation of palm stearin (<15%) that could be incorporated into margarine formulations. The choice of lower proportions of MLCT feedstock blend (40%–50%) might require a higher percentage of palm stearin to be added to increase the SFC of MLCT-enriched margarine formulations at room temperature (25ºC). Palm olein was then substituted with 5%, 10% and 15% palm stearin in MO 64 and MO 73 formulations to shift the SFC of the MLCT-enriched margarine formulations at 25ºC as similar to commercial margarines. From the six ternary formulations developed, only two formulations of MOS 603010 and MOS 702010 showed SFC similar to commercial margarines (Figure 2). Solid fat of all ternary formulations completely melted at temperature 55ºC.

Heating Profiles

Figure 3 shows the heating curves of commercial and binary MLCT-enriched margarine formulations. The heating curves had numerous shoulders which were not separable from the peaks. The complex nature of fats and oils which comprised various types of TAG might associate to the numerous peaks. Samples containing palm olein, palm kernel olein and tallow fat showed curves with an overlap of melting ranges and numbers of peak shapes of all the fats and oils components (Jin *et al*. 2008). The heating thermograms of binary formulations were not much different with ternary heating curves (Figure 4). It may be due to the fact that only small amounts of palm olein were substituted with palm stearin. Moreover, palm olein and palm stearin are fractionated products of palm oil which had similar fatty acid and TAG types. The commercial margarines showed similar patterns of heating curves indicating similarity in the TAG profiles for both margarines. As shown in Table 3, complete melting and onset melting temperatures of the binary formulations increased from 51.04ºC to 57.93ºC and 3.90ºC to 17.43ºC, respectively as the percentages of MLCT feedstock blend were increased (40%–90%). The high complete melting and onset melting points of MLCT-enriched margarine binary formulations were related to the high proportion of LCSFA in MLCT feedstock blend (47.8%–55.1%), as depicted in Table 2. On the other hand, the onset melting and complete melting temperatures of Planta and Daisy margarines were –1ºC and 0ºC, and 32.74ºC and 33.04ºC, respectively which were lower than MLCT enriched-margarine binary formulations (Table 3).

In Figure 3, there were two endothermic peaks observed at temperatures between 8ºC and 20ºC (peaks ‘a’ and ‘b’)

paper 2.indd 117 1/20/2011 11:18:05 AM

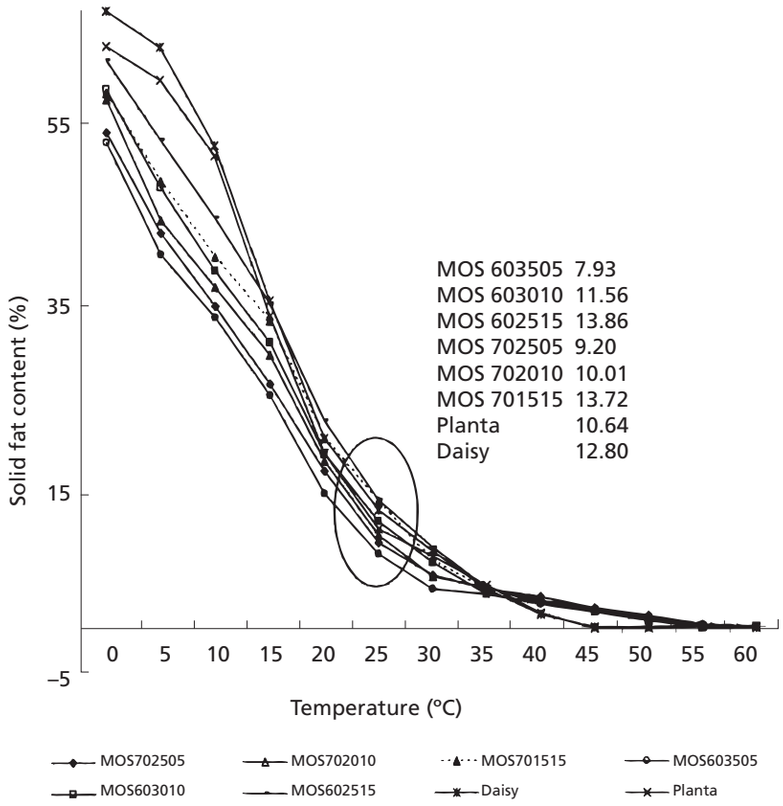

(M, medium- and long-chain triacylglycerols (MLCT); S, palm stearin; O, palm olein.)
Figure 2: Solid fat profiles of commercial and ternary MLCT-enriched margarine formulations.

on the thermograms of MO 46 and MO 55 formulations. However, these two peaks were not seen on MO 64, MO 73 and MO 91 formulations thermograms. This might be due to the solubility of higher melting peak glycerides of MLCT feedstock blend in the lower melting fraction of palm olein. Shi *et al.* (2005) stated that the disappearance of the original peaks indicated the formation of a solid solution composed of both high- and low-melting lipid classes due to the similarity in TAG molecules of the fat and oils components in the blends. Peaks 'a' and 'b' of MOS 603505 and MOS 701515 formulations were found to be sharp and narrow (Figure 4). The sharp peak indicated that all crystals in the formulations nucleated approximately at the same time (Humprey *et al.* 2003). As the proportion of substituted palm stearin increased, peaks 'a' and 'b' shifted to the higher temperature. Lee *et al.* (2008) suggested that the increment of melting peak temperature was associated with the formation of higher melting solid fat in the bakery shortening formulations with high palm stearin substitution.

From Table 3, the complete melting temperatures of the ternary formulations moved to the right corner (increase in temperature) as the percentages of palm stearin (5%–15%) were substituted in both MO 64 (53.97ºC–55.93ºC) and MO 73 (55.44ºC–57.07ºC) formulations. The increase in the amount of LCSFA might contribute to the increase in the complete melting point (Table 2). The substitutions of palm stearin (5%–15%) in the MO 64 and MO 73 binary formulations also increased the onset melting temperatures to 19.42ºC–19.72ºC and 20.15ºC–20.59ºC, respectively (Table 3).

The similarities in values ($P>0.05$) for melting peak temperatures between MO 46 and MO 55 margarine formulations were due to lower proportion of high-melting FA (myristic, palmitic and stearic acids) as compared to low-melting FA (capric, oleic and linoleic acids). On the contrary, significant ($P<0.05$) differences were found between these two formulations and MO 64, MO 73, MO 82 and MO 91 group formulations. The latter formulations had a higher percentage of high-melting FA compared to low-melting FA. The differences in amounts of high- and low-melting FAs in formulations were suggested to influence the melting peak temperatures.

paper 2.indd 118 1/20/2011 11:18:06 AM

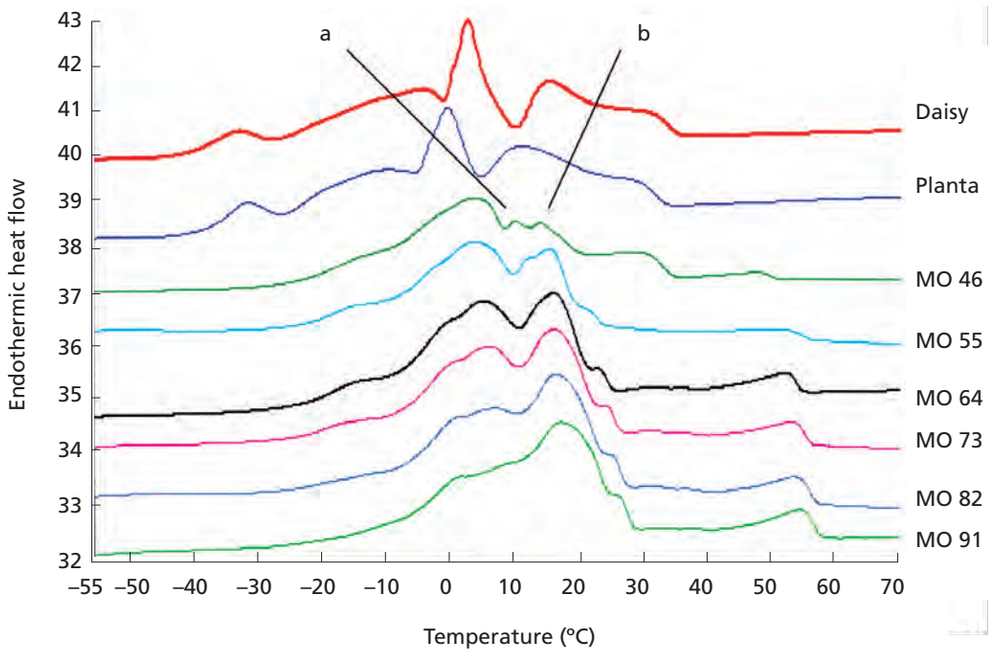

(M, medium- and long-chain triacylglycerol (MLCT); O, palm olein;
S, palm stearin; 'a' and 'b' endothermic peaks).
Figure 3. The heating curves of commercial and binary MLCT-enriched margarine formulations.

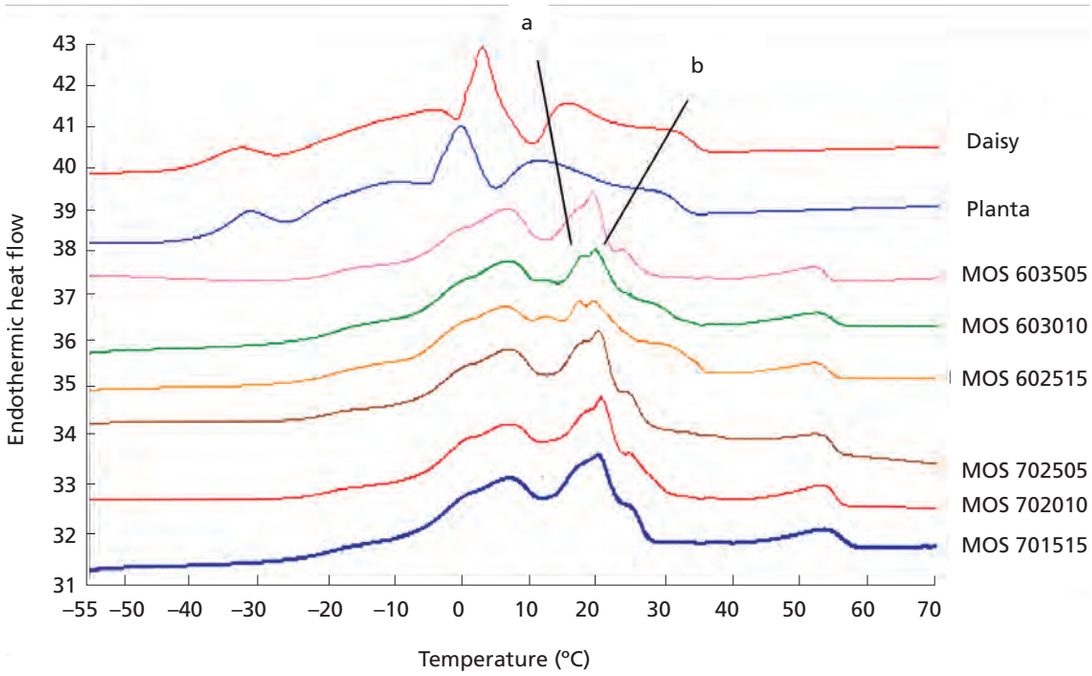

(M, medium- and long-chain triacylglycerol (MLCT); O, palm olein;
S, palm stearin; 'a' and 'b' endothermic peaks).
Figure 4. The heating curves of commercial and ternary MLCT-enriched margarine formulations.

paper 2.indd 119 1/20/2011 11:18:08 AM

Table 3. Peak and complete melting temperatures of binary and ternary MLCT-enriched margarine formulations [a].

Formulations [b]	Temperature (°C)	
	Onset melting	Complete melting
Planta	–1.00 ± 0.06	32.74 ± 0.04
Daisy	0.00 ± 0.05	33.04 ± 0.10
MO 46	3.90 ± 0.10	51.04 ± 0.12
MO 55	4.26 ± 0.08	56.42 ± 0.02
MO 64	16.34 ± 0.10	56.58 ±0.06
MO 73	16.46 ± 0.04	57.72 ± 0.10
MO 82	16.71 ± 0.12	57.86 ± 0.05
MO 91	17.43 ± 0.08	57.93 ± 0.11
MOS 603505	19.42 ± 0.16	53.93 ± 0.10
MOS 603010	19.59 ± 0.11	55.97 ± 0.15
MOS 602515	19.72 ±0.02	55.44 ± 0.02
MOS 702505	20.15 ± 0.08	55.44 ± 0.05
MOS 702010	20.22 ± 0.13	56.25 ± 0.11
MOS 701515	20.59 ± 0.10	57.07 ± 0.03

[a] Each value in the table represents the mean ± standard deviation of duplicate analyses.
[b] The fats and oil composition for each formulation are shown in Table 1.
Abbreviation: M, medium- and long-chain triacylglycerols (MLCT); S, palm stearin; O, palm olein.

Table 4. Textural properties of commercial and MLCT-enriched margarines[a].

Samples [b]	Hardness (g)		Adhesiveness (g sec^{-1})
	Force 1	Force 2	
Commercial	90.7b ± 0.34	83.8b ± 0.38	–121.1b ±0.26
MOS 603010	129.8a ± 0.51	106.5a ± 0.41	–171.5c ±0.40
MOS 702010	99.2b ± 0.48	78.8b ± 0.42	–133.2b ±0.48

[a] Each value in the table represents the mean ± standard deviation of triplicate analyses. Mean within each column with different letters are significantly ($p<0.05$) different.
[b] The fats and oil composition for each formulation are shown in Table 1.
Abbreviations: M, medium- and long-chain triacylglycerols (MLCT); S, palm stearin and O, palm olein.

Polymorphism

The polymorphism of the binary and ternary MLCT-enriched margarines formulations were determined by FTIR spectroscopy. This method was used due to its sensitivity towards molecular level structures of the polymorphic form of fats (Yano & Sato 1999). All the formulations showed a β′ crystal except for the formulation MO 46 which showed 'α' form. Low amount of higher-melting fats in the MO 46 formulations such as POO and OOO (unpublished data) did not lead to the formation of granular crystals in margarine as crystal nuclei. Consequently, no crystal growth could be observed. The formation of β′ crystals in most binary and ternary formulations were affected by the broad ranges of fatty acid chain lengths. de Man & de Man (1995) suggested that for an oil or fat to be in the β′-crystal from, it should have various numbers of fatty acid chain lengths.

Textural Properties

As shown in Table 4, the commercial margarine (Planta) showed lower values for hardness (Force 1 and Force 2) as compared to MLCT-enriched margarines. It indicated that commercial margarine was softer than the latter margarines. The higher values of hardness for margarine formulated with MOS 603010 compared to MOS 702010 margarine might be due to the high solid fat at the measured temperature. The values for Force 2 were lower than that of Force 1 due to the structural deformation of the margarines during the first compression. Even though the hardness 1 for commercial margarine was lower than for MOS 702010 margarine, Force 2 of the former margarine was lower than the latter. It suggested that the structure of the MLCT-enriched margarine was deformed excessively as compared to the commercial margarine. Adhesiveness value for commercial margarine was found to be the lowest followed by MOS 702010 and MOS 603010 margarines.

paper 2.indd 120 1/20/2011 11:18:08 AM

High adhesiveness values showed that the margarines were sticky. No significant differences (P>0.05) were found between commercial and MOS 702010 margarines for hardness (Force 1 and 2) and adhesiveness values.

The correlation study showed that the adhesiveness values of these margarines were highly correlated to the hardness values (force 1 and 2) with R^2 = 0.92 and R^2 = 0.99, respectively. There was positive correlation between hardness and SFC (R^2 = 0.81), and adhesiveness and solid fat content (R^2 = 0.80). The texture of margarine was influenced by SFC at that temperature (Chateris & Keogh 1991). Although Braipson-Danthine & Deroanne (2004) found a linear relationship between the firmness and SFC for several vegetables blends, they still believe that the hardness was also influenced by polymorphism and microstructure (Narine & Marangoni 1999).

CONCLUSION

Increment in MLCT feedstock blend percentage increased the solid fat content, onset melting and complete melting temperatures of the MLCT-enriched margarine formulations. These trends were due to an increase in the long chain saturated fatty acid proportion (myristic, palmitic and stearic acids) as the MLCT feedstock blend increased. FT-IR study showed that most of the MLCT-enriched formulations had β´-tending crystals. Margarine with formulations of MOS 603010 and MOS 702010 showing similar SFC to commercial margarines at 25ºC were chosen to produce margarine. The textural properties of the margarines were found to be highly correlated to solid fat content at 25ºC. MLCT-enriched margarines had harder and stickier texture as compared to commercial margarine. However, MOS 702010 and commercial margarines showed similar (P>0.05) values in hardness and adhesiveness.

ACKNOWLEDGEMENT

Financial support for this work from Golden Hope Sdn. Bhd. is gratefully acknowledged. The authors would like to thank Azmi and Mary Goh of MARDI for their kind technical assistance.

Date of submission: July 2009
Date of acceptance: June 2010

REFERENCES

AOCS American Oil Chemists' Society 1997, *Official methods and recommended practices of the American Oil Chemists' Society*, 4th edn, ed D Firestone, AOCS Press, Champaign, IL.

Aoyama, T, Nosaka, N & Kasai, M 2007, 'Research on the nutritional characteristics of medium-chain fatty acids', *The Journal of Medical Investigation*, vol. 54, pp. 385–388.

Arifin, N, Cheong, LZ, Koh, SP, Long, K, Tan, CP, Yusoff, MSA, Nor Aini, I, Lo, SK & Lai, OM 2009, 'Physicochemical properties and sensory attributes of medium- and long-chain triacylglycerols (MLCT) - enriched bakery shortening', *Food and Bioprocess Technology*, doi 10.1007/s11947-009-0204-0.

Braipson-Danthine, S & Deroanne, C 2004, 'Influence of SFC, microstructure and polyphorphism on texture (hardness) of binary blends of fats involved in the preparation of industrial shortening', *Food Research International*, vol. 37, pp. 941–948.

Chateris, W & Keogh, K 1991, 'Fat and oil in table spread', *Lipid Technology*, vol. 3, pp. 16–22.

Chrysam, MM 1985, 'Table spreads and shortenings', in Bailey's industrial oil and fat products, ed TH Applewhite, John Wiley and Sons, New York, vol. 3.

de Man, JM & de Man, L 1995, 'Palm oil as a component for high quality margarine and shortening formulations', in *Handbook No. 4, Malaysia Oil Science Technology (MOST)*, Kuala Lumpur.

Humphrey, KL, Moquin, PHL and Narine, SS 2003, 'Phase behavior of binary lipid shortening system: from molecules to rheology', *Journal of the American Oil Chemists' Society*, vol. 80, pp. 1175–1182.

Jin, Q, Zhang, T, Shan, L, Liu, Y & Wang, X 2008, 'Melting and solidification properties of palm kernel oil, tallow, and palm olein blends in the preparation of shortening', *Journal of the American Oil Chemists*' Society, vol. 85, pp. 23–28.

Karabulut, I, Turan, S & Ergin G 2004, 'Effects of chemical interesterification on solid fat content and slip melting point of fat/oil blends', *European Food Research Technology*, vol. 218, pp. 224–229.

Kasai, M, Nosaka, N, Maki, H, Negishi, S, Aoyama, T, Nakamura, M, Suzuki, Y, Tsuji, H, Uto, H, Okazaki, M & Kondo, K 2003, 'Effect of dietary medium - long chain triacylglycerols (MLCT) on accumulation of body fat in healthy humans', *Asia Pacific Journal of Clinical Nutrition*, vol. 12, pp. 151–160.

Koh, SP, Tan, CP, Lai, OM, Arifin, N, Yusoff, MSA & Long, K 2008, 'Enzymatic synthesis of medium- and long-chain triacylglycerols (MLCT): optimization of process parameters using response surface methodology', *Food and Bioprocess Technology*, doi 10.1007/s11947-008-0073-y.

Lai, OM, Low, CT & Akoh, CC 2005, 'Lipase-catalyzed acidolysis of palm olein and caprylic acid in a continuous bench-scale packed bed bioreactor', *Food Chemistry*, vol. 92, pp. 527–533.

Lee, JH, Akoh, CC & Lee, KT 2008, 'Physical properties of trans-free bakery shortening produced by lipase-catalyzed interesterification', *Journal of the American Oil Chemists' Society*, vol. 85, pp. 1–11.

Li, LK, Fehr, WR, Hammond, EG & White, PJ 1999, 'Trans-free margarine from highly saturated soybean oil', *Journal of*

paper 2.indd 121 1/20/2011 11:18:08 AM

the American Oil Chemists' Society, vol. 76, pp. 1175–1181.

List, GR 2004, 'Decreasing trans and saturated fatty acid content in food oils', Food Technology, vol. 58, pp. 23–31.

Litwinenko, JW, Rojas, AM, Gerschenson, LN & Marangoni, AG 2002, 'Relationship between crystallisation behaviour, microstructure, and mechanical properties in a palm oil-based shortening', *Journal of the American Oil Chemists' Society*, vol. 79, pp. 647–654.

Matsuo, T, Matsuo, M, Kasai, M & Takeuchi, H 2001, 'Effects of a liquid diet supplement containing structured medium- and long chain triacylglycerols on body fat accumulation in healthy young subjects', *Asia Pasific Journal of Clinical Nutrition*, vol. 10, pp. 46–50.

Matulka, RA, Noguchi, O & Nosaka, N 2006, 'Safety evaluation of a medium- and long-chain triacylglycerol oil produced from medium-chain triacylgycerols and edible vegetable oil', *Food and Chemical Toxicology*, vol. 44, pp. 1530–1538.

Moran, DPJ 1993, 'Reduced calorie spreads', in *PORIM Technology Palm Oil Research Institute Malaysia', Handbook No. 15*, Ministry of Primary Industries, Kuala Lumpur, Malaysia.

Narine, SS & Marangoni, AG 1999, 'Relating structure of fat crystal networks to mechanical properties: a review', *Food Research International*, vol. 32, pp. 1315–1319.

Nosaka, N, Suzuki, Y, Maki, H, Haruna, H, Ohara, A, Kasai, M, Tsuji, H, Aoyama, T, Okazaki, M & Kondo, K 2003a, 'Effects of ingestion of margarine containing medium-chain triacylglycerides for 4 weeks on blood parameters and postprandial thermogenesis', *Journal of Oleo Science*, vol. 52, pp. 571–581.

Nosaka, N, Maki, H, Suzuki, Y, Haruna, H, Ohara, A, Kasai, M, Tsuji, H, Aoyama, T, Okazaki, M, Igarashi, O & Kondo, K 2003b, 'Effects of margarine containing medium-chain triacylglycerols on body fat reduction in human', *Journal of Atherosclerosis and Thrombosis*, vol. 10, pp. 290–298.

Piska I, Zarubova, M, Louzecky, T, Karami, H & Filip, V 2006, 'Properties and crystallization of fat blends', *Journal of Food Engineering*, vol. 77, pp. 433–438.

Sandrou, DK & Arvanitoyannis, IS 2000, 'Low-fat/calorie foods: current state and perspectives', *Critical Reviews in Food Science and Nutrition* vol. 40, pp. 427–447.

SAS 2000, *SAS user's guide: statistic (version 8.2)*, SAS Institute Inc., Cary, North Carolina, USA.

Seriburi, V & Akoh, CC 1998, 'Enzymatic transesterification of triolein and stearic acid', *Journal of the American Oil Chemists' Society*, vol. 75, pp. 611–615.

Shi, Y, Liang, B & Hartel, RW 2005, 'Crystal morphology, microstructure and textural properties of model lipid systems', *Journal American Oil Chemists' Society*, vol. 82, pp. 399– 408.

Shinohara, H, Ogawa, A, Kasai, M & Aoyama, T 2005, 'Effect of randomly interesterified triacylglycerols containing medium-and long-chain fatty acids on energy expenditure and hepatic fatty acid metabolism in rats', *Bioscience Biotechnology and Biochemistry*, vol. 60, pp. 1811–1818.

TA.XT Plus Application Study 2006, *Measurement of firmness of margarine*, Stable Micro Systems Ltd., Godalming, Surrey,UK.

Yankah, VV & Akoh, CC 2000, 'Lipase catalyzed acidolysis of tristearin with oleic or caprylic acids to produce structured lipids', *Journal of the American Oil Chemists' Society*, vol. 77, pp. 495–500.

Yano, J & Sato, K 1999, 'FT-IR studies on polymorphism of fats: molecular structures and interactions', *Food Research International*, vol. 32, pp. 249–259.

Zainal, Z & Yusoff MSA 1999, 'Enzymatic interesterification of palm stearin and palm kernel olein, production of structured lipid containing oleic and palmitic acids in organic solvent free system', *Journal American Oil Chemists' Society*, vol. 76, pp. 1003–108.

paper 2.indd 122 1/20/2011 11:18:08 AM

ASM Sci. J., **4(2)**, 123–132

Expression of Receptor-interacting Protein (RIP 140) in Zebrafish Tissues and Embryonic Stages

P.H. Teoh[1], M.K. Kuah[1], P.S. Lim[1], T.S.T. Muhammand[2,3], N. Najimudin[1,4] and A.S.C. Chien[1,2]*

The receptor-interacting protein 140 (RIP 140) is a well known nuclear repressor and has been shown to be crucial for female reproduction and metabolism. However, the function of this repressor in developmental processes is still unknown. We conducted a study to investigate the expression patterns of RIP 140 in developing zebrafish embryos. Semi-quantitative RT-PCR analysis revealed that RIP140 was highly expressed in the eye, swim bladder, reproductive and metabolic organs of adult zebrafish. During embryogenesis, RIP 140 mRNA was continuously expressed throughout all the developmental stages with the highest expression at 24 hours of post-fertilization (hpf). Furthermore, *in situ* hybridization whole-mounts revealed that the expression of this gene was mainly localized in the eyes, mid-brain, pectoral fin buds and somites. Therefore, this present study has provided a starting point for future investigations to examine the role of RIP 140 in the development of these organs.

Key words: nuclear repressor; female reproduction; metabolism; embryogenesis; post-fertilization; *in situ* hybridization; whole-mounts; eyes; mid-brain; pectoral fin buds; somites; organ development

Nuclear receptors are ligand-activated transcription factors which subsequently bind to specific responsive elements located in the regulatory regions of target gene promoters. In this way, transcription is activated using both a constitutive amino-terminal and a ligand-dependent carboxyl terminal. In this context, recruitment of co-factors is an important element in regulating the stability of the transcription initiation complex or in changing the chromatic structure. While a number of such recruitments will activate transcriptional activities, repressors are also vital in the regulation of transcription through the exertion of an inhibitory effect on transcription initiation.

Receptor-interacting protein 140 (RIP 140), also known as nuclear receptor-interacting protein 1 (NRIP 1), is a known repressor of many nuclear receptors (Treuter *et al*. 1998; Lee & Wei 1999). Findings so far have revealed that the corepressor function of RIP 140 is regulated by the recruitment of histone deacetylases and the repressor C-terminal binding protein (Wei *et al.* 2000; Vo *et al.* 2001). The human RIP 140 protein comprises 1158 amino acids (Augereau *et al.* 2006). Studies have implicated the role of RIP140 in two major physiological processes —reproduction and metabolism. RIP 140-null female mice are infertile due to failure of the ovulation process, where mature follicles release oocytes (White *et al*. 2000). Upon further investigation, this failure is a result of ovary defect rather than perturbation of the hypothalamic-pituitary signaling. In addition to reproduction, studies have also shown the pivotal role in metabolism, with RIP 140-null mice showing an approximately 20% reduction of body weight as compared to wild type mice. A significant number of genes are upregulated and downregulated on either depletion or ablation of RIP 140, which further confirms the role of RIP 140 in repressing metabolic gene networks (Christian *et al.* 2006).

The zebrafish has rapidly gained status as a useful model for developmental biology. Attributes such as clarity of embryo and existence of useful molecular strategies such as large-scale genetic screening, mutagenesis, in situ hybridization and morpholino disruption have propelled the zebrafish as a useful model organism to complement the mouse in developmental biology (Kimmel *et al.* 1995; McGonnell & Fowkes 2006). At present, information on the role of RIP 140 in developmental processes is lacking as compared to its known roles in reproduction and metabolism. As a prerequisite to further unravel the role of RIP 140 during development, we describe here the cloning of a zebrafish RIP 140 cDNA fragment and proceed to examine its expression patterns in the selected adult tissues and developing embryos. Adult tissue expression

[1] School of Biological Sciences Universiti Sains Malaysia, 11800, Minden, Penang, Malaysia
[2]Malaysian Institute of Pharmaceuticals and Nutraceuticals, Sains@USM, Blok A, 10 Persiaran Bukit Jambul, 11900 Bayan Lepas, Penang, Malaysia
[3]Department of Biological Sciences, Universiti Malaysia Terengganu, 21030 Kuala Terengganu, Terengganu, Malaysia
[4]Centre for Chemical Biology, Universiti Sains Malaysia, 11800 Minden, Penang, Malaysia
*Corresponding author (e-mail: alex@usm.my)

paper 3.indd 123 1/20/2011 11:22:28 AM

profiles revealed the expression of this gene in the eye and swim bladder. Embryonic expression data localized the presence and identified the potential role of the zebrafish RIP 140 in the eye, mid-brain, pectoral fin bud and somite development.

MATERIALS AND METHODS

Animals

Wild-type zebrafish (*Danio rerio*) were maintained according to Westerfield (1994) in the fish facility of the Aquaculture Research Complex, Universiti Sains Malaysia. Embryos obtained through natural spawning were raised at 28.5°C and staged according to hours of post-fertilization (hpf) and morphological criteria (Kimmel *et al.* 1995).

Total RNA Isolation and Semi-quantitative RT-PCR Analysis

Total RNA was isolated from zebrafish embryo and adult fish tissue using TRI-Reagent® (Molecular Research Center, USA) as according to the manufacturer's instructions. For each single independent analysis, 100 embryos were collected for each age group and about 100 mg of tissue were pooled from 3–20 adult fish for each organ group. Concentration of the total RNA was determined by spectrophotometer analysis through A_{260}/A_{280} measurement and 2 µg of total RNA was treated with RQ1 RNase-Free DNase (Promega, USA). Treated RNA was then reverse transcribed to first-strand cDNA using M-MLV Reverse Transcriptase (Promega, USA) and Random Primers (Promega, USA) following the manufacturer's description.

The complete cDNA sequence of zebrafish RIP140 (XM_001341734) available from GenBank was used for primer design. Subsequently, a 488 bp cDNA fragment of zebrafish RIP 140 was amplified using gene-specific forward primer 5'-AAC TCC CAA CAG CAG CTC AC-3' and reverse primer 5'-GAG TCC TCT GGT GTG CCA AT-3', followed by cloning into pGEM®-T Easy Vector (Promega, USA) and sequencing. Sequence analysis revealed that the amplified cDNA fragment of RIP 140 was virtually 100% homologous to the published cDNA sequence of zebrafish RIP140 (XM_001341734). Therefore, this result verified the specificity of the primer set used in the semi-quantitative RT-PCR analysis.

For semi-quantitative RT-PCR analysis, zebrafish β-actin was included as an internal control. PCR amplification was performed in a final volume of 25 µl containing 2 µl of first-strand cDNA. The PCR program comprised an initial denaturation step at 94ºC for 1 min, amplification cycles at 94ºC for 30 s, 60ºC for 30 s and 72ºC for 30 s and a final extension step at 72ºC for 5 min. A negative control with water as the substitute of cDNA templates was included in each analysis to access any possible contamination. In total, the analysis was independently repeated for three times.

Equal amounts of PCR products were size-fractioned by 1.5% agarose gel stained with ethidium bromide. The amount of amplified cDNA was quantified by measuring the intensity emitted from the appropriate band using GeneTools software on the Gene Genius bio imaging system (Syngene, UK).

Whole-mount *in situ* Hybridization

The spatio-temporal expression pattern of zebrafish RIP 140 was analyzed by whole-mount *in situ* hybridization as previously described (Chai & Chan 2000). Digoxigenin (DIG)-labeled antisense and sense RNA probes for RIP 140 mRNA were synthesized using T7 or SP6 RNA Polymerase (Roche, Germany) with DIG RNA Labeling Mix, 10× conc. (Roche, Germany) according to the manufacturer's protocol. Embryos older than 18 hpf were incubated in 0.003% of 1-phenyl-2-thiourea to inhibit melanin formation.

RESULTS

Validation of semi-quantitative RT-PCR Analysis

A series of experimental optimizations had been carried out to quantify the gene expression levels accurately by ensuring the reactions were within the exponential phase of amplification. Samples were collected at different cycles and analyzed using GeneTools software (Syngene, USA). The readings of band intensity were converted to an amplification graph using GraphPad Prism v3.0 (GraphPad Software Inc., USA). Based on the constructed graphs, the half-maximal amplification cycles for zebrafish RIP 140 and β-actin were determined as 37 and 23, respectively (Figure 1).

Distribution of RIP 140 in Adult Tissue of Zebrafish

Due to the inconsistency in mRNA expression of β-actin among different adult tissue, a calculation method to adjust the expression of β-actin was used prior to the normalization of RIP 140 expression (Ings & Van Der Kraak 2006). Both the non-normalized raw input and the normalization with adjusted β-actin method showed similarity in the RIP 140 expression. Semi-quantitative RT-PCR analysis revealed that RIP 140 was widely distributed in various adult tissue of zebrafish. Relatively high expression of RIP 140 mRNA was detected in the ovary, testis and swim bladder, followed by moderate expression in the eye, brain, gill and liver (Figure 2). In tandem, a low level of RIP 140 transcript was expressed in heart, fin, muscle and intestine.

paper 3.indd 124 1/20/2011 11:22:29 AM

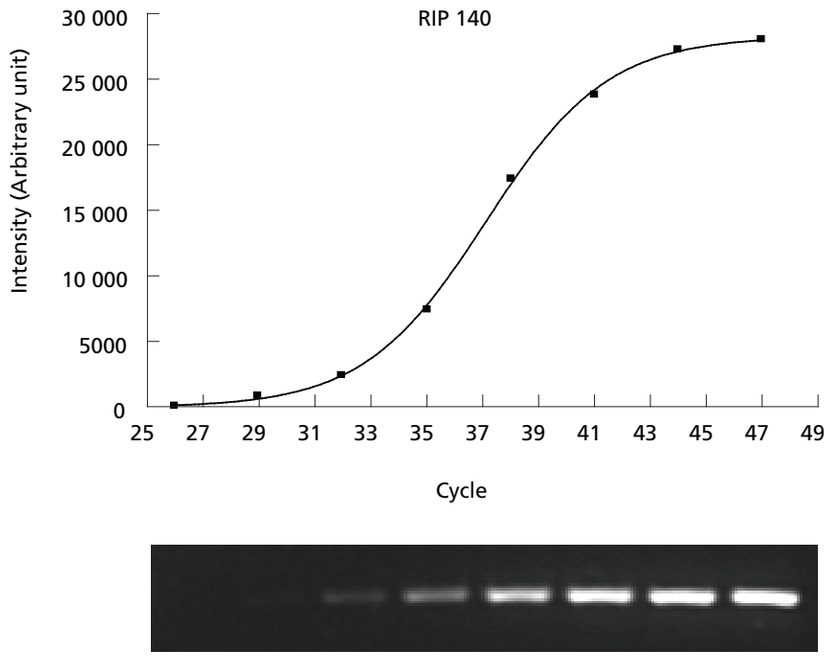

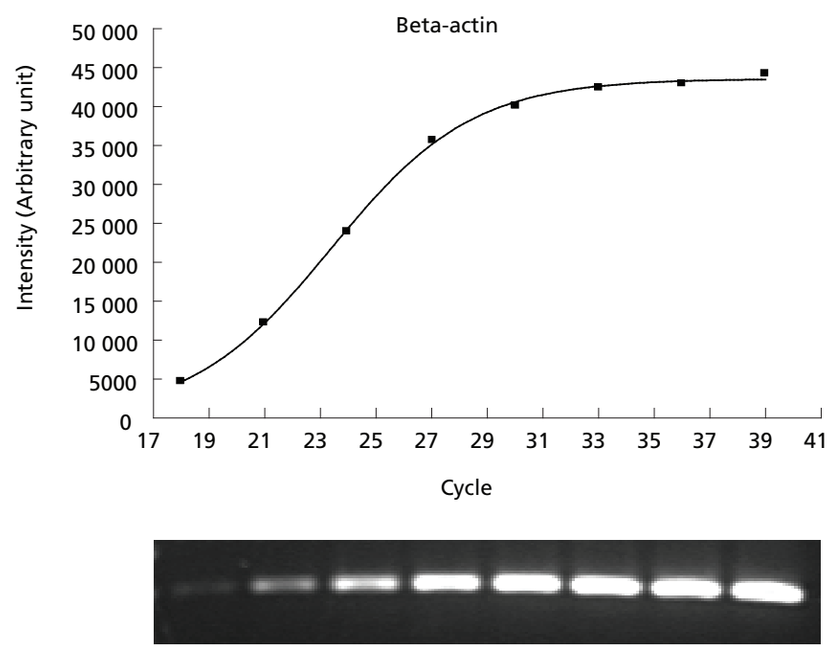

Figure 1. Kinetics of PCR amplifications with representatives of the electrophoretic images shown at bottom.

paper 3.indd 125 1/20/2011 11:22:29 AM

(A)

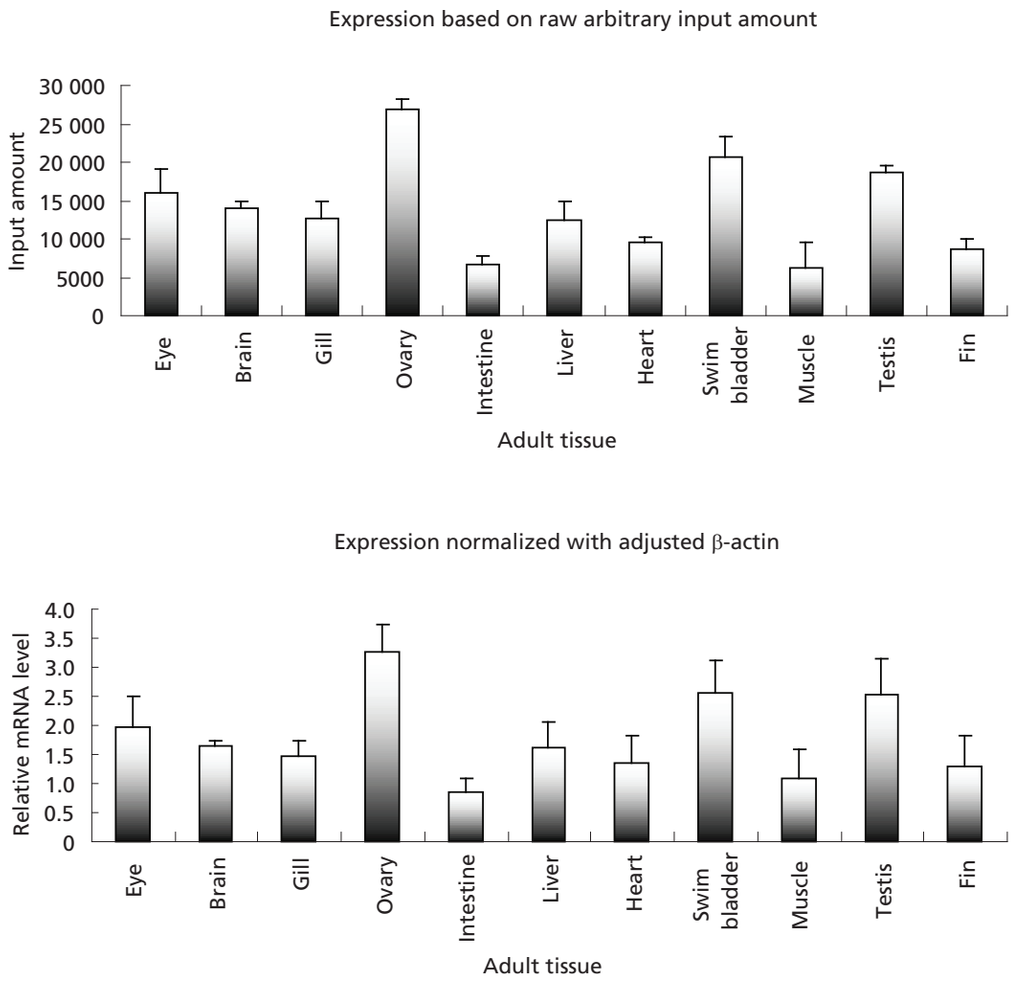

(B)

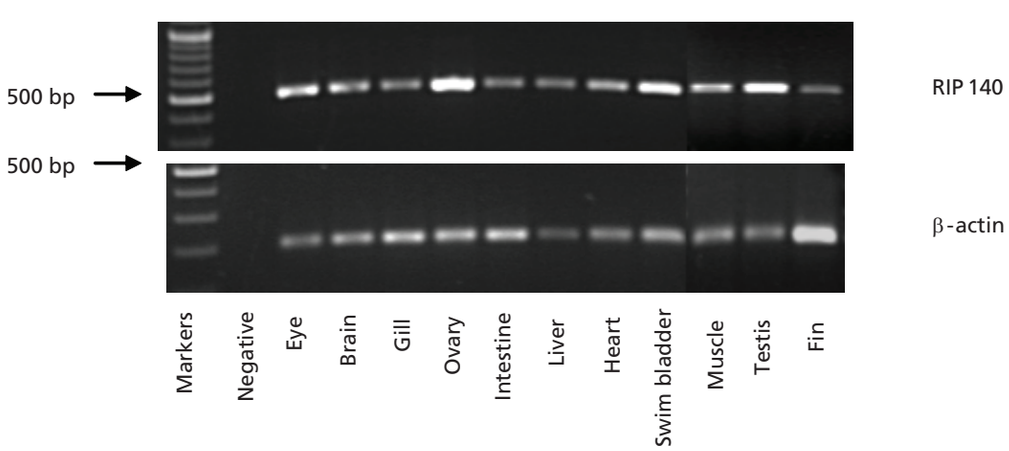

Figure 2. (A) Expression of RIP 140 in various adult tissue of zebrafish by semi-quantitative RT-PCR analysis based on raw input amount and after normalization to adjust β-actin value. Each bar represents mean ± SEM of 3 replicates. (B) Representative of the electrophoretic images of RT-PCR analysis, showing the expected band size of RIP140 (488 bp) and β–actin (201 bp).

Expression of RIP140 during Zebrafish Early Development

The RIP 140 transcripts were detectable starting from 0 hpf to 72 hpf, indicating that RIP 140 mRNA was continuously expressed throughout the early developmental stages (Figure 3). The highest level of RIP 140 transcript was observed at the 0 hpf stage, suggesting that a high amount of maternal mRNA RIP 140 was stored in the eggs while relatively low levels of RIP 140 mRNA were present at 6 hpf. The embryos started to express high levels of RIP 140 at 12 hpf and reached maximum levels at 24 hpf. Following this, the expression of RIP 140 gradually declined through the next 48 h, while maintaining a moderate level. It is noteworthy that these expression patterns were consistent with the results of whole-mount *in situ* hybridization. Figure 4 shows that RIP 140 transcripts were detected at the 1-cell stage (0 hpf) and the segmentation stage (11 hpf), but were very low at the glastula stage (6 hpf). During the segmentation period, RIP 140 was detected at the somites. At 24 hpf, a relatively strong expression of RIP 140 was found in the eye, mid-brain, pectoral fin bud and somite. At 36 hpf, the expression at mid-brain and pectoral fin buds remained high (Figure 5). At this stage, a high expression of RIP 140 was observed at the tectum but expression at the eye was reduced to a very low level. At 48 hpf, expression was restricted at the pectoral fins although a relatively low expression was also found at the hindbrain (Figure 6). At 72 hpf, expression was identified at the epiphysis and tegmentum, but expression at the pectoral fin disappeared (Figure 7).

DISCUSSION

The detection of RIP 140 transcripts in zebrafish and muscle is consistent with the known vital roles of these genes in metabolism (Parker *et al*. 2003; White *et al.*

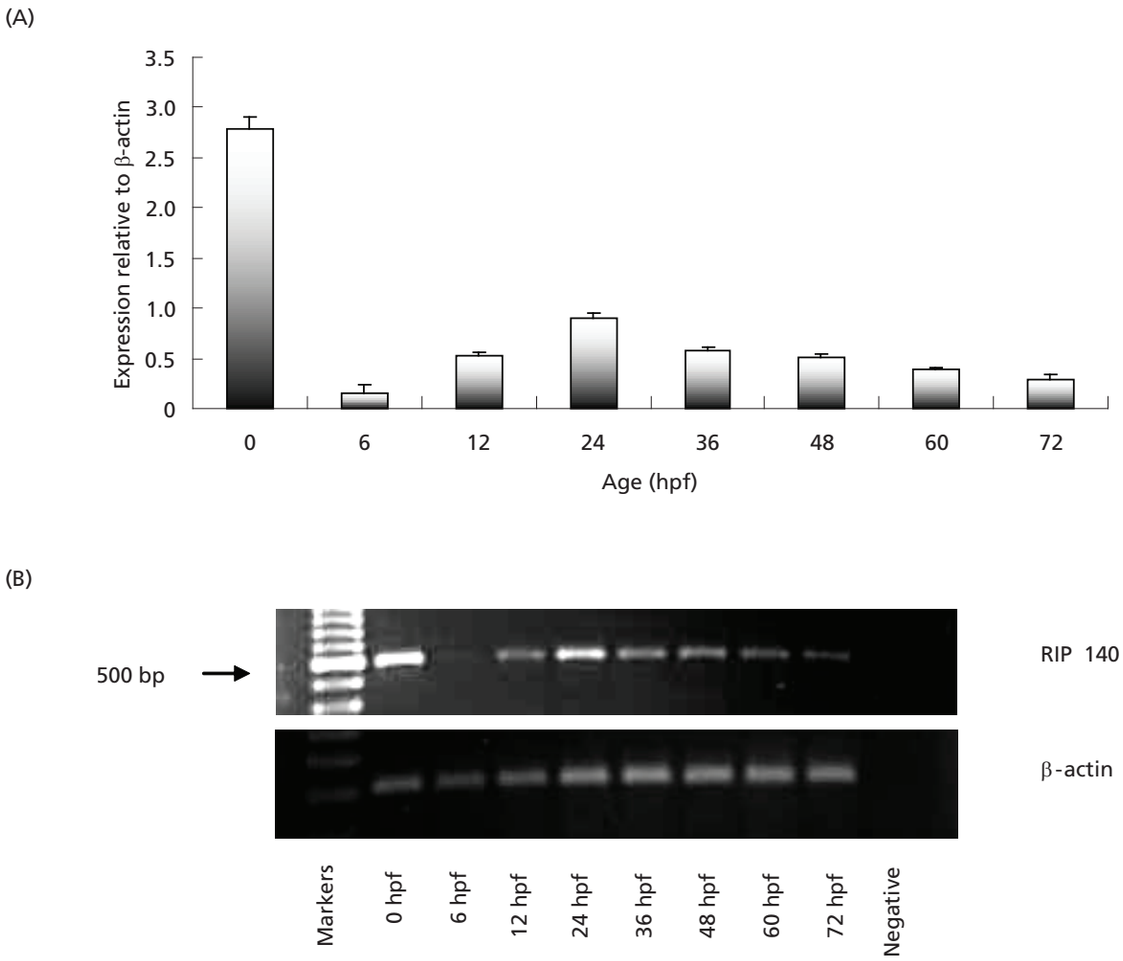

Figure 3. (A) Expression of RIP 140 during the zebrafish embryogenesis by semi-quantitative RT-PCR analysis. Each bar represents mean ± SEM of 3 replicates. (B) Representative of the electrophoretic images of RT-PCR analysis, showing the expected band size of RIP 140 (488 bp) and β–actin (201 bp).

paper 3.indd 127 1/20/2011 11:22:30 AM

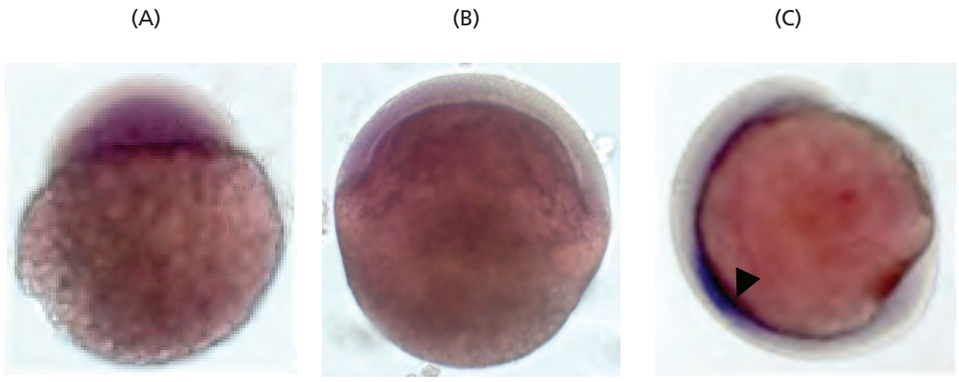

Figure 4. Expression of RIP 140 in developing zebrafish embryos. (A) 0 hpf embryo; (B) 6 hpf embryo; (C) 11 hpf embryo. Black arrow head: somite.

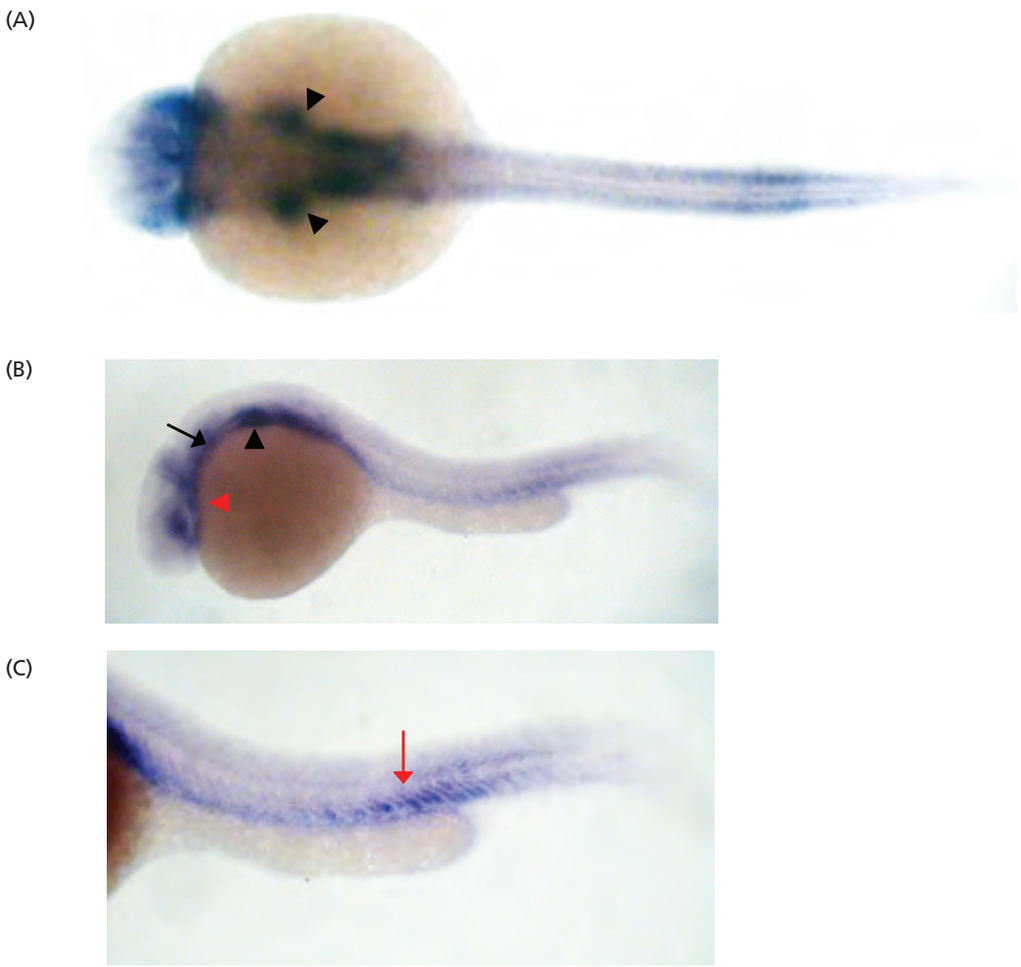

Figure 5. Expression of RIP 140 in developing zebrafish embryos. (A) 24 hpf embryo, dorsal view; (B) 24 hpf embryo, lateral view; (C) Trunk region. Black arrow head: pectoral fin bud; black arrow: hindbrain; red arrow head: eye; red arrow: somite.

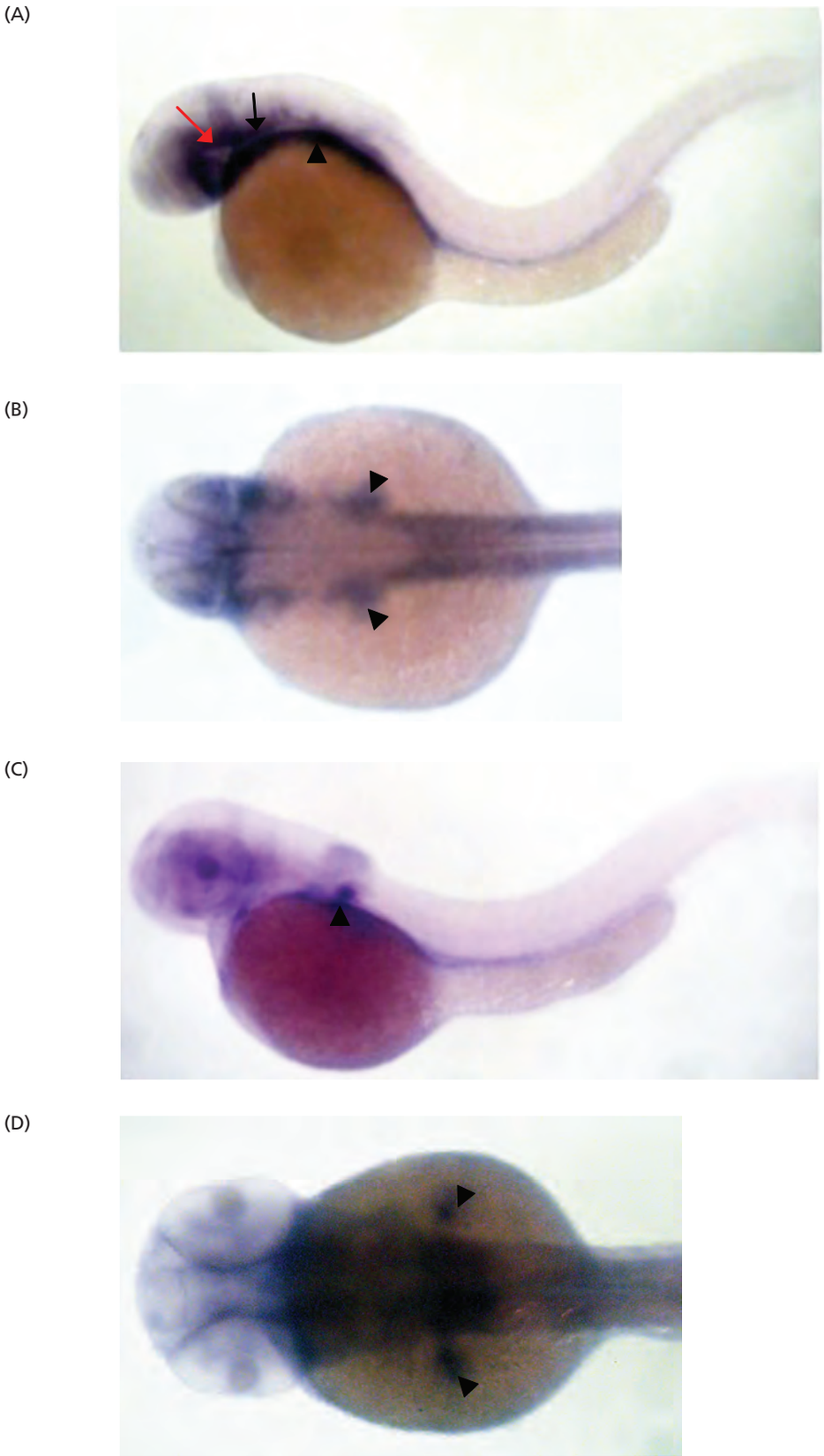

Figure 6. Expression of RIP 140 in developing zebrafish embryos. (A) 36 hpf embryo, lateral view; (B) 36 hpf embryo, dorsal view; (C) 48 hpf embryo, lateral view. Red arrow: tegmentum; black arrow: mid-brain, black arrow head: pectoral fin bud.

paper 3.indd 129 1/20/2011 11:22:35 AM

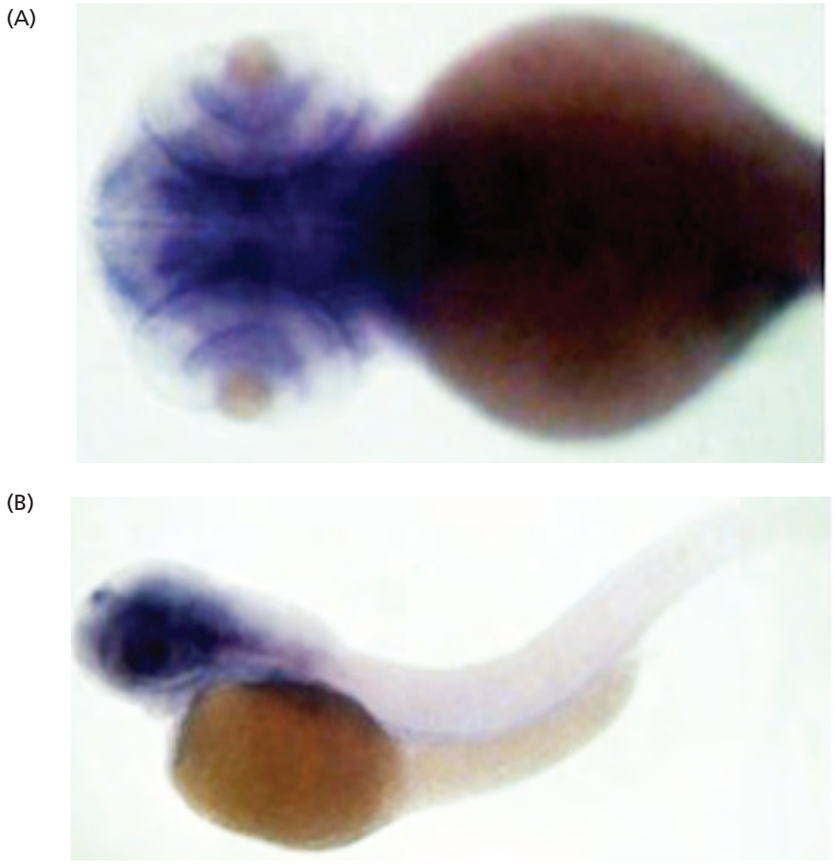

Figure 7. Expression of RIP 140 in developing zebrafish embryos. (A) 72 hpf embryo, lateral view; (B) 72 hpf embryo, dorsal view.

2008). A survey on mice tissue expression suggested that although expression of RIP 140 was widespread, it was primarily present in specific cell types at specific stages of development or hormonal control (White *et al.* 2000). In mice, RIP 140 appeared to regulate expression of lipogenic enzymes and prevented expression of key metabolic genes in white adipose tissue (Leonardsson *et al.* 2004). Furthermore, mice devoid of RIP 140 were smaller than their wild-type littermates, a phenomenon that could be partly due to reduction in white adipose tissue.

The detection of RIP 140 transcripts in the ovary of zebrafish is also in agreement with the known roles of RIP 140 in reproduction. RIP 140-null mice had been reported to be totally infertile due to failure of mature follicles to ovulate (White *et al.* 2000; Tullet *et al.* 2005). However, to-date, the underlying mechanisms involving RIP 140 signaling remain to be elucidated. Interestingly, it has been suggested that understanding the pathways governed by RIP 140 may even serve as a potential target for contraceptives development since impairment of its activities prevents oocyte release without adversely affecting other events related to the normal ovarian cycle (Parker *et al.* 2003). The zebrafish has been proposed as a viable model to understand folliculogenesis, or the process of oocyte development, where primary oocytes are recruited to go through the process of vitellogenesis, maturation and ovulation as eggs (Ge 2005). The zebrafish oocyte development can be categorised to about 5 stages based on size and microscopic appearance (Selman *et al.* 1993). In addition, a hormonal-dependent *in vitro* technique to enable spontaneous maturation of zebrafish oocytes has been developed (Selman *et al.* 1994). The detection of RIP140 in zebrafish oocytes in the present study and the known effect of RIP 140 in mammalian reproduction warrant future study to dissect the pathways regulated by RIP 140 in oocyte development, using the zebrafish as a model system.

At present, the role of RIP 140 in development is virtually unknown. Our expression study showed that the two major RIP 140 expression domains in zebrafish embryos were the developing fin and eye. The zebrafish pectoral fin is known to be an excellent model for the development of the mammalian forelimb since a large number of genes required for forelimb development have been shown to be crucial

paper 3.indd 130 1/20/2011 11:22:35 AM

for the morphogenesis of zebrafish pectoral fin (Mercader 2007). A major event in zebrafish fin development is the formation of the apical ectodermal ridge (AER) from the epidermis, initiated by signaling processes in the limb bud subsequent to the 24 hpf stage embryo. The genes required for the early stages of fin induction have been well-characterized and include signaling molecules such as *Wnt2b*, *Fgf24* and the T-box transcription factor, Tbx5 (Ng *et al*. 2002; Fischer *et al*. 2003). It will be interesting to investigate the existence of a possible interaction between RIP 140 and these major players of AER patterning. In addition, a possible mechanism explaining the involvement of RIP 140 in the development of pectoral fin bud could be via interaction with the retinoid acid receptors (RAR) as *in vitro* studies have shown interaction between these two groups of receptors (Christian *et al*. 2006). In zebrafish, the expression of RAR has been reported in the fin bud, brain and eye regions (Hale *et al*. 2006). In addition, retinoid signaling has also be reported to be pivotal in pectoral fin development (Gibert *et al*. 2006).

In conclusion, this present study showed that RIP 140 is highly expressed in the ovary, swim bladder and testis of adult zebrafish tissue. In addition, embryonic developmental patterns reveal the potential role of this gene in development of the pectoral fin, eye and brain region, providing useful insights for detailed future experiments.

ACKNOWLEDGEMENTS

We wish to thank the Academy of Sciences, Malaysia for funding this project under the Scientific Advancement Granting Allocation (SAGA), project no. M2-003-M50.

Date of submission: May 2008
Date of acceptance: June 2010

REFERENCES

Augereau, P, Badia, E, Carascossa, S, Castet, A, Fritsch, S, Harmand, PO, Jalaguier, S & Cavailles, V 2006, 'The nuclear receptor transcriptional coregulator RIP140', *Nuclear Receptor Signaling*, vol. 4, e024.

Chai, C & Chan, W-K 2000, 'Developmental expression of a novel Ftz-F1 homologue, *ff1b* (NR5A4), in the zebrafish *Danio rerio*', *Mechanisms of Development*, vol. 91, no. 1–2, pp. 421–426.

Christian, M, White, R & Parker, MG 2006, 'Metabolic regulation by the nuclear receptor corepressor RIP 140', *Trends in Endocrinology & Metabolism*, vol. 17, no. 6, pp. 243–250.

Fischer, S, Draper, BW & Neumann, CJ 2003, 'The zebrafish *fgf*24 mutant identifies an additional level of Fgf signaling involved in vertebrate forelimb initiation', *Development*, vol. 130, no. 15, pp. 3515–3524.

Ge, W 2005, 'Intrafollicular paracrine communication in the zebrafish ovary: the state of the art of an emerging model for the study of vertebrate folliculogenesis', *Molecular and Cellular Endocrinology*, vol. 237, no. 1–2, pp. 1–10.

Gibert, Y, Gajewski, A, Meyer, A & Begemann, G 2006, 'Induction and prepatterning of the zebrafish pectoral fin bud requires axial retinoic acid signaling', *Development*, vol. 133, no. 14, pp. 2649–2659.

Hale, LA, Tallafuss, A, Yan, YL, Dudley, L, Eisen, JS & Postlethwait, JH 2006, 'Characterization of the retinoic acid receptor genes*raraa*, *rarab* and *rarg* during zebrafish development', *Gene Expression Patterns*, vol. 6, no. 5, pp. 546–555.

Ings, JS & Van Der Kraak, GJ 2006, 'Characterization of the mRNA expression of StAR and steroidogenic enzymes in zebrafish ovarian follicles', *Molecular Reproduction and Development*, vol. 73, no. 8, pp. 943–954.

Kimmel, CB, Ballard, WW, Kimmel, SR, Ullmann, B & Schilling, TF 1995, 'Stages of embryonic development of the zebrafish', *Developmental Dynamics*, vol. 203, no. 3, pp. 253–310.

Lee, CH & Wei, LN 1999, 'Characterization of receptor-interacting protein 140 in retinoid receptor activities', *Journal of Biological Chemistry*, vol. 274, no. 44, pp. 31320–31326.

Leonardsson, G, Steel, JH, Christian, M, Pocock, V, Milligan, S, Bell, J, So, PW, Medina-Gomez, G, Vidal-Puig, A, White, R & Parker, MG 2004, 'Nuclear receptor corepressor RIP 140 regulates fat accumulation', *Proceedings of the National Academy of Sciences*, vol. 101, no. 22, pp. 8437–8442.

McGonnell, IM & Fowkes, RC 2006, 'Fishing for gene function — endocrine modelling in the zebrafish', *Journal of Endocrinology*, vol. 189, no. 3, pp. 425–439.

Mercader, N 2007, 'Early steps of paired fin development in zebrafish compared with tetrapod limb development', *Development, Growth & Differentiation*, vol. 49, no. 6, pp. 421–437.

Ng, JK, Kawakami, Y, Buscher, D, Raya, A, Itoh, T, Koth, CM, Esteban, CR, Rodriguez-Leon, J, Garrity, DM, Fishman, MC & Belmonte, JCI 2002, 'The limb identity gene *Tbx5* promotes limb initiation by interacting with *Wnt2b* and *Fgf10*', *Development*, vol. 129, no. 22, pp. 5161–5170.

Parker, M, Leonardsson, G, White, R, Steel, J & Milligan, S 2003, 'Identification of RIP 140 as a nuclear receptor cofactor with a role in female reproduction', *FEBS Letters*, vol. 546, no. 1, pp. 149–153.

Selman, K, Petrino, TR & Wallace, RA 1994, 'Experimental conditions for oocyte maturation in the zebrafish, *Brachydanio rerio*', *Journal of Experimental Zoology*, vol. 269, no. 6, pp. 538–550.

Selman, K, Wallace, RA, Sarka, A & Qi, X 1993, 'Stages of oocyte development in the zebrafish, *Brachydanio rerio*', *Journal of Morphology*, vol. 218, no. 2, pp. 203–224.

Treuter, E, Albrektsen, T, Johansson, L, Leers, J & Gustafsson, JA 1998, 'A regulatory role for RIP 140 in nuclear receptor

paper 3.indd 131 1/20/2011 11:22:35 AM

activation', *Molecular Endocrinology*, vol. 12, no. 6, pp. 864–881.

Tullet, JMA, Pocock, V, Steel, JH, White, R, Milligan, S & Parker, MG 2005, 'Multiple signaling defects in the absence of RIP 140 impair both cumulus expansion and follicle rupture', *Endocrinology*, vol. 146, no. 9, pp. 4127–4137.

Vo, N, Fjeld, C & Goodman, RH 2001, 'Acetylation of nuclear hormone receptor-interacting protein RIP 140 regulates binding of the transcriptional corepressor CtBP', *Molecular and Cellular Biology,* vol. 21, no. 18, pp. 6181–6188.

Wei, LN, Hu, X, Chandra, D, Seto, E & Farooqui, M 2000, 'Receptor-interacting protein 140 directly recruits histone deacetylases for gene silencing', *Journal of Biological Chemistry*, vol. 275, no. 52, pp. 40782–40787.

Westerfield, M 1994, *The zebrafish book: a guide for the laboratory use of the zebrafish* (Danio rerio), University of Oregon, Eugene OR, USA.

White, R, Leonardsson, G, Rosewell, I, Jacobs, MA, Milligan, S & Parker, M 2000, 'The nuclear receptor co-repressor Nrip1 (RIP 140) is essential for female fertility', *Nature Medicine*, vol. 6, no. 12, pp. 1368–1374.

White, R, Morganstein, D, Christian, M, Seth, A, Herzog, B & Parker, MG 2008, 'Role of RIP 140 in metabolic tissues: connections to disease', *FEBS Letters*, vol. 582, no. 1, pp. 39–45.

paper 3.indd 132 1/20/2011 11:22:35 AM

ASM Sci. J., **4(2)**, 133–141

Ambient Noise Reduction Using Improved Least Mean Square Adaptive Filtering

A.O.A. Noor[1]*, S.A. Samad[1] and A. Hussain[1]

In this paper, an improved method of reducing ambient noise in speech signals is introduced. The proposed noise canceller was developed using a computationally efficient (DFT) filter bank to decompose input signals into sub-bands. The filter bank was based on a prototype filter optimized for minimum output distortion. A variable step-size version of the (LMS) filter was used to reduce the noise in individual branches. The sub-band noise canceller was aimed to overcome problems associated with the use of the conventional least mean square (LMS) adaptive algorithm in noise cancellation setups. Mean square error convergence was used as a measure of performance under white and ambient interferences. Compared to conventional as well as recently developed techniques, fast initial convergence and better noise cancellation performances were obtained under actual speech and ambient noise.

Key words: Noise cancellation; adaptive filtering; LMS algorithm; filter banks; prototype filter; minimum output distortion; step-size; sub-band noise

Noisy environments such as streets, factories and noisy rooms can degrade speech communications significantly. The type of interference arriving from these sources is non-stationary in nature. In this context, recovering clean speech in a noisy acoustical environment has been a difficult task for many speech related applications such as hands-free telephony, hearing aids, video or teleconferencing, speaker identification and speech-controlled devices. These applications require clean speech to function properly. In the past few decades various algorithms have emerged, aimed at reducing the background noise from the target speech signal (Poularikas & Ramadan 2006). Among these algorithms is the least mean square LMS algorithm which is often used to adapt a full-band transversal filter with relatively low computation complexity and good performance (Vaseghi 2006). However, the conventional (LMS) solution suffers from significantly degraded performance with coloured interfering signals due to the eigenvalue spread of the autocorrelation matrix of the input signals (Haykin 2002, p. 425). Furthermore, the computational complexity increases as with the length of the adaptive filter. This can be a problem in applications such as acoustic noise and echo cancellation that demand long adaptive filters to model the noise path response. These issues are particularly important in applications where processing power must be kept as low as possible (Johnson *et al.* 2004). In recent literature, the issue of using filter-banks to improve the performance of adaptive filtering is considered from the view point of application to line echo cancellation in telecommunication systems (Mingsian *et al*. 2009), (Schüldt *et al*. 2008) and (Choiand & Bae 2007). In critically sampled filter banks, the presence of aliasing distortions require the use of adaptive cross filters between subbands (Kim *et al.* 2008; Petraglia & Batalheiro 2008). However, systems with cross adaptive filters generally converge slowly and have high computational cost, while gap filter banks produce spectral holes. The objective of the current work is to develop an improved sub-band noise cancellation system that is capable of removing ambient noise from speech signals.

METHODOLOGY

Commonly used noise cancellation schemes are based on the model that is depicted in Figure 1. This classical scheme was modified to sub-band configuration by the insertion of analysis and synthesis filter banks in the signal paths as shown in Figure 2. In the sub-band setup, the unknown noise path *P(z)* was estimated using a set of parallel, independently updated filters (k). For coloured input signals, with large eigenvalue spread such as speech and coloured noise, full-band (LMS) filters show slow convergence and degraded performance. In the sub-band case, the branch signals would have a flatter frequency amplitude spectrum and therefore improved convergence behaviour.

In sub-band systems, the design of alias-free and perfectly reconstructed filter banks require certain conditions to be

[1]Department of Electrical, Electronic and System Engineering, Faculty of Engineering and Built Environment, Universiti Kebangsaan Malaysia, 43600 Bangi, Selangor, Malaysia

*Corresponding author (e-mail: ali511@vlsi.eng.ukm.my)

paper 4.indd 133 1/20/2011 11:24:46 AM

met by the analysis and synthesis filters (Alhava & Renfors 2008). However, any filtering operation in the individual branches causes a possible phase and amplitude change and therefore alters the perfect reconstruction property. There are tradeoffs in controlling the aliasing effect and the amplitude distortion level to improve the overall performance in non-critically sampled filter banks (Cedric *et al*. 2006). Using downsampling factors of less than the number of channels i.e. oversampling, has the advantage of reducing the aliasing distortion of the sub-band system and permitting non-ideal filters to be used in signal decomposition. Referring to Figure 2, the analysis filters can be expressed as:

$$H_k(z) = \sum_{m=0}^{L-1} h_k(m) z^{-m} \tag{1}$$

where, k is the decomposition index, $h(m)$ is the impulse response of a finite impulse response filter (FIR), m is a time index, M is the number of sub-bands and L is the filter length. Defining $e(m)$ as the error signal and $y(m)$ as the output of the adaptive filter calculated at the downsampled rate (Dm), $\hat{w}(m)$ is the filter coefficient vector at m iteration, μ is the adaptation step-size factor, α is proportional to the inverse of the power input to the adaptive filter, then

$$y_k(m) = \hat{\mathbf{w}}_k^{\,T}(m)\mathbf{x}_k(m) \tag{2}$$

$$e_k(m) = v_k(m) - y_k(m) \tag{3}$$

$$\hat{\mathbf{w}}_k(m+1) = \hat{\mathbf{w}}_k(m) + \mu_k.\alpha_k.e_k(m)\mathbf{x}_k(m) \tag{4}$$

Equation 4 represents the branch update of the sub-band adaptive filters. With upper case letters representing the z-domain version of the discrete time domain signals, relation (3) can be expressed as:

$$E_k(z) = V_k(z) - Y_k(z) \tag{5}$$

The input/output relationship can be expressed as:

$$\hat{\mathrm{S}}_k(z) = \frac{1}{D}\sum_{k=0}^{M-1} G_K(z)U_k(z) \tag{6}$$

where, $U_k(z) = E_K(z^D)$

It can be shown that distortions due to insertion of filter banks can be expressed by the following input-output relationship:

$$\hat{\mathrm{S}}_k(z) = A_0(z)S(z) + \sum_{i=0}^{D-1} A_i(z)S(ze^{-j2i\pi/M}) \tag{7}$$

where,

$$\mathrm{A}_0(z) = \frac{1}{M}\sum_{k=0}^{M-1} G_K(z)H_k(z) \tag{8}$$

and

$$\mathrm{A}_i(z) = \frac{1}{D}\sum_{k=0}^{M-1} G_K(z)H_k(ze^{-2\pi i/D}) \tag{9}$$

for $i=1,2,\ldots D-1$. Here, $\mathrm{A}_0(z)$ represents the total distortion transfer function of the filter bank for the non-aliased component of the system input $S(z)$, while $A_i(z)$ represents aliasing distortion and determines how well the aliased components of the system are attenuated. In this work, a two-fold oversampled filter bank was utilized, therefore it was assumed that a sufficient sub-band separation did exist, and we concentrated on minimizing the total system

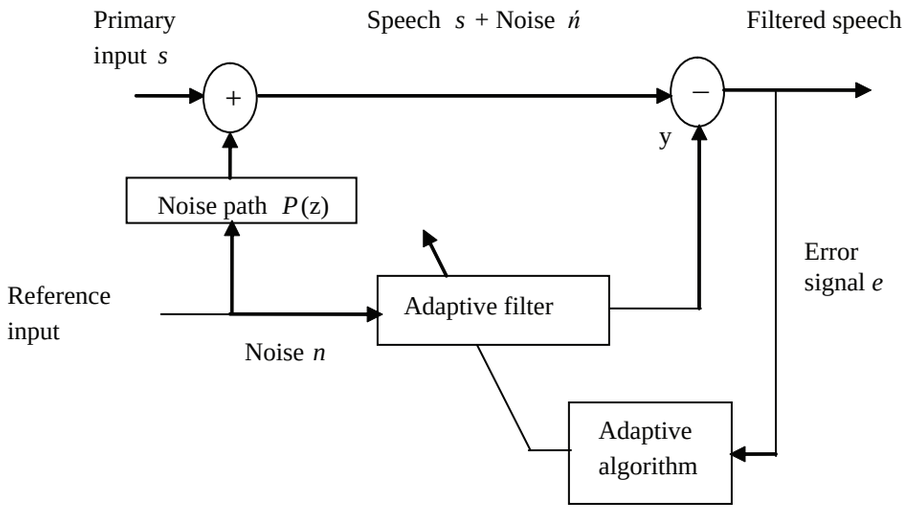

Figure 1. Conventional noise cancellation model.

paper 4.indd 134 1/20/2011 11:24:49 AM

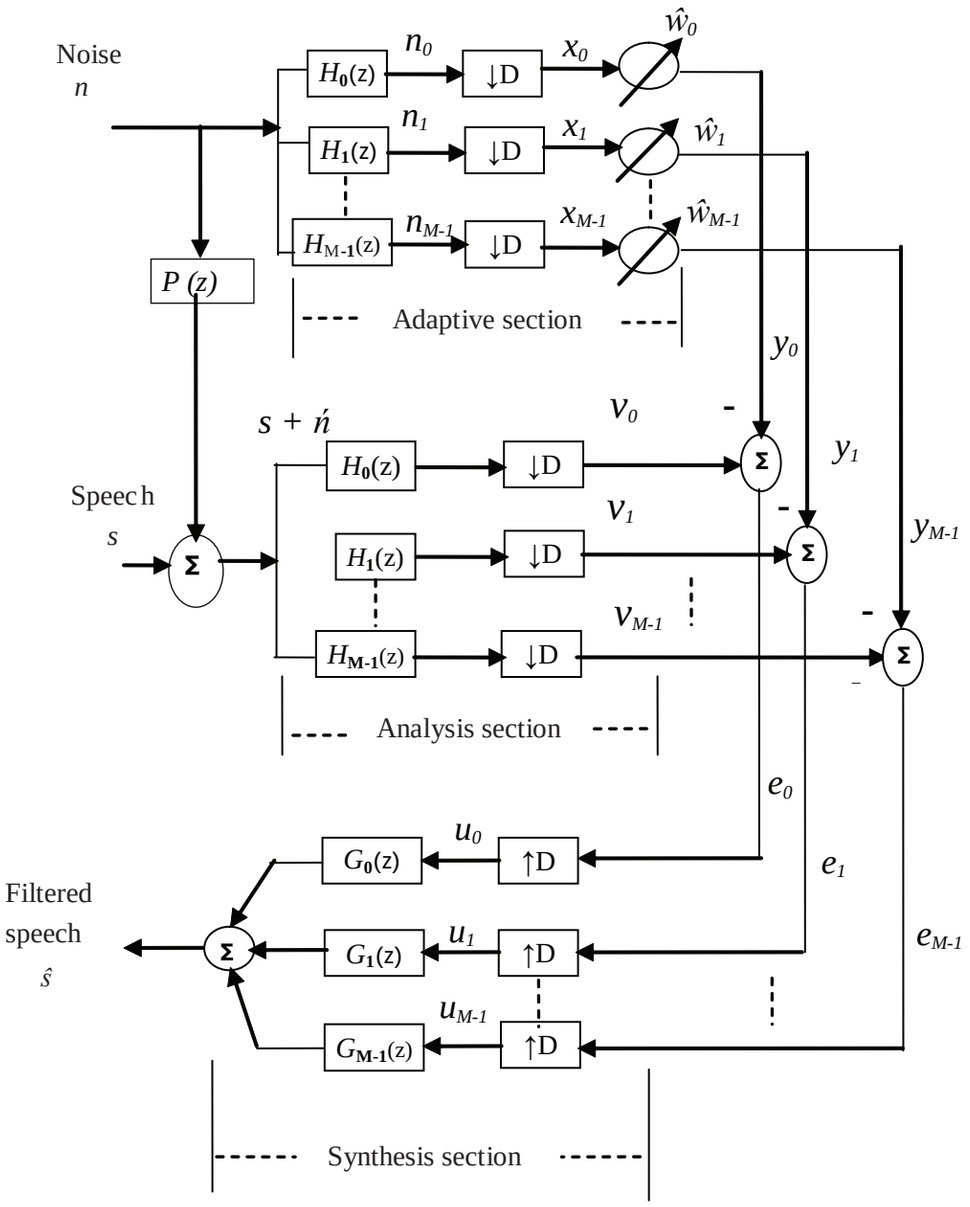

Figure 2. The proposed sub-band noise canceller.

distortion. The branch filters $H_K(z)$ and $G_K(z)$, could be derived from prototype filters $H_0(z)$, $G_0(z)$ according to:

$$H_k(z) = H_0(zW_M^k) \tag{10}$$

and,

$$G_k(z) = G_0(zW_M^k) \tag{11}$$

where $W_M = e^{-j2\pi/M}$

This way we obtained a discrete Fourier transform (DFT) filter bank (Viholainen *et al*. 2006). If we constrain $H_0(z)$ and $G_0(z)$ to be linear phase (FIR) filters, then Equation 8 becomes the amplitude distortion in the system equation. In frequency domain, $A_0(z)$ can be represented as:

$$A_0(e^{j\omega}) = \sum_{k=0}^{M-1} H_k(e^{j\omega})G_k(e^{j\omega}) \tag{12}$$

The aim was to find prototype filters $H_0(e^{jw})$ and $G_0(e^{jw})$ to minimize an objective function $A_0(e^{jw})$ according to:

$$A_d(e^{j\omega}) = \left| 1 - \left| A_0(e^{j\omega}) \right| \right| \tag{13}$$

paper 4.indd 135 1/20/2011 11:24:51 AM

$A_d(e^{jw})$ was evaluated over a dense grid of frequencies in the fundamental frequency range (0–½). For a given number of sub-bands M, a downsampling factor D and for a certain length of prototype filter L, we designed the normalized cut-off frequency $0<f<½$ and the corresponding window function. The Kaisar and the Dolph-Chebyshev windows have been reported to have good performance in the presence of aliasing (Cedric *et al.* 2006). However, these methods possess additional design parameters which should be controlled in the optimization problem. In this paper, we use the Hamming window, for simplicity.

The analysis filter bank was implemented efficiently as a tapped delay line with D- fold downsampling, followed by polyphase components of the prototype filter followed by fast Fourier transforms (FFT) (Vaidyanathan 1990). The synthesis bank was constructed in a similar fashion with inverse (FFT), the overall implementation is shown in Figure 3.

RESULTS AND DISCUSSION

Signal decomposition was produced using an eight-band discrete Fourier transform (DFT) filter bank, the magnitude frequency response of which is shown in Figure 4. This filter bank was constructed using a single prototype finite impulse response (FIR) filter that was optimized in a Hamming window function with an order of 128. Reconstruction and aliasing errors are depicted in Figure 5. It is clear from Figure 5 that the optimized filter bank had very low amplitude and aliasing distortions.

To examine the convergence behaviour of the proposed sub-band noise cancellation system, a linear chirp signal was used to provide full excitation to the system. This signal was corrupted with white Gaussian noise that had been convolved with an impulse response representing the noise path. The resulting noisy signal was then applied to the primary input of the sub-band noise canceller, while white Gaussian noise with zero mean and unit variance was applied directly to the reference input of the noise canceller. A variable step size sub-band version of the LMS algorithm was used for adaptation with the adaptation gain factor μ set to 0.08 in all branches. Mean square error MSE convergence was used as a measure of performance. Plots of MSE were produced and smoothed with a 200 point moving average filter. A comparison was made with a conventional full-band system as well as with a critically sampled system developed by Kim *et al*. 2008 as shown in Figure 6.

To test the behaviour under environmental conditions, a speech signal was then applied to the primary input of the proposed noise canceller. This speech was in the form of a Malay language utterance "Kosong, Satu, Dua, Tiga" as spoken by a woman, sampled at 16 kHz as shown in Figure 7. Engine noise was used as an ambient interference to corrupt this speech. MSE plots were produced as shown in Figure 8. A similar comparison as in Figure 6 was made in Figure 8.

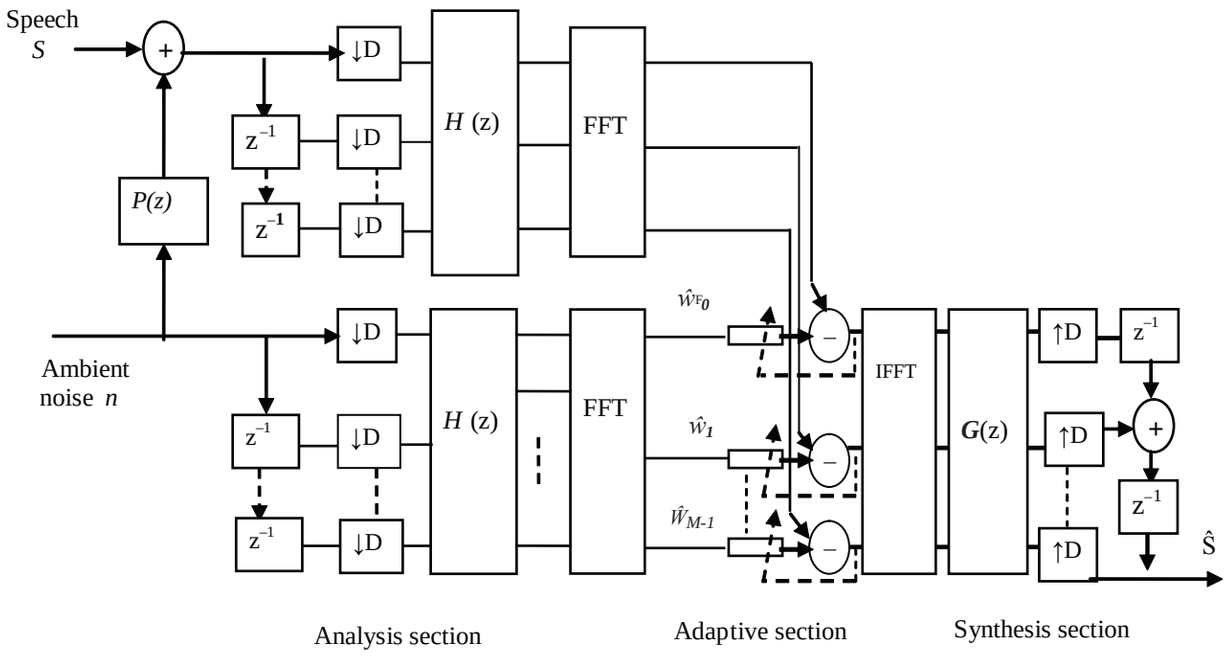

Figure 3. Efficient implementation of the ambient noise canceller.

paper 4.indd 136 1/20/2011 11:24:52 AM

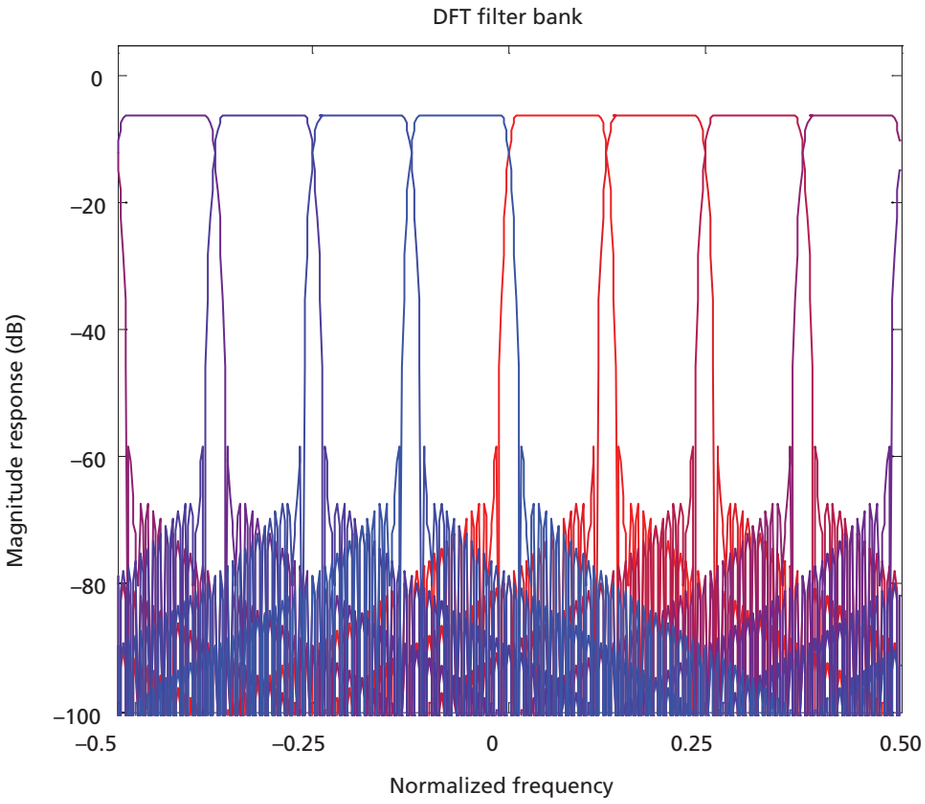

Figure 4. Magnitude frequency response of the filter bank used in the noise canceller.

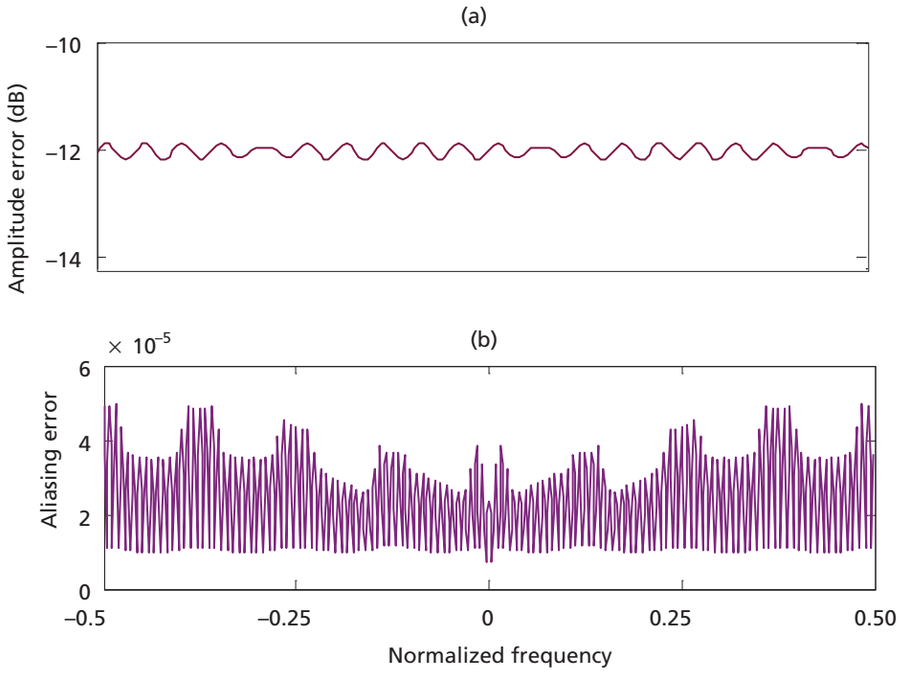

Figure 5. (a) Reconstruction error; (b) Aliasing error of the analysis filter bank.

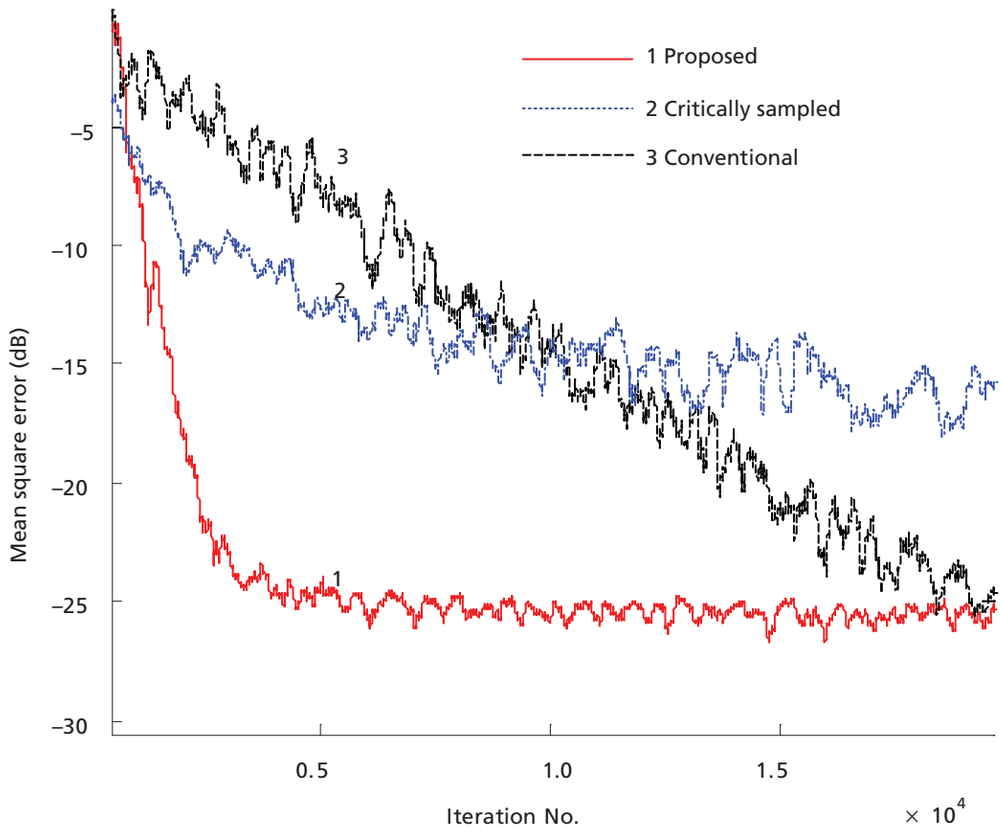

Figure 6. Mean square error performance of the proposed noise canceller compared to a critically sampled system developed by Kim *et al.* (2008) and a conventional full-band model under white noise.

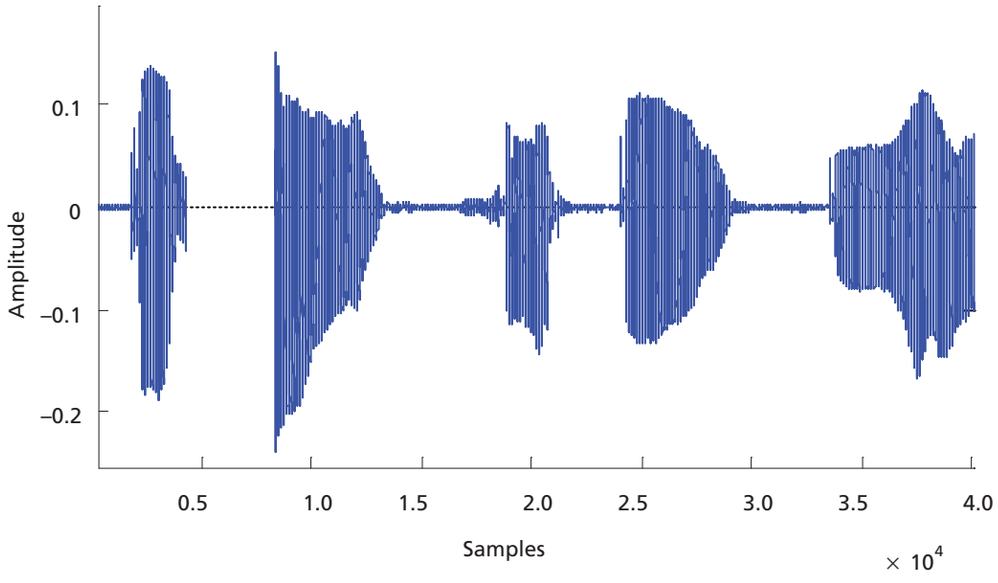

Figure 7. Malay utterance "Kosong, satu, dua, tiga" used in the tests.

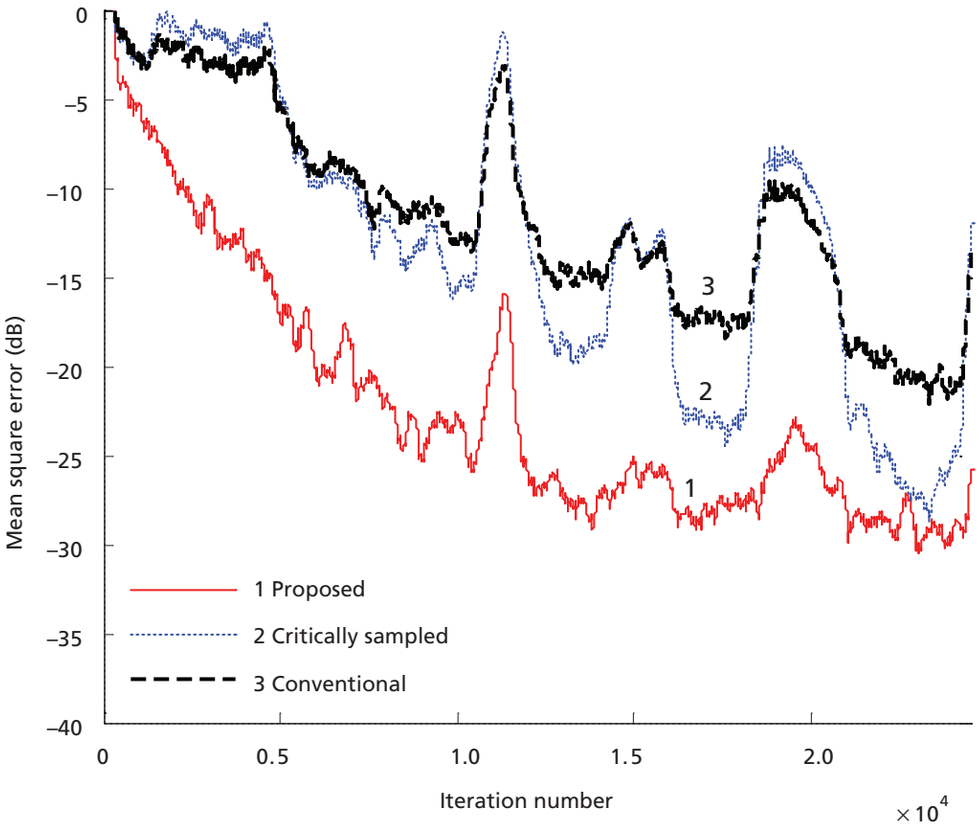

Figure 8. Mean square error performance comparison under actual speech and ambient noise.

From Figure 6, it is clear that the proposed oversampled system converges faster than both critically sampled and conventional full-band systems. While the full-band system was still converging slowly, the proposed noise canceller had removed 25 dB of the noise in about 5000 iterations. This increase in the convergence rate is of particular importance in environments where the impulse response of the noise path is changing over a shorter period of time than the initial convergence period, as in the case of speech communications where changes in the response of the path can result from the change of the speaker's head position or the movement of the noise source. In these cases, initial convergence plays a major role in cancellation quality. On the other hand, the recently developed critically sampled case (Kim *et al.* 2008) converges in a slow way, which is obviously due to the inability to model properly in the presence of aliasing. With two-fold oversampling, reduced aliasing levels are a tradeoff for extra computation costs.

It is obvious from Figure 8 that the conventional full-band noise canceller exhibits reduced modeling behaviour with ambient noise as the input to the adaptive filter. The amount of residual noise could be severely high if the input noise was highly coloured. It is evident from Figure 8 that the proposed system achieves a noise reduction improvement of about 10 dB compared to the conventional single rate full-band system and better behaviour than the critically sampled technique developed recently. Finally, as a demonstration of the success of the approach, the recovered Malay utterance is shown in Figure 9. A close inspection of this figure shows how the engine noise was removed from totally buried speech, the remaining noise at a steady state had of little or no effect on subjective hearing tests. Apart from the beginning of the sentence 'kosong' which was totally corrupted with engine noise, the rest of the sentence "satu dua tiga" was identified easily by average listeners.

CONCLUSION

In this work, a sub-band noise canceller with optimized oversampled (DFT) filter bank was developed to mitigate problems of slow convergence and increased computational complexity associated with conventional LMS noise cancellation schemes. A single prototype filter was optimized in a two-fold oversampled (DFT) filter bank

paper 4.indd 139 1/20/2011 11:24:53 AM

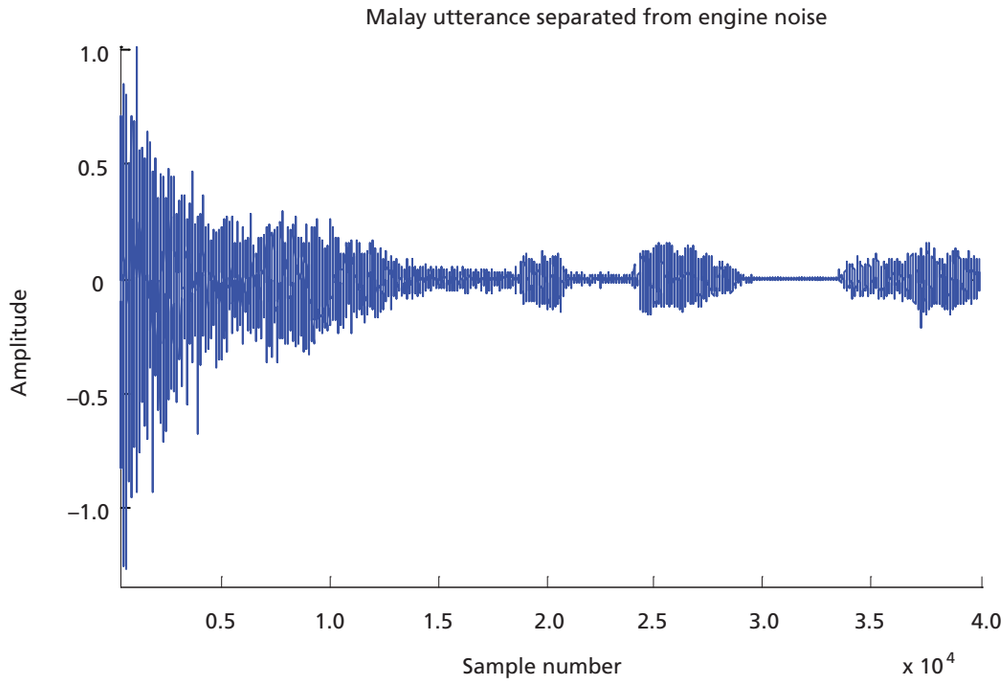

Figure 9. The recovered utterance.

and used in the noise canceller. Efficient implementation was obtained using polyphase components of the analysis and synthesis filters, and fast Fourier/inverse fast Fourier (FFT/IFF) transforms. To reduce the noise in the individual branches of the system, a variable step size version of the (LMS) algorithm was used for adaptation. The system showed better performance compared to the conventional full-band model as well as to a recently developed critically sampled scheme. The convergence behaviour under white and ambient noises was greatly improved. An increase in the amount of noise reduction by approximately 10 dB compared to the full-band model was achieved.

Date of submission: May 2009
Date of acceptance: August 2010

REFERENCES

Alhava, J & Renfors, M 2008, 'Prototype filter design for arbitrary delay exponentially modulated filter banks', in *Proceedings of ISCCSP 2008*, Malta, 12–14 March 2008, pp. 111–1114.

Cedric, KF, Grbic, N, Nordholm, S & Teo, KL 2006, 'A hybrid method for the design of oversampled, uniform DFT filter banks', *Elsevier Signal Processing*, vol. 86, pp. 549–557.

Choiand, H & Bae, HD 2007, 'Subband affine projection algorithm for acoustic echo cancellation system', *EURASIP Journal on Advances in Signal Processing*, vol. 2007, pp. 1–12.

Haykin, S 2002, *Adaptive filter theory*, 4th ed, Upper Saddle River, NJ. Prentice Hall. USA.

Johnson, J, Cornu, E , Choy G & Wdowiak, J 2004, 'Ultra low-power sub-band acoustic echo cancellation for wireless headsets', in *Proceeding of the 2004 IEEE International Conference Acoustics, Speech and Signal Processing V3*, pp. 57–60.

Kim, SG, Yoo, CD & Nguyen, TQ 2008. 'Alias-free sub-band adaptive filtering with critical sampling', *IEEE Transactions on Signal Processing*. Vol. 56, No. 5, pp. 1894–1904.

Mingsian, R, Yang, CK & Hur, KN 2009, 'Design and implementation of a hybrid sub-band acoustic echo canceller (AEC)', *Elsevier Journal of Sound and Vibration*, vol. 321, issues 3–5,April 2009, pp. 1069–1089.

Petraglia, MR & Batalheiro, P 2008, 'Nonuniform sub-band adaptive filtering with critical sampling', *IEEE Trans. Signal Processingy*, vol. 56, no. 2, pp. 549–557,

Poularikas, AP & Ramadan, ZM 2006. *Adaptive filtering primer with matlab*. Taylor & Francis Group, New York 2006.

Schüldt, C, Lindstrom, F & Claesson, I 2008, 'A low-complexity delayless selective sub-band adaptive filtering algorithm', *IEEE Trans. Signal Processing*, vol. 56, no. 22, pp. 5840–5850.

paper 4.indd 140 1/20/2011 11:24:54 AM

Vaidyanathan, PP 1990, 'Multirate digital filters, filter banks, polyphas networks, and applications: a tutorial', *IEEE Trans*. vol. 78, no. 1, pp. 56–93.

Vaseghi, VS 2006. *Advanced digital signal processing and noise reduction*. Third Edition, John Willey and Sons Ltd. West Sussex PO198SQ, England.

Viholainen, A, Alhava, J & Renfors, M 2006, 'Efficient implementation of complex modulated filter banks using cosine and sine modulated filter banks', *EURASIP Journal on Applied Signal Processing,* vol. 2006, Article ID 58564, 10 pages.

paper 4.indd 141 1/20/2011 11:24:54 AM

ASM Sci. J., **4(2)**, 142–148

Preliminary Characterization Study Based on Cyclic Voltammetry and Reliability of a Fabricated Au/Ti Microfluidic Three-electrode Sensor

I.H. Hamzah[1,2,3], A. Abd Manaf[1,2]* and O. Sidek[1,2]

A preliminary study was carried out to fabricate a three electrode system based on electrochemical sensoring. The cyclic voltammetry (CV) technique was chosen to select the type of metal suitable for evaporation and to compare the results produced from the fabricated gold electrode with the conventional macro-electrode system. The methodology and apparatus used involved low cost apparatus and methodology such as soft lithography, wet-etching, thermal evaporation, direct current sputtering, polymethylmethacrylate moulding and polydimethylsiloxane coating. The experiment was conducted at a fixed scan rate of 100 mV/s by using 0.01 M $K_3Fe(CN)_6$ in 0.1M KCl and well known method using Randles-Sevcik equation, peak current ratio and voltage separation was used to analyze the characterization on the fabricated sensors. Electrodes of 6.5 mm^2 and 0.26 mm^2 were fabricated to prove the adsorption effect of the reactant and the influence of the electrode area on the value of the peak current. CV analysis proved that the fabricated sensor was reliable for a range of 24 h at 25ºC room temperature.

Key words: microfluidic; PDMS; cyclic voltammetry; electrochemical; three-electrode systems; redox; evaporation; lithography; wet-etching; thermal evaporation; current sputtering; polymethylmethacrylate moulding; polydimethylsiloxane coating; Randles-Sevcik equation

Electrochemical

Electrochemistry is a branch of chemistry that studies chemical reactions which involve electron transfer between the electrode and the electrolyte in solution. A three electrode system consisting of a working electrode (WE), a reference electrode (RE) and a counter electrode (CE) is well known and used extensively in electrochemistry. An appropriate value of potential is applied at WE to facilitate the transfer of electrons, RE measures and controls the WE potential while CE supplies the appropriate current needed by WE.

The fundamental principle of all electrochemical sensors is the transfer of electrons to or from the conduction band of an electronic conductor (usually metal or carbon) to or from a redox active species at the electrode surface (Patel *et al*. 2007). Oxidation involves the loss of electrons from the highest occupied molecular orbital while reduction involves electrons being injected into the lowest unoccupied molecular orbital.

Recent developments in micro-fabrication influenced the design of the three-electrode system in micro-electrode size. A cost effective method such as soft lithography using thin film of photoresistant mask had expanded the micro-size design and gold (Au) fabrication technique on various material substrate. Morita *et al.* (1988) reported the use of Chromium (Cr) as an adhesive layer for Au deposition on the silicon wafer substrate and Triroj *et al.* (2006) introduced the adhesion layer of Titanium (Ti) for Au evaporation on the glass substrate.

Polydimethylsiloxane (PDMS)

Most microfluidic devices were made of glass and silicon (Knight *et al.* 1998) but recent trends have focused on the use of advanced materials such as polydimethylsiloxane (PDMS) that are flexible, durable and versatile yet low-cost in a research environment (McDonald & Whitesides 2002). PDMS offers an ability to be sealed reversibly and irreversibly on various kinds of materials such as PDMS itself (Duffy *et al*. 1998), silicon, glass and SiO_2.

[1]Collaborative Micro-electronic Design Excellence Centre (CEDEC), Universiti Sains Malaysia, Engineering Campus, 14300 Penang, Malaysia
[2]School of Electrical and Electronic Engineering, Universiti Sains Malaysia, Engineering Campus, 14300 Penang, Malaysia
[3]Faculty of Electrical Engineering, Universiti Teknologi MARA, Malaysia
*Corresponding author (e-mail: eeasrulnizam@eng.usm.my)

paper 5.indd 142 1/20/2011 11:29:09 AM

A reversible seal can be easily formed on glass but there is a possibility of leakage and seal reversal. An irreversible seal is needed to produce a robust microfluidic device. The method of forming an irreversible bond between the PDMS and glass is well documented in literature (Bhattacharya *et al*. 2005). It involves the activation of the PDMS surface by oxygen plasma, and the subsequent conformal contact of the glass and the PDMS surfaces. If both surfaces are relatively clean, the bond will be successful if the surfaces are pressed together for less than a minute after the plasma treatment.

Hydrophobic to Hydrophilic Property

An irreversible seal involves changing the property of PDMS from hydrophobic to hydrophilic (McDonald *et al*. 2000). A hydrophobic surface makes it difficult for polar solvents to wet the PDMS surface and may lead to adsorption of hydrophobic contaminants. Plasma oxidation can be used to alter the surface property by adding silanol (SiOH) groups to the surface. This treatment renders the PDMS surface hydrophilic. The method involves the treatment of either oxygen (O_2) itself or a mixture of nitrogen (N_2) and O_2 (Sperandio *et al*. 2010). The activated PDMS then adheres strongly and covalently to glass when brought into contact with it; creating an irreversible bond (Oh 2008). This irreversible sealing method was used in this research project to create the bonding between PDMS and the glass substrate.

METHODS AND APPARATUS

Electrode Design and Fabrication

Mask patterns were designed by using AutoCAD 2002. A film was used to print a positive mask (Hapmax (M) Sdn. Bhd Penang, Malaysia) for the mask patterns.

A glass slide was chosen as a base material for the sensor. It was first cleaned sequentially with acetone, then isopropanol and dried with nitrogen. DC sputtering (Auto 500: BOC Edwards) using 100% Ar, RF power at 210 W, vacuum pressure at 5×10^{-3} Torr and 2 min exposure produced 30 nm of Ti as an adhesion layer. Then a thermal evaporator (Auto 306: Edwards UK) of 6.0×10^{-5} mbar at 68A produced 1 um Au electrode layer.

The electrode layer was then spin-coated for 10 s with positive photoresistant material (PR1-500A: Futurrex Inc, USA). A positive mask (Hapmax (M) Sdn. Bhd Penang, Malaysia) was then put on the coating electrode layer and this was UV-exposed (OAI 150 Exposure Timer: Teltec HK) for 30 s. It was then patterned by using the wet etching technique of aqua regia, a mixture of nitric acid and hydrochloric acid in a volumetric ratio of 1:3, respectively. Similarly, the Ti layer was removed by using a mixture of H_2O, H_2O_2 and HF in a volumetric ratio of 20:1:1, respectively. It was then dried under nitrogen flow.

Mould Preparation

Hamzah *et al*. (2009) reported the use of polymethylmethacrylate (PMMA) as an alternative for glass or silicon as base material. This procedure and technique were used for this project. A PMMA of 1 mm thickness was cut into a square sized 1 cm $\times$ 1 cm with four side walls of 0.5 cm $\times$ 1 cm. The square PMMA and all the side walls were cleaned with isopropyl alcohol (IPA) and deionized (DI) water. All these were dried in an oven (UNB 200: Memmert GmbH & Co using a computer numerical controlled (CNC) machine (CCD 2: Bungard Elektronik GmbH & Co. KG). The PMMA cutting was again cleaned with isopropyl alcohol (IPA) and deionized (DI) water. Then it was dried in an oven (UNB 200: Memmert GmbH & Co. KG) at 90ºC for 30 min. These cuttings were merged together through the solvent bonding process (Lin *et al*. 2007) using chloroform.

PDMS Fabrication and Sealing

The PMMA mould was placed in a petri dish onto which PDMS (Dow Corning Sylgard 184) was poured. PDMS was mixed with the curing agent at a rate of PDMS:curing agent = 10:1. The PDMS was defoamed in a vacuum desiccator for 24 h. After that, the PDMS was peeled off from the petri dish.

Sealing Process

Before the bonding process, an electrode fabricated on a glass slide was cleaned by the following procedure. First, it was immersed in heptane solvent for 5 min, then rinsed with ethanol, dried with nitrogen and baked in an oven (E28: Memmert GmbH & Co. KG) at 110ºC for 5 min. The PDMS relief was immersed into ethanol, sonicated for 5 min and fully dried with nitrogen. Then the PDMS relief and the electrode pattern on the glass slide were exposed to oxygen plasma in the ICP-RIE chamber (Plasmalab 80 Plus: Oxford Instruments) with the pressure at 50 mtorr, oxygen flow rate of 10 sccm for an exposure time of 2 min at 120 W RF power. After taking the PDMS relief and the electrode pattern on the glass slide out of the chamber, the PDMS relief are then quickly aligned and sealed to the glass slide. Figure 1(a) shows the final fabricated Au three-electrode cell after the PDMS was irreversibly assembled on glass slide while the graphical cross sectional view was as shown in Figure 1(b).

Apparatus for experiments

The instrument consists of a custom-built potentiostat (EC epsilon: BASi Analytical Instruments) with a computer-controlled user interface and miniature alligator clips

paper 5.indd 143 1/20/2011 11:29:09 AM

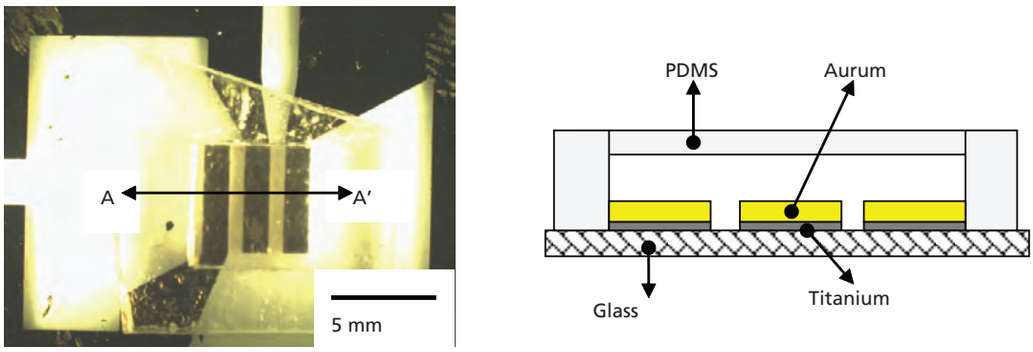

Figure 1. (a) Fabricated Au electrode with PDMS coating; (b) Cross-sectional structure view A–A′.

soldered to insulate three colour-coded electric cables. The data of the cyclic voltammetry technique was captured and analyzed using DigiSim Simulation Software (BASi Analytical Instruments).

The supporting electrolyte of 0.1 M KCl was added to the 10 mM $K_3Fe(CN)_6$ solution. Without further cleaning, the PDMS container was loaded with the solution using the syringe pump.

RESULTS AND DISCUSSION

CV Analysis

A start-up experiment had been conducted to investigate the performance of various kinds of metals based on cyclic voltammetry technique as shown in Figure 2. The range of potential voltage was set to be –1V to +1V. Six kinds of metal, which were aluminium (Al), zinc (Zn), Au, platinum (Pt), silver (Ag) and copper (Cu) had been analyzed as standard electrodes of 0.5 mm diameter in the electrolyte 0.1M KCl. The reactant used was 10 mM $K_3Fe(CN)_6$ in which the redox system occurs as :

$$\underset{\text{Ferricyanide (Reactant)}}{Fe^{3+} + e^-} \rightleftharpoons \underset{\text{Ferrocyanide (Product)}}{Fe^{2+}}$$

Figure 3 shows the cyclic voltammetry results for these metals. From the plotted CV, it is obvious that Au produced the triangular curve at both sides, which shows the convincing pattern for redox reaction. Therefore, Au was selected to be used for the sensor fabrication. Another reason of Au selection was because the final product to be developed was a sensor device for DNA hybridization detection. Au had been used widely and found to be suitable for DNA immobilization in the previous research. Lee & Lee (2004) reported that oligonucleotides with thiol group having a short length of N-alkyl chain (C1-C4) were found to have the most stable immobilization on Au wettability surface. The finding had been used by Choi *et al.* (2005, p. 379) in their integrated multichannel electrochemical DNA sensor.

Analysis results of the CV on the fabricated Au electrodes as compared to the conventional electrochemistry macroelectrode system is as shown in Figure 4. The peak-shape voltammograms of fabricated electrode is similar to the Au three electrode conventional macroelectrode system. Choi *et al* (2005, p. 381) and Triroj *et al.* (2006, p. 1399) produced similar CV results for the multichannel fabricated Au with the same reactant (ferricyanide), the same electrolyte (KCl) and the same scan rate of 100 mV/s.

The fabricated Au electrode was left at the room temperature of 25ºC for reliability tests. It was left hooked to the potentiostat for 24 h. The CV measurement graph is as shown in Figure 5. All the measurements were done at the scan rate of 100 mV/s.

The decrement in peak current, I_p was due to the Au erosion in the electrolyte. The erosion caused the area of electrode size to decrease thus influencing the value of peak current to decrease. The difference in the peak current, I_p could be explained by Randle-Sevcik (Bard & Faulkner 1980) as in Equation 1:

$$I_p = (2.69 \times 10^5) n^{3/2} A D^{1/2} C v^{1/2} \quad \ldots 1$$

where I_p is the peak current (in ampere), n is the electron stoichiometry, A is the electrode area (in centimeter square), D is the diffusion coefficient (in centimeter square per second), C is the concentration of the electroactive species (in moles per centimeter cubic) and v is the scan rate (in volts per second). From this relationship, it is observed that I_p is proportional to the area size of the electrode, A when all the other parameters were fixed.

paper 5.indd 144 1/20/2011 11:29:09 AM

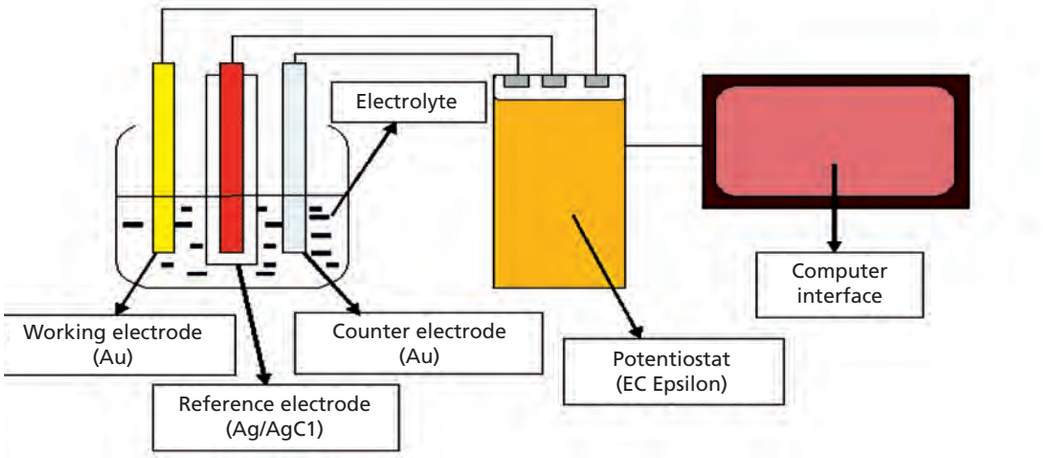

Figure 2. Conventional macro-electrode electrochemical system.

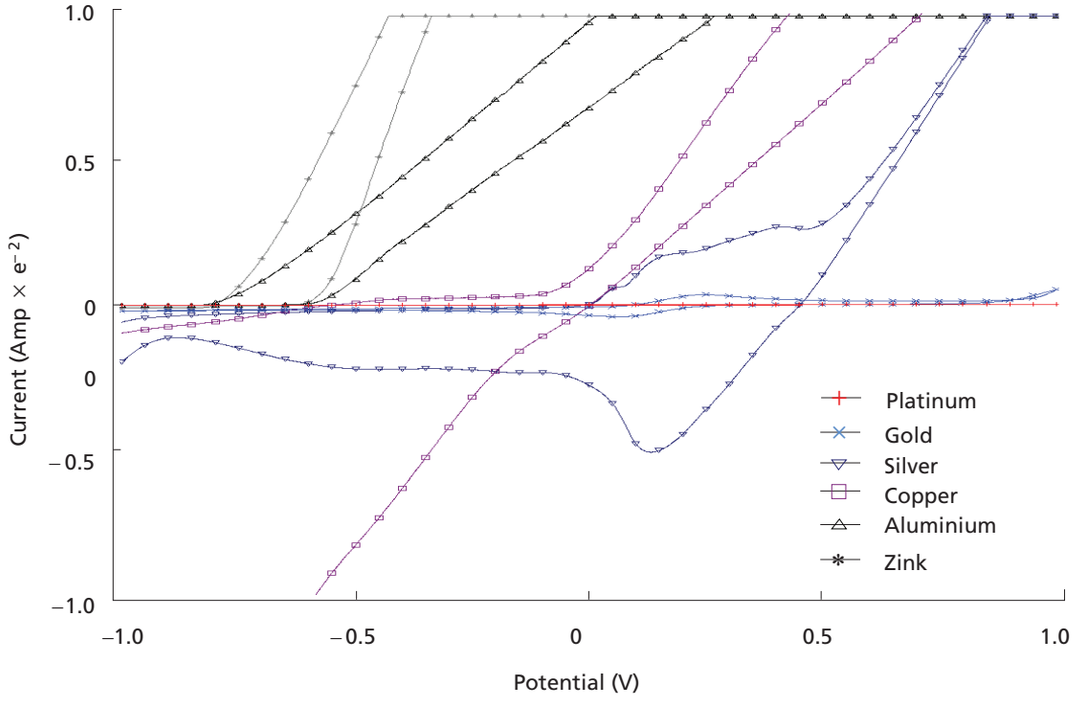

Figure 3. Cyclic voltammetry and metals comparison of 10 mM $K_3Fe(CN)_6$ in 0.1M KCl.

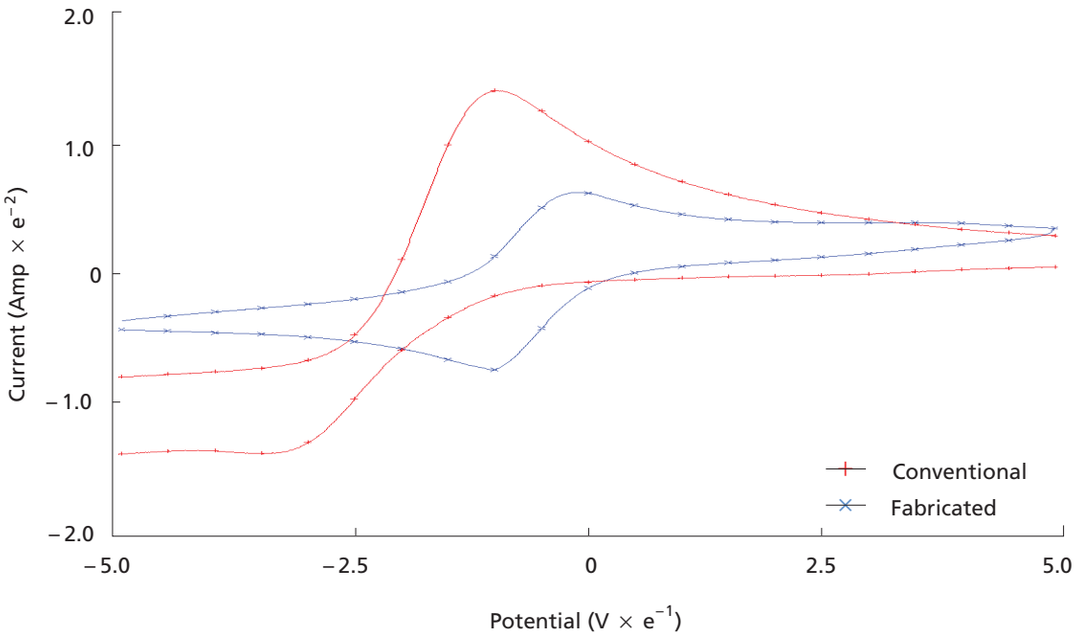

Figure 4. CV for conventional electrochemical system vs 6.5 mm^2 fabricated Au electrode.

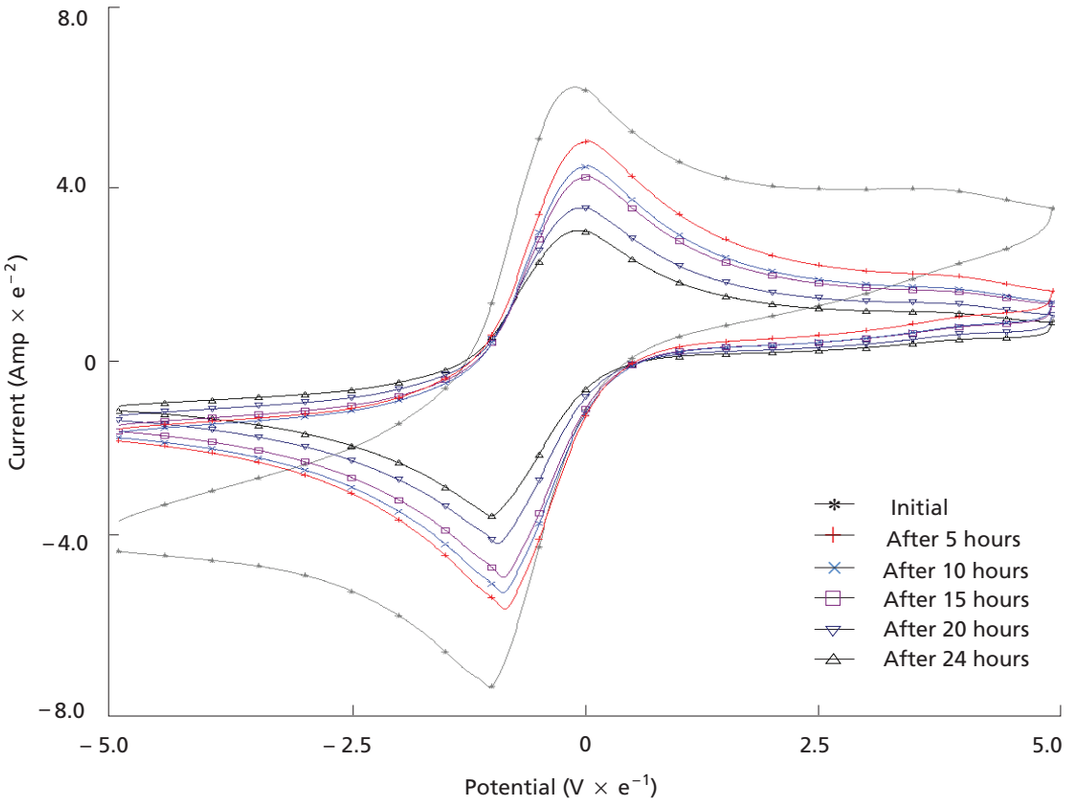

Figure 5. Results of 24 h reliability test for 6.5 mm^2 fabricated Au electrodes.

Table 1. Peak current parameters for fabricated electrode.

Electrode area (A)	I_{pa} (uA)	I_{pc} (uA)	Ratio of I_{pa}/I_{pc}	E_{pa} (mV)	E_{pc} (mV)	$\|\Delta E_p\| = E_{pa} - E_{pc}$ (mV)
6.50 mm^2	47.4	38.7	1.22	–88	2	90
0.26 mm^2	8.2	10.3	0.80	–149	32	181

The cyclic voltammogram for a reversible redox couple holds a relationship:

$$I_{pa} / I_{pc} = 1 \quad \ldots 2$$

where I_{pa} is the anodic peak current and I_{pc} is the cathodic peak current. From Equation 2 above, the fabricated Au electrode was found to have the reading as shown in Table 1.

Table 1 depicts that the peak current ratio for 6.50 mm^2 it was 1.22 and for 0.26 mm^2 was 0.80. The results proved that the size of the electrode does affect the value of the peak current explained by Equation 1.

The peak current ratio of less than unity indicated weak adsorption of the reactant (ferricyanide) (Wopschall & Shain 1967) due to the decrease in electrode surface area. The weak adsorption of reactant lead generally to an enhancement of the cathodic peak current and on the reverse scan, to a smaller increase in the anodic peak current. With the adsorption of reactant sufficiently weak, the adsorbed reactant was more difficult to reduce and the reduction occured at a more cathodic potential. This in turn caused the cathodic peak to be increased.

The peak current ratio of greater than unity was due to the anodic peak current being enhanced dramatically while the cathodic peak current showed a smaller increase. Thus, the product (ferrocyanide) was weakly adsorbed on the electrode surface (Wopschall & Shain 1967).

The separation of peak potentials ΔE_p (ΔE_p > 59 mV) indicated a quasi reversible redox process. However, measured values for a reversible process were generally higher than ideal due to the condition of the electrode surface. For example, the formation of a passivating film on the electrode surface would decrease the reversible nature of the electron transfer reaction (Triroj *et al*. 2006).

CONCLUSION

The fabricated Au electrode that was developed in this research project was confirmed to be suitable for usage as an electrochemical sensor as the produced CV results were similar with the conventional macro-electrode electrochemistry system. The fabricated Au electrode for electrochemical sensoring by using cost effective techniques and apparatus as presented in this paper displayed the potential of being further developed as a microfluidic sensor that would be inexpensive, disposable and functional. The fabricated Au electrode was found to be reliable for 24 h at 25ºC room temperature.

The use of PMMA as a base offers a cost effective and flexibility material compared to the conventional silicon wafer. The irreversible sealing method of PDMS-glass created a robust microfluidic fabricated Au electrode could be used as a handy and disposable electrochemical sensor. One such useful application in CV electrochemical signal detection of the microfluidic device is in DNA hybridization based on the redox activity of Au surfaces.

The effect of peak current ratio with regard to the electrode size was investigated in this paper. As stated by Equation 1, with the molarity of reactant and product as used in this research project, a smaller dimension of electrode size produced a decrement in the value of peak current, thus giving a peak current ratio of less than unity.

ACKNOWLEDGEMENTS

This work was sponsored by the internal grant from the Collaborative Microelectronic Design Excellence Centre (CEDEC), Universiti Sains Malaysia, Penang, Malaysia. The financial support is gratefully appreciated.

Date of submission: March 2010
Date of acceptance: September 2010

REFERENCES

Bard, AJ & Faulkner, LR (eds) 1980, *Electrochemical methods: fundamentals and application*, Wiley, New York.

Bhattacharya, S, Datta, A, Berg, JM & Gangopadhyay, S 2005, 'Studies on surface wettability of Poly(dimethyl) siloxane (PDMS) and glass under oxygen-plasma treatment and correlation with bond strength', *J. Microelectromech. Syst*., vol. 14, pp. 590–597.

Choi, YS, Lee, KS & Park, DH 2005, 'Hybridization by an electrical force and electrochemical genome detection using an indicator-free DNA on a microelectrode-array DNA chip', *Bull. Korean Chem. Soc*., vol. 26, no. 3, pp. 379–383.

Duffy, DC, McDonald, JC, Schueller, OJA & Whitesides, GM 1998, 'Rapid prototyping of microfluidic systems in poly(dimethylsiloxane)', *Anal. Chem*., vol. 70, pp. 4974–4984.

paper 5.indd 147 1/20/2011 11:29:10 AM

Hamzah, IH, Abd Manaf, A & Sidek, O 2009, 'Fabrication technique of a 3 dimensional SU8 mold on PMMA substrate', *IEICE Electronics Express*, vol. 6, no. 24, pp 1726-1731.

Knight, JB, Vishwanath, A, Brody, JP & Robert, H 1998, 'Hydrodynamic focusing on a silicon chip: mixing nanoliters in microseconds', *Austin Phys. Rev. Lett*., vol. 80, pp. 3863–3866.

Lee, BS & Lee, SG 2004, 'Synthesis of thiol-functionalized ionic liquids and formation of self-assembled monolayer on gold surfaces: effects of alkyl group and anion on the surface wettability', *Bull. Korean Chem. Soc*., vol. 25, no. 10, pp. 1531–1537.

Lin, CH, Chao, CH & Lan, CW 2007, 'Low azeotropic solvent for bonding PMMA microfluidic devices', *Sensors and Actuators B: Chemical*, vol. 121, no. 2, pp. 698–705.

McDonald, JC, Duffy, DC, Anderson, JR, Chiu, DT, Wu, H, Schueller, OJA & Whitesides, GM 2000, 'Fabrication of microfluidic systems in poly(dimethylsiloxane)', *Electrophoresis, Wiley InterScience*, vol. 21, no. 1, pp. 27–40.

McDonald, JC & Whitesides, GM 2002, 'Poly(dimethylsiloxane) as a material for fabricating microfluidic devices', *Acc. Chem. Res*., vol. 35, pp. 491–499.

Morita, M, Longmire, ML & Murray RW 1988, 'Solid-state voltammetry in a three electrode electrochemical cell-on-a-chip with a microlithography defined microelectrode', *Anal. Chem.*, vol. 60, pp. 2770–2775.

Oh, SR 2008, 'Thick single-layer positive photoresist mold and poly(dimethylsiloxane) (PDMS) dry etching for the fabrication of a glass-PDMS-glass microfluidic device', *J. Micromech. Microeng*., vol. 18, p. 115025.

Patel, BA, Anastassiou, CA & O'Hare, D 2007, 'Biosensor design and interfacing', in *Body sensor networks*, ed Yang, Springer-Verlag, New York.

Sperandio, C, Bardon J, Laachachi, A, Aubriet, H & Ruch, D 2010, 'Influence of plasma surface treatment on bond strength behaviour of an adhesively bonded aluminium-epoxy system', *International Journal of Adhesion & Adhesives*, vol. 30, no. 5, pp. 1–9.

Triroj, N, Lapierre-Devlin, MA, Kelley, SO & Beresford, R 2006, 'Microfluidic three electrode cell array for low-current electrochemical detection', *IEEE Sensors Journal*, vol. 6, no. 6, pp. 1395–1402.

Wopschall, RH & Shain, I 1967, 'Effects of adsorption of electroactive species in stationary electrode polaro-graphy', *Anal. Chem.*, vol. 39, no. 13, pp. 1514–1527.

paper 5.indd 148 1/20/2011 11:29:11 AM

ASM Sci. J., **4(2)**, 149–157

Forced Convection Boundary Layer Flow over a Moving Thin Needle

S. Ahmad[1], N.M. Arifin[2], R. Nazar[3]* and I. Pop[4]

In this paper, the problem of steady laminar boundary layer flow of an incompressible viscous fluid over a moving thin needle is considered. The governing boundary layer equations were first transformed into non-dimensional forms. These non-dimensional equations were then transformed into similarity equations using the similarity variables, which were solved numerically using an implicit finite-difference scheme known as the Keller-box method. The solutions were obtained for a blunt-nosed needle. Numerical computations were carried out for various values of the dimensionless parameters of the problem which included the Prandtl number Pr and the parameter a representing the needle size. It was found that the heat transfer characteristics were significantly influenced by these parameters. However, the Prandtl number had no effect on the flow characteristics due to the decoupled boundary layer equations.

Key words: forced convection; boundary layer flow; moving thin needle; variable wall temperature

The flow and heat transfer stirred up by a moving surface in an ambient fluid are of great practical importance. For example, materials which are manufactured by extrusion processes and heat-treated substances proceeding between a feed roll and a wind-up roll can be classified as continuously moving surfaces. In order to acquire the top-grade property of the final product, the cooling procedure should be effectively controlled. The heat transfer of moving cylinders is important for fibre making and extrusion processes, fabrication of adhesive tapes and application of coating layers onto rigid substrates, among others. From an industrial point of view, the wall shear stress distribution is perhaps the most important parameter in this type of flow because it directly determines the driving force (or torque) required to withdraw from the surface (Sadeghy & Sharifi 2004). The thermal boundary layer for continuous moving slender cylinders with constant surface temperature was first studied by Sakiadis (1961), and Bourne and Elliston (1970) using the Karman-Pohlhausen approximate method. Further, Karnis and Pechoc (1978) solved this problem by using the perturbation method, while Lin and Shih (1980) used the local similarity method to solve the forced convection laminar boundary layer flow and heat transfer along static and moving cylinders with prescribed surface temperature or surface heat flux.

The problems of forced, free and mixed convection boundary layer flows over thin needles have been investigated by many researchers. Chen and Smith (1978), Narain and Uberoi (1972; 1973), Chen (1987), Lee *et al*. (1987) and Ahmad *et al*. (2008a) have studied various aspects of this problem. Wang (1990) has studied the problem of mixed convection boundary layer flow on a vertical adiabatic thin needle with a concentrated heat source at the tip of the needle. This situation may be applied, for example, to a stick burning at the bottom end. Agarwal *et al*. (2002) have investigated numerically the momentum and thermal boundary layers for power-law fluids over a moving thin needle under wide ranges of kinematic and physical conditions. We also notice to this end that Gorla (1979; 1990; 1993) has studied the boundary layer flow in the vicinity of an axisymmetric stagnation point on a circular cylinder placed in a Newtonian or a micropolar fluid.

A thin needle is a body of revolution whose diameter is of the same order as the velocity or thermal boundary layers that it develops. By appropriately varying the radius of the needle, the partial differential boundary layer equations admit similarity solutions which are more revealing than the direct numerical integration of the partial differential equations. As is well-known, an important aspect of experimental studies for flow and heat transfer characteristics are the measurements of velocity and the temperature profiles of the flow field. The probe of the measuring devices, such as a hot wire anemometer or shielded thermocouple, is often

[1] School of Mathematical Sciences, Universiti Sains Malaysia, 11800 USM, Penang
[2] Institute for Mathematical Research & Department of Mathematics, Universiti Putra Malaysia, 43400 UPM Serdang, Selangor
[3] School of Mathematical Sciences, Faculty of Science and Technology, Universiti Kebangsaan Malaysia, 43600 UKM Bangi, Selangor
[4] Faculty of Mathematics, University of Cluj, CP 253, R-3400 Cluj, Romania
*Corresponding author (e-mail: rmn@ukm.my)

paper 6.indd 149 1/20/2011 11:30:35 AM

a very thin wire or needle. The detailed analysis of the flow over such slender needle-shaped bodies is, therefore, of considerable practical interest.

All studies mentioned above on forced, free or mixed convection boundary layer flow over thin needles refer to fixed needles immersed in a viscous and incompressible fluid. However, the solution for boundary layer flows past moving thin needles in a vertical direction in a quiescent fluid with variable heat flux has been reported recently by Ahmad *et al*. (2008b). However, it is worth mentioning that the two previously published papers by the same author (Ahmad *et al*. 2008a; 2008b) are on mixed convection while the present paper is on forced convection. Moreover, the previously published papers are for vertical thin needles while the present paper is for horizontal thin needles. All these different geometries and different kind of convections lead to different kind of problems to be considered separately.

The aim of this paper is to study the problem of steady forced convection boundary layer flow over a moving thin needle with variable wall temperature in a quiescent fluid. It should also be mentioned that due to entrainment by the ambient fluid, this flow situation represents an intrinsically different class of boundary layer flow, which has substantially different type of solutions as compared to the case of a static needle. The partial differential equations governing the flow and temperature fields are reduced to ordinary differential equations which are solved numerically using an implicit finite-difference scheme called the Keller-box method. The influence of the needle size and the Prandtl number on the flow and heat transfer characteristics is presented in tabular and graphical forms.

BASIC EQUATIONS

Consider a steady laminar boundary layer flow of an incompressible viscous fluid over a moving thin needle in a bulk fluid at a constant temperature T_∞. Figure 1 shows the slender paraboloid needle whose radius is described by $\bar{r} = \bar{R}(\bar{x})$, where $\bar{x}$ and $\bar{r}$ are the axial and radial co-ordinates, respectively, with the $\bar{x}$ axis measured from the needle leading edge. The needle is considered thin when its thickness does not exceed that of the boundary layer over it. Under this assumption, the effect of transverse curvature is of importance, but the pressure variation along the surface due to the presence of the needle can be neglected (Lee 1967). It is assumed that the needle moves with the velocity $\bar{U}(\bar{x})$ and is subjected to a variable wall temperature $\bar{T}_w(\bar{x})$. Under the boundary layer approximations, the basic boundary layer equations written in cylindrical co-ordinates are:

$$\frac{\partial}{\partial \bar{x}}(\bar{r}\,\bar{u}) + \frac{\partial}{\partial \bar{r}}(\bar{r}\,\bar{v}) = 0 \tag{1}$$

$$\bar{u}\frac{\partial \bar{u}}{\partial \bar{x}} + \bar{v}\frac{\partial \bar{u}}{\partial \bar{r}} = \frac{\upsilon}{\bar{r}}\frac{\partial}{\partial \bar{r}}\left(\bar{r}\frac{\partial \bar{u}}{\partial \bar{r}}\right) \tag{2}$$

$$\bar{u}\frac{\partial \bar{T}}{\partial \bar{x}} + \bar{v}\frac{\partial \bar{T}}{\partial \bar{r}} = \frac{\alpha}{\bar{r}}\frac{\partial}{\partial \bar{r}}\left(\bar{r}\frac{\partial \bar{T}}{\partial \bar{r}}\right) \tag{3}$$

where, $\bar{u}$ and $\bar{v}$ are the velocity components along the $\bar{x}$– and $\bar{r}$– axes, respectively, $\bar{T}$ is the local fluid temperature, ν is the kinematic viscosity and α is the constant thermal diffusivity of the fluid. We assume that the boundary conditions of Equations 1 – 3 are:

$$\begin{aligned} &\bar{v} = 0, \quad \bar{u} = \bar{U}(\bar{x}), \quad \bar{T} = \bar{T}_w(\bar{x}) \quad \text{at} \quad \bar{r} = \bar{R}(\bar{x}) \\ &\bar{u} \to 0, \quad \bar{T} \to T_\infty \quad \text{as} \quad \bar{r} \to \infty \end{aligned} \tag{4}$$

where, $\bar{R}(\bar{x})$ describes the surface shape of the axisymmetric body. We introduce now the following non-dimensional variables:

$$\begin{aligned} &x = \bar{x}/L, \quad r = \mathrm{Re}^{1/2}(\bar{r}/L), \quad R(x) = \mathrm{Re}^{1/2}(\bar{R}(\bar{x})/L), \\ &u = \bar{u}/U_0, \quad v = \mathrm{Re}^{1/2}(\bar{v}/U_0), \quad U(x) = \bar{U}(\bar{x})/U_0, \\ &T = (\bar{T} - T_\infty)/T_0, \quad T_w(x) = (\bar{T}_w(\bar{x}) - T_\infty)/T_0 \end{aligned} \tag{5}$$

where, L is a characteristic length of the needle, U_0 is the characteristic velocity, T_0 (> 0)is the characteristic temperature and R_e (= $U_0 L/\nu$) is the Reynolds number. Substituting Equation 5 into Equations 1–3, we get:

$$\frac{\partial}{\partial x}(ru) + \frac{\partial}{\partial r}(rv) = 0 \tag{6}$$

$$u\frac{\partial u}{\partial x} + v\frac{\partial u}{\partial r} = \frac{1}{r}\frac{\partial}{\partial r}\left(r\frac{\partial u}{\partial r}\right) \tag{7}$$

$$u\frac{\partial T}{\partial x} + v\frac{\partial T}{\partial r} = \frac{1}{\mathrm{Pr}}\frac{1}{r}\frac{\partial}{\partial r}\left(r\frac{\partial T}{\partial r}\right) \tag{8}$$

where, Pr is the Prandtl number, with the boundary conditions (Equation 4) become:

$$\begin{aligned} &v = 0, \quad u = U(x), \quad T = T_w(x) \quad \text{at} \quad r = R(x) \\ &u = 0, \quad T = 0 \quad \text{as} \quad r \to \infty \end{aligned} \tag{9}$$

In order that Equations 6–8 become similar, we take:

$$U(x) = x^m, \quad T_w(x) = x^{2m} \tag{10}$$

where, m is a constant. We introduce now the following similarity variables:

$$\psi = x\,f(\eta), \quad T(x) = x^{2m}\theta(\eta) \tag{11a}$$

where,

$$\eta = x^{m-1}r^2 \tag{11b}$$

paper 6.indd 150 1/20/2011 11:30:38 AM

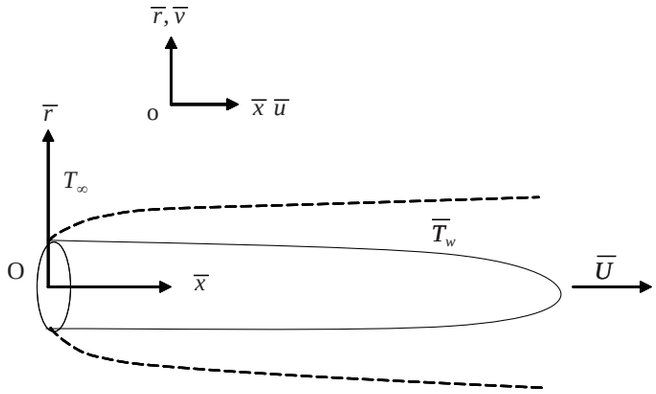

Figure 1. Physical model and coordinate system.

and ψ is the stream function which is defined in the usual way as u = (1/r) ∂ψ / ∂r and v = – (1/r) ∂ψ / ∂x. The surfaces of constant η = α, where α is a non-dimensional constant and is numerically small for a slender body, correspond to the surfaces of revolution. Setting η = α, Equation 11b describes both shape and size of the body with its surface given by:

$$R(x) = a^{1/2}\, x^{(1-m)/2} \tag{12}$$

Of practical interest is the pointed bodies and cylinders for which we must have $m \leq 1$ from Equation 12. For example, the body is a cylinder when m = 1, a paraboloid when m = 0, and a cone when m = –1. Substituting Equation 11 into Equations 7 and 8, we get the following ordinary differential equations:

$$2(\eta f'')' + ff'' - mf'^2 = 0 \tag{13}$$

$$\frac{2}{\mathrm{Pr}}(\eta\theta')' + f\theta' - 2mf'\theta = 0 \tag{14}$$

subject to the boundary conditions:

$$f(a) = \frac{(1-m)}{2}a, \quad f'(a) = \frac{1}{2}, \quad \theta(a) = 1$$
$$f'(\infty) \to 0, \quad \theta(\infty) \to 0 \tag{15}$$

where, primes denote differentiation with respect to η.
The physical quantities of interest are the skin friction coefficient C_f and the local Nusselt number Nu_x which are defined as:

$$C_f = \frac{\tau_w}{\rho \bar{U}^2/2}, \quad Nu_x = \frac{\bar{x}q_w}{k(\bar{T}_w - T_\infty)L} \tag{16}$$

where, the surface shear stress τ_w and the heat flux from the surface q_w of the needle are given by:

$$\tau_w = \mu\left(\frac{\partial \bar{u}}{\partial \bar{r}}\right)_{\bar{r}=\bar{R}(\bar{x})}, \quad q_w = -k\left(\frac{\partial \bar{T}}{\partial \bar{r}}\right)_{\bar{r}=\bar{R}(\bar{x})} \tag{17}$$

Using Equations 5, 11 and 17, we get:

$$C_f\, \mathrm{Re}_x^{1/2} = 8a^{1/2} f''(a), \quad Nu_x\, \mathrm{Re}_x^{-1/2} = -2a^{1/2}\theta'(a) \tag{18}$$

where Re_x (= $\bar{U}(\bar{x})\bar{x}/\nu$) is the local Reynolds number.

RESULTS AND DISCUSSION

Generally, of practical interest for needles is the pointed bodies and cylinders for which we must have m≤1 in Equation 12. For example, the body is a cylinder when m = 1, a paraboloid when m = 0 and a cone when m = –1 (Chen 1987). However, when a solid object of any shape, such as a needle in this present problem, exhibits a rectilinear translational motion through a fluid medium, then all parts of the solid object (needle) must have the same velocity. This implies that the velocity of its surface U has to be a constant and therefore, based on Equation 10, only the value m = 0 should be considered in the present paper. However, the only exception one may think of is an elastic body. The most typical example is an elastic sheet that is being stretched, in which the sheet velocity varies along the sheet or along x. Therefore, in the present problem which is a solid needle, the results for m = –1 and m = +1 were not of any physical relevance since the velocity of the body's surface U in Equation 10 would vary with x and this was inconsistent with the velocity of a solid needle. Still, these results were solutions of the mathematical problem posed, but without any physical realism of this present problem.

paper 6.indd 151 1/20/2011 11:30:40 AM

According to Equation 12, the value of $m = 0$ corresponds to a blunt-nosed needle or a paraboloid with $R(x) = a^{1/2} x^{1/2}$.

The system of decoupled ordinary differential Equations 13 and 14 subject to the boundary conditions (Equation 15) was solved numerically using an implicit finite-difference method known as the Keller-box scheme, as described in the book by Cebeci and Bradshaw (1988) for $m = 0$ (a blunt-nosed needle with uniform wall temperature) and some values of the governing parameter a (in the range of $0.001 \leq a \leq 0.1$). We consider that the needle moves in a fluid with different Prandtl numbers, i.e. Pr varies in the range of $0.01 \leq \text{Pr} \leq 100$. It is worth mentioning that small values of Pr (<<1) physically correspond to liquid metals, which have high thermal conductivity but low viscosity, while Pr>1 corresponds to diatomic gases including air. On the other hand, large values of Pr (>>1) correspond to high-viscosity oils and Pr = 6.8 corresponds to water at room temperature. Results are presented in tables and figures. In order to verify the accuracy of the present method, the values of the skin friction coefficient $C_f \text{Re}_x^{1/2}$ and the values of $\theta'(a)$ for fixed needles with $m = 0$ were compared with those reported by Chen and Smith (1978) in Tables 1 and 2, respectively. These results were found to be in good agreement. It can be seen from Table 1 that the skin friction coefficients for fixed and moving needles are in positive and negative signs, respectively. It is worth mentioning that a positive sign of the skin friction coefficient physically implies that the fluid exerts a dragging force on the surface and a negative sign implies the opposite. Table 2 shows that for any fixed value of Pr, the values of $\theta'(a)$ for a fixed needle are larger than moving needle, which meant that the heat transfer over a moving thin needle was greater than for a fixed thin needle.

The variations with a of the skin friction coefficient $C_f \text{Re}_x^{1/2}$ and the local Nusselt number $\text{Nu}_x \text{Re}_x^{-1/2}$, given by expressions (Equation 18) for $m = 0$, are shown in Figures 2 and 3 for Pr = 0.01, 0.7, 1, 6.8, 10. Due to the decoupled boundary layer (Equations 13 and 14), it is seen from Figure 2 that there is only a unique skin friction coefficient for all considered values of Pr at different values of a. It can also be seen from Figure 2 that the skin friction coefficient decreases with the increase of a for $0.001 \leq a \leq_{\text{min}}$ where a_{min} is the value of a when the skin friction coefficient is minimum. Figure 2 also shows that for $a_{\text{min}} < a \leq 0.1$, the skin friction coefficient increases with the increase of a.

Figures 3 and 4 show the variation with a and Pr, respectively, for the local Nusselt number $Nu_x \text{RE}_x^{-1/2}$ of a blunt-nosed needle with uniform wall temperature ($m = 0$). It can be seen from those figures that at any fixed value of a, the increase of Pr promotes heat transfer, i.e. the local Nusselt number increases with the increase of Pr. Figure 3 shows that for a fixed value of Pr, the local Nusselt number increases with the increase of a for $0.001 \leq a \leq a_{\text{max}}$ (Pr) where a_{max} (Pr) is the value of a when the local Nusselt number is maximum and depending on Pr. Figure 3 also shows that for a_{max} (Pr) $< a \leq 0.1$, the local Nusselt number decreases when a increases. Furthermore, it can be seen from Figure 4 that for $\text{Pr} < \text{Pr}_{in}^{0.05, 0.1}$ where $\text{Pr}_{in}^{0.05, 0.1}$ is the value of Pr when the curves $a = 0.05$ and $a = 0.1$ intersect, the local Nusselt number decreases with the increase of a. On the other hand, Figure 4 also shows that the local Nusselt number increases with the increase of a when $\text{Pr} < \text{Pr}_{in}^{0.01, 0.5}$ where $\text{Pr}_{in}^{0.01, 0.5}$ is the value of Pr when the curves $a = 0.01$ and $a = 0.05$ intersect.

The axial velocity profiles $f'(\eta)$ and the non-dimensional temperature profiles $\theta(\eta)$ for a blunt-nosed needle with uniform wall temperature ($m = 0$) are plotted against η in Figures 5 and 6, respectively, for three needle sizes, namely $a = 0.01, 0.05$ and 0.1. Figure 5 shows that at any fixed value of a, there is only a unique velocity profile for all values

Table 1. Skin friction coefficient $C_f \text{Re}_x^{1/2}$ over thin needles for $m = 0$.

a	$C_f \text{Re}_x^{1/2}$		
	Fixed needle		Moving needle
	Chen and Smith (1978)	Present	Present
0.1	3.26045	3.26289	–3.22553
0.01	6.79395	6.80883	–3.64781
0.001	15.72632	15.73317	–1.82632

Table 2. Values of $\theta'(a)$ over thin needles for $m = 0$ and $a = 0.1$.

Pr	$\theta'(a)$		
	Fixed needle		Moving needle
	Chen and Smith (1978)	Present	Present
0.020	–1.459	–1.490	–2.131
0.733	–2.434	–2.436	–2.535
100.000	–7.046	–7.064	–30.556

paper 6.indd 152 1/20/2011 11:30:40 AM

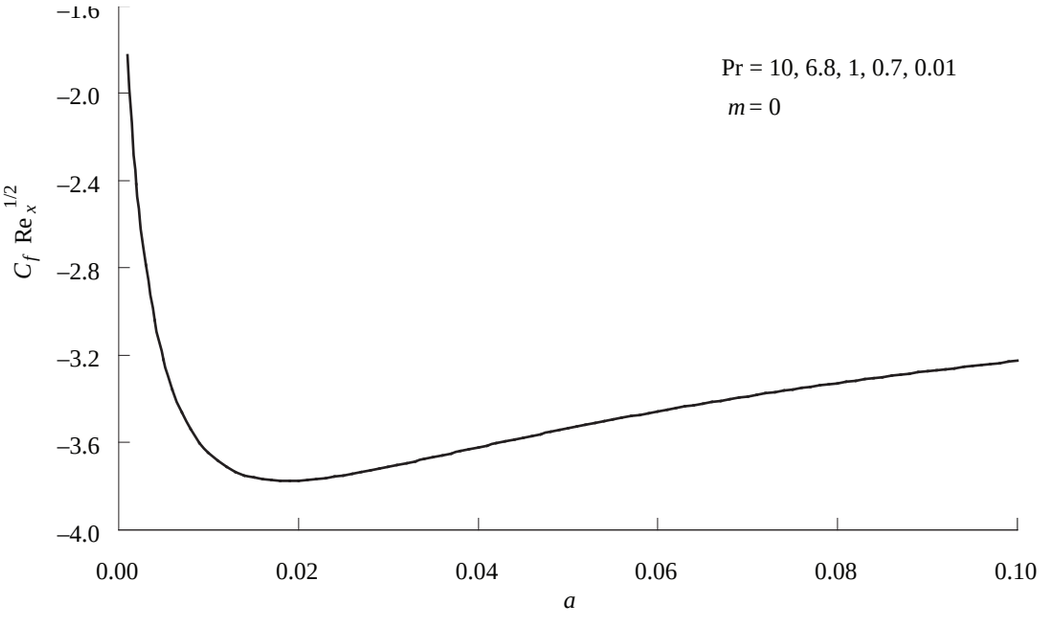

Figure 2. Variation of the skin friction coefficient with a for various values of Pr and $m = 0$.

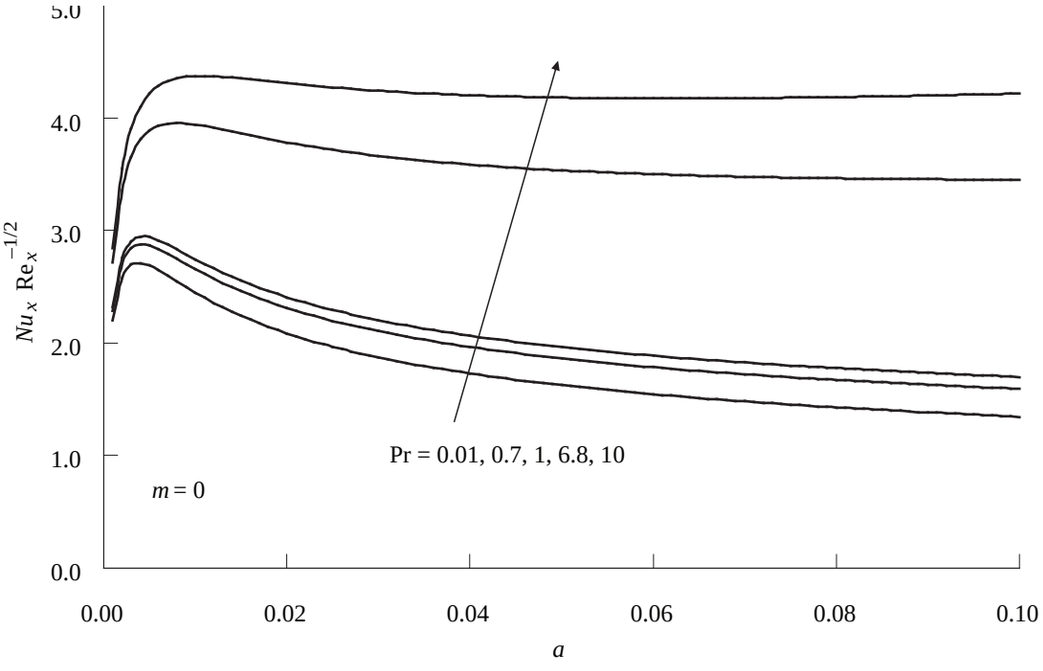

Figure 3. Variation of the local Nusselt number with a for various values Pr when $m = 0$.

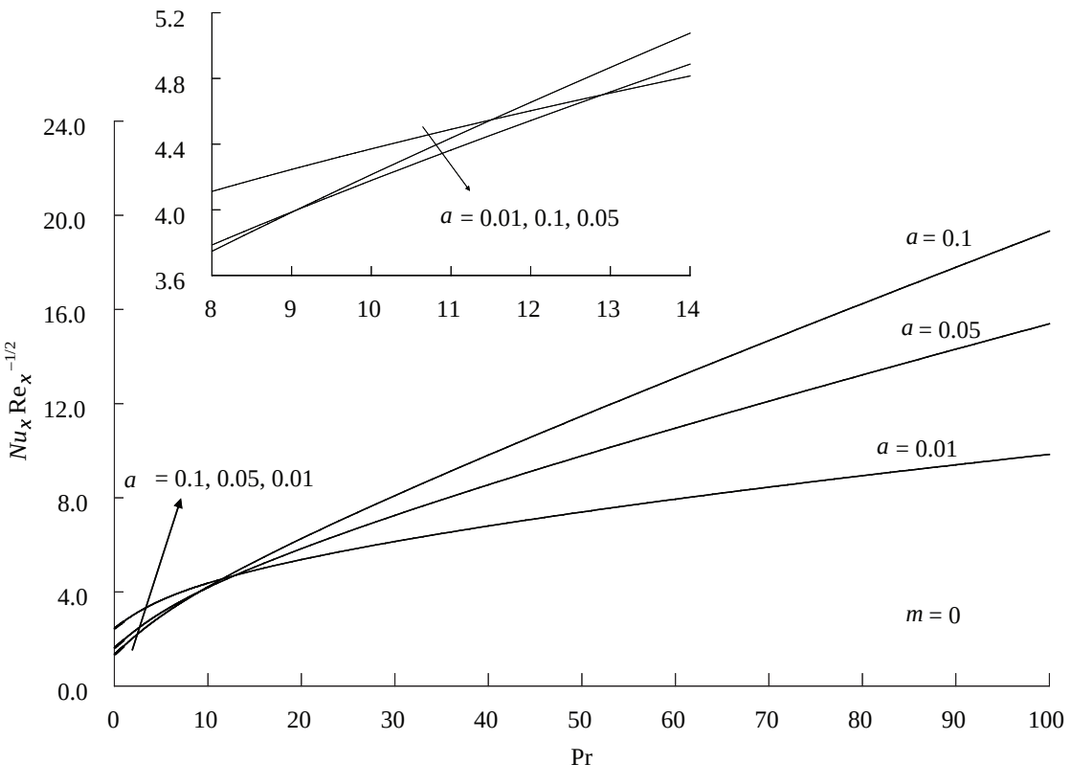

Figure 4. Variation of the local Nusselt number with Pr for various values *a* when *m* = 0.

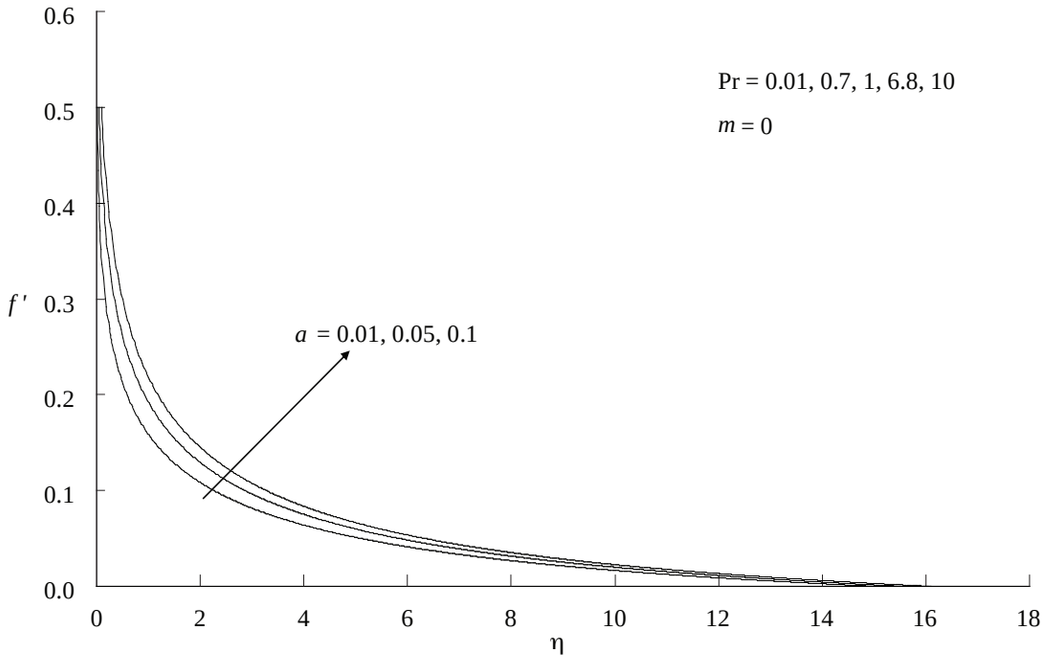

Figure 5. Velocity profiles for various values of *a* and Pr with *m* = 0.

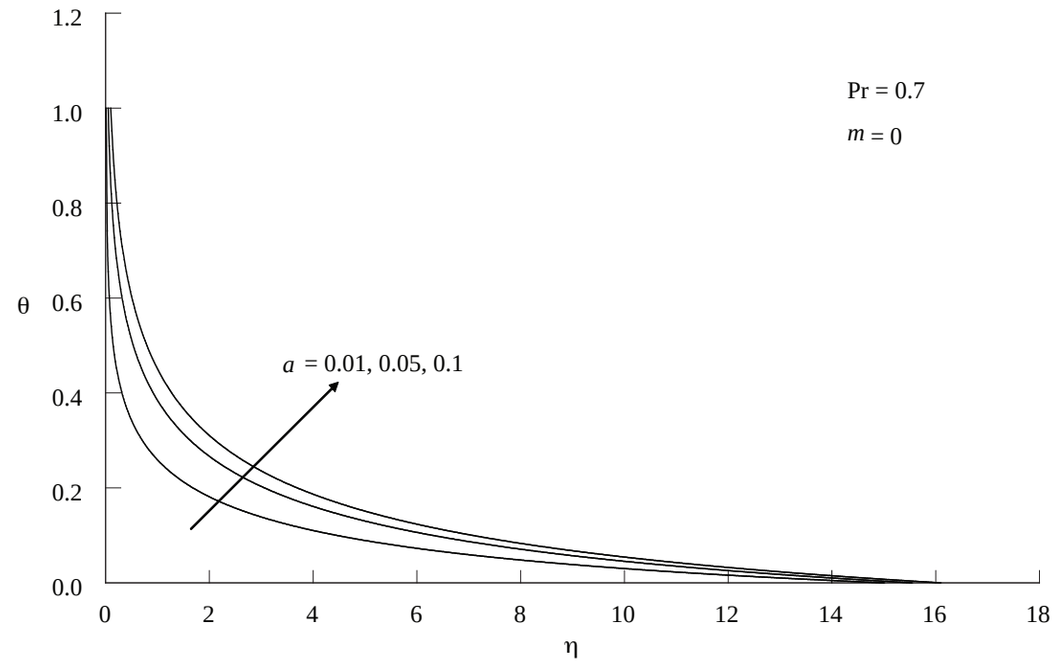

Figure 6. Temperature profiles for various values of *a* with Pr = 0.7 and *m* = 0.

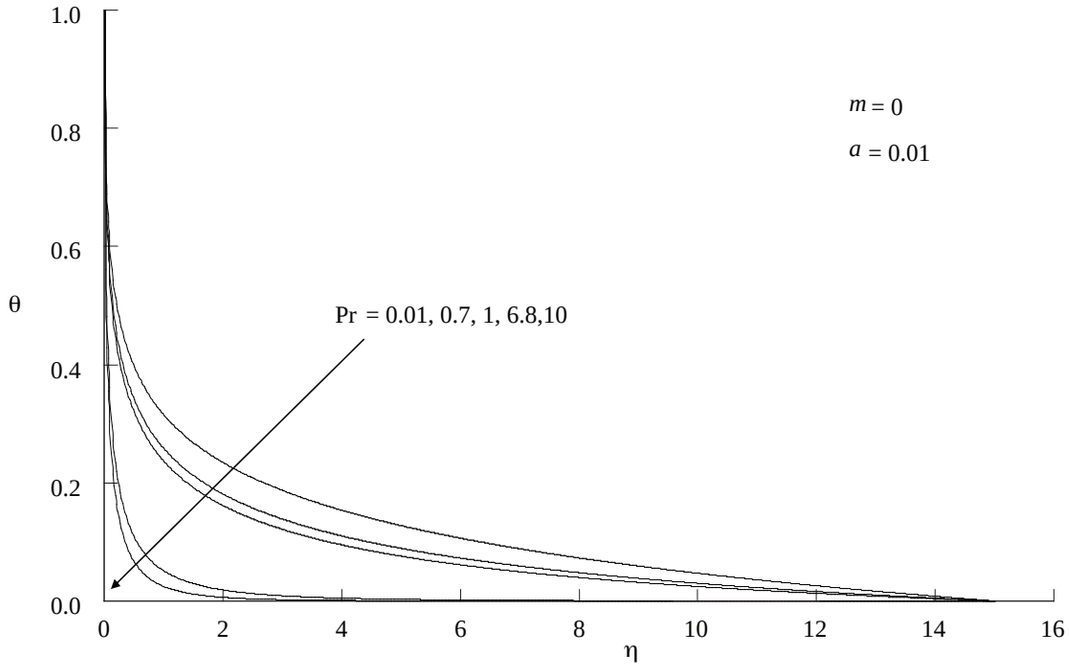

Figure 7. Temperature profiles for various values of Pr with *m* = 0 and *a* = 0.01.

of Pr. It is seen from Figures 5 and 6 that the velocity and thermal boundary layer thicknesses increase, respectively, with the increase of the needle size a. It is worth mentioning that the thickness of the boundary layer is measured by the value of η when the velocity and temperature gradients first become zero. An inspection of these figures (Figures 5 and 6) clearly shows that the thinner the needle, the smaller is the value of η for the free stream conditions to be attained, i.e. the boundary layer thickness decreases with the decreasing values of a. It can also be clearly seen from Figure 5 that $f''(\eta) \to 0$ as $\eta \to \infty$, i.e. the shear stress vanishes outside the momentum boundary layer. Figure 7 displays the non-dimensional temperature profile $\theta(\eta)$ for a blunt-nosed needle with uniform wall temperature ($m = 0$) for various values of Pr (Pr = 0.01, 0.7, 1, 6.8 and 10.0) and $a = 0.01$. It is seen that as Pr increases, the temperature profile decreases. It is also shown that the thermal boundary layer thickness decreases with an increase in Pr. Physically, this is because, as Pr increases, the thermal diffusivity decreases. This leads to the decreasing of energy transfer ability that reduces the thermal boundary layer.

CONCLUSION

The problem of a steady boundary layer flow of an incompressible viscous fluid over a moving thin needle in an ambient fluid was studied. Calculations were carried out for a blunt-nosed needle with uniform wall temperature ($m = 0$), which moved in a fluid with a wide range of the Prandtl numbers ($0.01 \leq \text{Pr} \leq 100$). The numerical results were also obtained for various values of the dimensionless parameters, which included the Prandtl number Pr and the parameter a representing the needle size. The results showed that the shape and the size of the needles had strong effects on the velocity and the thermal characteristics of the problem. Generally, it could be concluded that the local Nusselt number and the temperature profiles were significantly influenced by these parameters. However, the Prandtl number had no effect on the local skin friction coefficient and the velocity profiles due to the decoupled boundary layer equations.

ACKNOWLEDGEMENTS

The authors gratefully acknowledge the financial support received in the form of a fundamental research grant (SAGA Fund) from the Academy of Sciences Malaysia. The first author also acknowledges the Incentive Grants from Universiti Sains Malaysia. The authors also wish to express their very sincere thanks to the reviewers for the valuable comments and suggestions.

Date of submission: February 2009
Date of acceptance: November 2010

REFERENCES

Agarwal, M, Chhabra, RP, & Eswaran, V 2002, 'Laminar momentum and thermal boundary layers of power-law fluids over a slender cylinder', *Chemical Engineering Science*, vol. 57, pp. 1331–1341.

Ahmad, S, Arifin, NM, Nazar, R, & Pop, I 2008a, 'Mixed convection boundary layer flow along vertical thin needles: Assisting and opposing flows', *International Communications in Heat and Mass Transfer*, vol. 35, pp. 157–162.

Ahmad, S, Arifin, NM, Nazar, R & Pop, I 2008b, 'Mixed convection boundary layer flow along vertical moving thin needles with variable heat flux', *Heat and Mass Transfer*, vol. 44, pp. 473–479.

Bourne, DE & Elliston, DG 1970, 'Heat transfer through the axially symmetric boundary layer on a moving fibre', *International Journal of Heat and Mass Transfer*, vol. 13, pp. 583–593.

Cebeci, T & Bradshaw, P 1988, *Physical and computational aspects of convective heat transfer*, Springer, New York.

Chen, JLS 1987, 'Mixed convection flow about slender bodies of revolution', *Journal of Heat Transfer*, vol. 109, pp. 1033–1036.

Chen, JLS & Smith, TN 1978, 'Forced convection heat transfer from nonisothermal thin needles', *Journal of Heat Transfer*, vol. 100, pp. 358–362

Gorla, RSR 1979, 'Unsteady viscous flow in the vicinity of an axisymmetric stagnation point on a circular cylinder', *International Journal of Engineering Science*, vol. 17, pp. 87–93.

Gorla, RSR 1990, 'Boundary layer flow of a micropolar fluid in the vicinity of an axisymmetric stagnation point on a cylinder', *International Journal of Engineering Science*, vol. 28, pp. 145–152.

Gorla, RSR 1993, 'Mixed convection in an axisymmetric stagnation flow on a vertical cylinder', *Acta Mechanica*, vol. 99, pp. 113–123.

Karnis, J & Pechoc, V 1978, 'The thermal laminar boundary layer on a continuous cylinder', *International Journal of Heat and Mass Transfer,* vol. 21, pp. 43–47.

Lee, LL 1967, 'Boundary layer over a thin needle', *Physics of Fluids*, vol. 10, pp. 820–822.

Lee, SL, Chen, TS, & Armaly, BF 1987, 'Mixed convection along vertical cylinders and needles with uniform surface heat flux', *Journal of Heat Transfer*, vol. 109, pp. 711–716.

Lin, HT & Shih, YP 1980, 'Laminar boundary layer heat transfer along static and moving cylinders', *Journal of Chinese Institute of Engineers*, vol. 3, pp. 73–79.

Narain, JP & Uberoi, MS 1972, 'Combined forced and free-convection heat transfer from vertical thin needles in a uniform stream', *Physics of Fluids*, vol. 15, pp. 1879–1882.

paper 6.indd 156 1/20/2011 11:30:46 AM

Narain, JP & Uberoi, MS 1973, 'Combined forced and free-convection over thin needles', *International Journal of Heat and Mass Transfer*, vol. 16, pp. 1505–1511.

Sadeghy, K & Sharifi, M 2004, 'Local similarity solution for the flow of a "second-grade" viscoelastic fluid above a moving plate', *International Journal of Non-Linear Mechanics*, vol. 39, pp. 1265–1273.

Sakiadis, BC 1961, 'Boundary-layer behaviour on continuous solid surfaces III. The boundary layer on a continuous cylindrical surface', *AIChE Journal,* vol. 7, pp. 467–472.

Wang, CY 1990, 'Mixed convection on a vertical needle with heated tip', *Physics of Fluids*, vol. A 2, pp. 622–625.

paper 6.indd 157 1/20/2011 11:30:46 AM

ASM Sci. J., **4(2)**, 158–172

Intrinsic Couplings between the Primary Motor Area and Supplementary Motor Areas during Unilateral Finger Tapping Task

A.N. Yusoff[1]*, M. Mohamad[1], K.A. Hamid[1], A.I.A. Hamid[1], H.A. Manan[1,2] and M.H. Hashim[1]

In this multiple-subject study, intrinsic couplings between the primary motor (M1) and supplementary motor areas (SMA) were investigated. Unilateral (UNI_{right} and UNI_{left}) self-paced tapping of hand fingers were performed to activate M1 and SMA. The intrinsic couplings were analysed using statistical parametric mapping, dynamic causal modeling (DCM) and Bayesian model analysis. Brain activation observed for UNI_{right} and UNI_{left} showed contralateral and ipsilateral involvement of M1 and SMA. Ten full connectivity models were constructed with right and left M1 and SMA as processing centres. DCM indicated that all subjects prefer M1 as the intrinsic input for UNI_{right} and UNI_{left} as indicated by a large group Bayes factor (GBF). Positive evidence ratio (PER) that showed strong evidence of Model 3 and Model 6 against other models in at least 12 out of 16 subjects, supported GBF results. The GBF and PER results were later found to be consistent with that of BMS for group studies with high expected posterior probability and exceedance probability. It was concluded that during unilateral finger tapping, the contralateral M1 would act as the input centre which in turn triggered the propagation of signals to SMA in the same hemisphere and to M1 and SMA in the opposite hemisphere.

Key words: self-paced tapping; statistical parametric mapping; dynamic causal modeling; Bayesian model analysis; group Bayes factor; signal

The analysis of neuroimaging data normally results in the production of activation maps which are static or time independent in nature. It cannot be used to estimate and make inferences about the coupling among brain areas and how that coupling is influenced by changes in experimental manipulations (Friston *et al*. 2003). The neurodynamics of brain activation, however, can be studied by means of dynamic causal modeling (DCM) which can be described by the following multivariate differential equation (Friston *et al*. 2003):

$$z_t = (\boldsymbol{A} + \sum_{j=1}^{M} u_t(j)\,\boldsymbol{B}^j)\,z_t + \boldsymbol{C}u_t \qquad (1)$$

In Equation 1, **A** is the matrix that represents the fixed or context-independent strength of connections between the modeled regions (intrinsic couplings) and the matrices $\boldsymbol{B}^j$ represent the modulation of these connections. The matrix $\boldsymbol{C}$ is free of z_t but its role is to model the extrinsic influences of input on neuronal activity. The absence of u_t, $\dot{z}_t = Az_t$, implies that the only existing connectivities are those of the intrinsic couplings between the regions of interest (ROIs) (Friston *et al*. 2003; Penny *et al*. 2004; Stephan *et al*. 2007).

Connectivity models that can be constructed from Equation 1 normally consist of several ROIs as processing centres. The models are then estimated, fitted and later compared so that given the observed data, there will be one optimal model that represents the best balance between accuracy and complexity (Stephan *et al*. 2007).

Model comparisons are made based on Akaike Information Criterion (AIC) and Bayesian Information Criterion (BIC) (Penny *et al*. 2004). Empirically, AIC is observed to be biased towards complex models and BIC towards simple models. For a model to be accepted as the most probable model, a good agreement between AIC and BIC must be achieved. This means, the probability of getting a correct model (m) given the data (y), or $p(y|m)$, is high in both AIC and BIC frameworks. During model comparisons, the relative goodness between the two models

[1]Functional Image Processing Laboratory, Diagnostic Imaging and Radiotherapy Program, Faculty of Allied Health Sciences, Universiti Kebangsaan Malaysia, 50300 Kuala Lumpur
[2]Medical Imaging Program, Masterskill University College of Health Sciences, 43000 Cheras, Selangor, Malaysia
*Corresponding author (e-mail: nazlim@medic.ukm.my)

paper 7.indd 158 1/20/2011 11:33:56 AM

m_i and m_j, which is the difference in their log-evidences is computed using the equation (Stephan *et al.* 2007)

$$BF_{ij} = \frac{p(y|\, m_i)}{p(y|\, m_j)} \tag{2}$$

The Bayes factor (BF) for a comparison between model m_i and model m_j is the ratio of the model evidence of model m_i to model m_j. BF is the summary of the evidence provided by the observed data in favour of one statistical model as opposed to another. BF may take the values ranging from 1 to infinite numbers. $BF_{ij} = 1$ means that there is no evidence of model m_i to be in favour of model m_i. For $BF_{ij} > 1$, the data favours model m_i over model m_j and when $BF_{ij} < 1$, the data favours model m_j. A detailed interpretation of the ranges of BF values in terms of percentage can be found in Penny *et al*. (2004) suggesting weak ($BF < 3$), positive ($3 \leq BF < 20$), strong ($20 \leq BF < 150$) and very strong ($BF \geq 150$) evidence of one model over another. For example, if the value of BF_{ij} is 20, one is 95% sure that the data show strong evidence in favour of model m_i while a 99% confidence level is obtained for BF = 150.

For a single subject, the evidence for a particular model must be high in both the AIC and BIC criteria for that model to be chosen as the most optimal model that would represent the observed data. However, the BF value obtained from any model comparison would not be able to conclude any particular model as the most optimum model over a group of subjects under study. To make a conclusion over a group of subjects, the group Bayes factor (GBF) for any model comparison (model m_i and model m_j) must be computed. The formula is (Stephan *et al*. 2009):

$$GBF_{ij} = \prod_{n=1}^{N} BF_{ij}^{(n)} \tag{3}$$

which is simply the product of Bayes factors obtained from a model comparison between model m_i and model m_j over N subjects with n denoting the n-th subject. Equation 3 is very sensitive to between-subject variability in making a conclusion about the most optimal model over a group of subjects. A complementary measure to GBF is the positive evidence ratio (PER) which is defined as the number of subjects where there is positive or stronger evidence for model m_j divided by the number of subjects with positive or stronger evidence for model m_j. PER is given as (Stephan *et al*. 2007):

$$PER_{ij} = \frac{|\, k : BF_{ij}^{k} > 3|}{|\, k : BF_{ji}^{k} > 3|} \tag{4}$$

with subject $k = 1 \ldots N$. In contrast to GBF, PER is not sensitive to between-subject variability but describes the reproducibility of model comparison over subjects qualitatively (Stephan *et al.* 2007). In computing PER, one must only consider the BF for subject k which is larger than 3 because consistent evidence for any model comparison can only be regarded if both AIC and BIC provide Bayes factors of at least e (the natural exponent 2.7183) which is rounded to 3 as shown in Equation 4 (Penny *et al.* 2004).

It is very clear that GBF and PER are complementing each other in the sense that GBF provides a quantitative measure about model comparison across subjects while PER describe the qualitative reproducibility of model comparison over subjects. In short, PER will conclude on the number of subjects that prefer a particular model in a model comparison against the number of subjects that prefer a competing model. To overcome the drawbacks of GBF and PER, a novel hierarchical approach, Bayesian model selection (BMS) for group studies, has been formulated (Stephan *et al.* 2009) that would be able to consider the presence of outliers that may arise in any subject under study.

In this work, firstly, group analyses were conducted by means of random (RFX) effects analyses and inferences based on the group responses which were made onto the whole subject. A conjunction analysis was then performed to search for common activated areas among the subjects and to define the ROI for later use. Secondly, the connectivity measure between regions of interest was studied and evaluated by implementing the DCM to model interactions among neuronal populations at cortical level. Full connective models with various input are constructed based on the ROIs defined in conjunction analysis. Thirdly, the models are estimated using the DCM and compared by means of Bayes rule. The GBF, PER and BMS for group studies were finally implemented in order to obtain the most probable model that would represent the intrinsic couplings during unilateral finger tapping for all subjects.

MATERIALS AND METHODS

Functional magnetic resonance imaging (fMRI) examinations were performed on 16 healthy right-handed male and female subjects. The average age was 22.31 ± 2.65 years old. Sample size, together with significance level (α) and effect size (t-value) influence the power of an fMRI study. Estimation of statistical power in an fMRI study requires knowledge of the expected percentage signal change between baseline and active states as well as estimates of the variability in percentage signal change (PSC). Desmond and Glover (2002) illustrated how PSC (μ_D), intra (σ_W) and intersubject (σ_B) variability as well as the number of time points (n) affect the power. For a typical fMRI study that consists of active and baseline conditions, a value of 0.75% for σ_W is typically observed in spatially smoothed data with 100 time points per condition. They concluded that with μ_D and σ_B of 0.5%, 11 – 12 subjects were

paper 7.indd 159 1/20/2011 11:33:57 AM

needed to achieve 80% power at $\alpha = 0.05$. With reference to that, in this study, we decided to take 16 subjects.

The subjects were given formal consent and screening forms as required by the Institutional Ethics Committee. The subjects were interviewed on their health condition prior to the scanning session and were confirmed to be healthy.

Functional magnetic resonance imaging (fMRI) data were acquired using 1.5 tesla magnetic resonance imaging (MRI) system (Siemens Magnetom Vision VB33G) equipped with functional imaging option, echo planar imaging (EPI) capabilities and a radiofrequency (RF) head coil (Siemens 1596696K2125) used for signal transmission and reception. The imaging parameters for the structural (T1) and functional (T2*) scans have been described elsewhere (Yusoff *et al.* 2006).

The subjects were instructed on how to perform the motor activation task and were allowed to practice prior to the scanning. The subjects had to press all four fingers against the thumb beginning with the thumb-index finger contact and proceed to the other fingers in sequence which would then begin anew with contact between thumb and index finger. This study produced a robust self-paced finger movement. The tapping of the fingers was approximately twice per second (using an intermediate force between too soft and too hard). A six-cycle active-rest paradigm which was alternately cued between active and rest was used with each cycle consisting of 10 series of measurements during active state and 10 series of measurements during resting state. The tapping of the fingers was done unilaterally (UNI_{left} or UNI_{right}) (Yusoff *et al.* 2006).

All the functional (T2*-weighted) and structural (T1-weighted) images were analysed using a personal computer (PC) with a high processing speed and large data storage capacity. The MATLAB 7.4 – R2006a (Mathworks Inc., Natick, MA, USA) and Statistical Parametric Mapping (SPM5 and SPM8) (Functional Imaging Laboratory, Wellcome Department of Imaging Neuroscience, Institute of Neurology, University College of London) software packages were used for the purposes. Activated voxels were identified by the general linear model estimating the parameters of the model and by deriving the appropriate test statistic (*T* statistics) at every voxel. Statistical inferences were finally obtained on the basis of SPM and the Gaussian random field theory (Friston 2004). The inferences were made using *T* statistics at uncorrected ($\alpha = 0.001$) significance level, wherelse for the analysis of conjunction, the significance level was taken at $\alpha = 0.1$.

DCM (Friston *et al.* 2003) was applied to evaluate the effective connectivity between the ROIs within and between the right and left hemispheres. The two cortical brain regions which have been found to be involved in motor processing are the primary motor area (M1) in the precentral gyrus (PCG) and supplementary motor area (SMA). The peak co-ordinates of the ROIs on the statistical parametric maps (SPMs) produced from conjunction analysis were taken as the anatomical landmark and the corresponding anatomical structures were confirmed by superimposing the SPMs onto the coplanar high resolution T1-weighted images using the Anatomy Toolbox (Eickhoff *et al.* 2005) and by using the Wakeforest University Pick Atlas software (Maldijan *et al*. 2003). The anatomical constraints were (1) the M1 co-ordinates had to be in the PCG and (2) the SMA co-ordinates had to be in the dorsal medial wall within the inter-hemispheric fissure (Grefkes *et al.* 2008). A spherical volume of 4 mm in radius was extracted from the ROIs and named as the left M1 [M1(L)], left SMA [SMA(L)], right M1 [M1(R)] and right SMA [SMA(R)], from which the effective connectivities between the ROIs were computed via DCM. Their Tailarach-MNI co-ordinates were (–36, –24, 58), (–6, 8, 50), (36, –20, 62) and (8, 4, 48), respectively.

In DCM analyses, the input centres for UNI_{right} and UNI_{left} were initially determined. Ten full connectivity models were constructed with the direct input (u) assumed to be through M1 or SMA or through both (Figure 1). The ten models were fed into DCM and estimated for each subject to obtain the influence of the direct input on the system which were the values of the matrix $\mathbf{C}$ and the strength of intrinsic connections or couplings between the modeled regions which were the values of the matrix $\boldsymbol{A}$ (Equation 1). All the elements of the two matrices are rate constants and are thus in units of s^{-1} (Friston *et al*. 2003).

Using the Bayesian model selection (BMS), the ten estimated models were then compared by quantifying the relative goodness of any two models i.e. Model 1 vs. Model 2, Model 1 vs. Model 3, Model 1 vs Model 4 etc., continuing with Model 2 vs. Model 1, Model 2 vs. Model 3, Model 2 vs Model 4 etc., until any one model was compared to all other models. For each model comparison between two models, m_i and m_j, a BF was quantified by transforming the differences in their log evidences (Equation 2). To make a comparison between all the ten models over all the 16 subjects, the GBF for any given model m_i, relative to model m_j was computed (Equation 3). Since GBF is sensitive to outliers and the magnitude of differences across subjects, a complementary index to GBF which was the PER was calculated which was defined as the number of subjects where there was positive (or stronger) evidence for model m_i divided by the number of subjects with positive (or stronger) evidence for model m_j (Equation 4). PER would then indicate the most probable model that represented the network system during the unilateral left and right tapping of hand fingers by describing the qualitative reproducibility of model comparisons over subjects. Finally, the results of GBF and PER were compared with the results of BMSfor group studies.

paper 7.indd 160 1/20/2011 11:33:57 AM

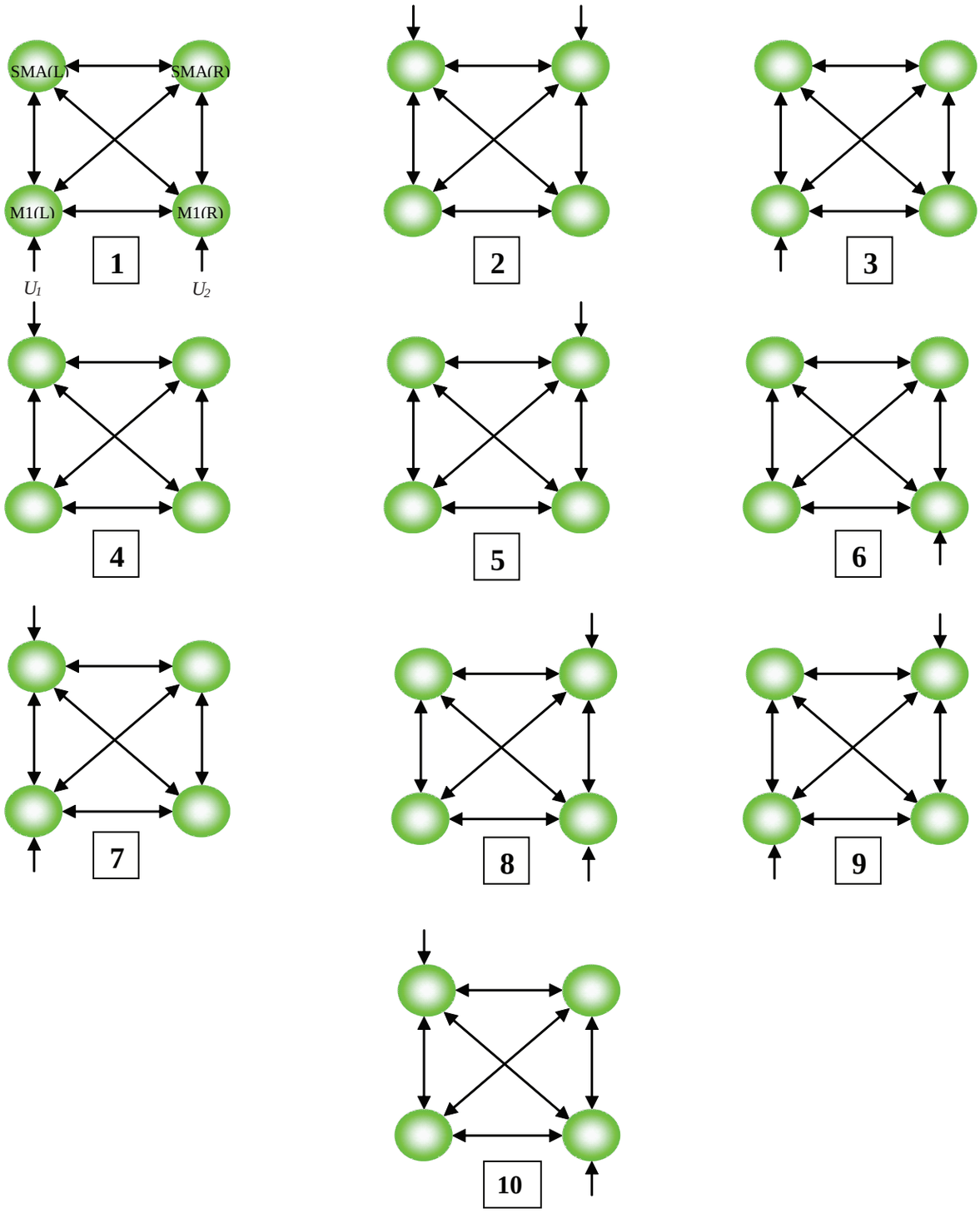

Figure 1. Ten full connectivity models for UNI_{right} and UNI_{left}. (⟶) represents the input while (⟷) represents forward and backward connections between any two areas. Model 1, 2, 7, 8, 9 and 10 have double input while Model 3, 4, 5, and 6 are single-input models. A complete labeling is shown only for Model 1.

The coupling values of the full connectivity models determined for both UNI_{right} and UNI_{left} were analysed to identify the most probable connections. This was done by first, justifying the connectivity values and their posterior probability for each connection and averaging the values over 16 subjects. Second, the average values for all connections were tested against 0 by means of Statistical Packages for Social Sciences (SPSS) at $\alpha/12 = 4.2 \times 10^{-3}$ (95% CI). Third, the connection that was significant, could be presented by at least 8 subjects with posterior probability larger than 0.9. It could be finally concluded that it was significant and the connectivity existed in at least half of the total number of subject under study. The most probable connectivity models for UNI_{right} and UNI_{left} were then suggested.

RESULTS

Figure 2 shows the SPMs obtained from random-effects (RFX) analysis showing contralateral and ipsilateral brain activations due to (a) UNI_{right} and (b) UNI_{left}. The crossing of the hair-line indicates the point of maximum intensity which occurred at (–32,–22, 50) and (38,–20, 62) in the left and right hemispheres, respectively. In order to illustrate several ipsilateral regions, Figure 2 was taken at a lower significant level $\alpha = 0.01$.

Table 1(a) shows the GBF and PER that were obtained from all model comparisons among the 10 full connectivity models shown in Figure 1 for UNI_{right}. Table 1(b) represents similar results obtained from UNI_{left}. The results were obtained from all subjects. The objective of the analysis was to determine the most probable input centre during the left and right hand finger tapping with the assumption that all the ROIs which were M1(L), SMA(L), M1(R) and SMA(R) were fully connected (forward and backward). This entailed taking into consideration both the contra- and ipsilateral behaviour of brain activation during the left and right hand finger tapping. BF and GBF for model comparison were computed based on Equations 2 and 3, respectively while PER was computed from Equation 4. It can be seen from Table 1(a) and (b) that both GBF and PER indicate Model 3 as the most preferred model for UNI_{right} while Model 6 is found to be the most probable model for UNI_{left}. The input for both models was determined to be through M1. For UNI_{right}, the GBF for model comparison 3 vs. 5 indicated the highest value of $+1.11 \times 1033$ with a very strong evidence of Model 3 as compared to Model 5. The PER was 12:0, which meant that 12 out of 16 subjects prefered Model 3 to Model 5. For UNI_{left}, Table 4(b) shows the highest value of $+6.03 \times 10^{21}$ for model comparison 6 vs. 5 with a very strong evidence of Model 6. The PER of 13:0, indicated that Model 6 was preferred by 13 out of 16 subjects under study.

Group BMS results for right and left hand finger tapping over 16 right handed subjects are shown in Figures 3(a) and 3(b), respectively. The results were obtained by means of random effects analysis (RFX) for BMS. For UNI_{right}, BMS results clearly showed evidence of the superiority of Model 3 as compared to the other 9 models indicating the Left M1 as the most probable input center during right hand finger tapping. For UNI_{left}, the group BMS results clearly showed evidence of the superiority of Model 6 as compared to the other 9 models indicating the Right M1 as the most probable input centre during left hand finger tapping. For the 16 subjects under study, the exceedance probability was almost 1.0 and the expected posterior probability was slightly larger than 0.5 for both Model 3 and Model 6. Tables 2(a) and 2(b) summarise the group BMS analyses for UNI_{right} and UNI_{left}, respectively for all models. Both types of finger tapping exhibited a constant sum of negative free energy (ΣF) for all models. All the Dirichlet parameter estimates (α_d), expected posterior probability ($\langle r \rangle$) and exceedance probability (φ) showed high preference for Model 3 and Model 6 as the most probable model for UNI_{right} and UNI_{left}.

The average intrinsic input (through M1) and intrinsic couplings between all ROIs within and between hemispheres for all subjects together with their statistics are tabulated in Tables 3(a) and 3(b) for UNI_{right} (Model 3) and UNI_{left} (Model 6), respectively. To test for the significance of the intrinsic input and couplings, the average values of the input and intrinsic couplings for all connections for each subject were entered into a one-sample *t*-test with '0' as target value. All the input and connections were found to be significant ($p < \alpha = 4.2 \times 10^{-3} = 0.05/12$; 95% CI) as shown in both tables. However, not all couplings showed posterior probability values higher than 0.9 which was the cut-off value for connectivity between any two regions which were considered as significant in the Bayesian framework. The couplings were small whenever their posterior probability was less than 0.9.

DISCUSSION

The statistical parametric maps (SPMs) depicted in Figure 2 clearly reveal significant activated areas not only in the hemisphere contralateral to the side of movement but also in the hemisphere opposite to the contralateral hemisphere. For UNI_{right}, ipsilateral activation occured in the right postcentral gyrus, right Rolandic operculum, right precentral gyrus, right middle frontal gyrus, right superior frontal gyrus, right SMA and right middle cingulate gyrus. For UNI_{left}, the activated ipsilateral areas were in the left precentral gyrus, left SMA and left middle frontal gyrus.

The existence of ipsilateral activation in the motor cortex during motor-related tasks has been widely reported and discussed (Grefkes *et al.* 2008; Newton *et al*. 2005; Walsh *et al.* 2008). It shows evidence of the involvement of ipsilateral areas in co-ordinating motor-related movement.

paper 7.indd 162 1/20/2011 11:33:58 AM

Table 1(a). Group Bayes factor and positive evidence ratio for all model comparisons for UNI_{right}.

Model	GBF	$k: BF_{ij}^{k} > 3$	$k: BF_{ij}^{k} > 3$	PER_{ij}
1 vs. 2	1.81E+10	7	2	7:2
1 vs. 3	2.74E-01	1	6	1:6
1 vs. 4	5.31E+09	5	2	5:2
1 vs. 5	5.50E+27	7	1	7:1
1 vs. 6	1.75E+06	3	6	3:6
1 vs. 7	3.00E+08	2	2	2:2
1 vs. 8	2.71E+10	7	2	7:2
1 vs. 9	3.51E+06	2	4	2:4
1 vs. 10	1.85E+17	9	1	9:1
2 vs. 1	1.18E-13	2	7	2:7
2 vs. 3	1.27E-10	0	11	0:11
2 vs. 4	4.41E-01	0	4	0:4
2 vs. 5	1.73E+17	1	6	1:6
2 vs. 6	1.23E-06	1	8	1:8
2 vs. 7	8.60E-07	3	6	3:6
2 vs. 8	9.84E-06	2	5	2:5
2 vs. 9	2.10E-09	1	9	1:9
2 vs. 10	9.06E-01	2	3	2:3
3 vs. 1	2.73E+00	6	1	6:1
3 vs. 2	4.68E+14	11	0	11:0
3 vs. 4	3.43E+13	11	0	11:0
3 vs. 5	1.11E+33	12	0	12:0
3 vs. 6	8.00E+05	8	2	8:2
3 vs. 7	7.76E+05	7	0	7:0
3 vs. 8	1.92E+08	10	1	10:1
3 vs. 9	2.64E+05	5	0	5:0
3 vs. 10	1.15E+16	12	0	12:0
4 vs. 1	1.70E-12	2	5	2:5
4 vs. 2	1.24E+02	3	1	3:1
4 vs. 3	1.04E-13	0	11	0:11
4 vs. 5	6.12E+19	6	1	6:1
4 vs. 6	3.83-08	2	8	2:8
4 vs. 7	5.55E-03	3	2	3:2
4 vs. 8	1.20E-05	3	3	3:3
4 vs. 9	5.12E-07	2	4	2:4
4 vs. 10	5.93E+00	5	3	5:3
5 vs. 1	1.54E-24	1	7	1:7
5 vs. 2	4.95E-11	3	2	3:2
5 vs. 3	3.54E-22	0	12	0:12
5 vs. 4	6.09E-10	1	6	1:6
5 vs. 6	4.97E-17	1	8	1:8
5 vs. 7	1.74E-13	1	4	1:4
5 vs. 8	5.22E-17	0	4	0:4
5 vs. 9	6.95E-21	0	6	0:6
5 vs. 10	5.09E-13	3	4	3:4
6 vs. 1	1.25E-04	6	3	6:3
6 vs. 2	2.22E+08	7	2	7:2
6 vs. 3	1.25E-06	2	8	2:8
6 vs. 4	2.60E+07	8	2	8:2
6 vs. 5	8.80E+26	8	1	8:1
6 vs. 7	7.97E+03	7	1	7:1
6 vs. 8	1.29E+04	6	0	6:0
6 vs. 9	5.60E+01	6	2	6:2
6 vs. 10	2.30E+09	8	0	8:0

paper 7.indd 163 1/20/2011 11:33:58 AM

Table 1(a) (cont.). Group Bayes factor and positive evidence ratio for all model comparisons for UNI_{right}.

Model	GBF	$k: BF_{ij}^{k} > 3$	$k: BF_{ij}^{k} > 3$	PER_{ij}
7 vs. 1	6.88E-07	1	3	1:3
7 vs. 2	3.27E+07	7	2	7:2
7 vs. 3	1.41E-03	0	7	0:7
7 vs. 4	3.01E+01	2	3	2:3
7 vs. 5	1.41E+19	4	1	4:1
7 vs. 6	1.25E-02	1	8	1:8
7 vs. 8	8.56E+01	6	2	6:2
7 vs. 9	2.04E-02	1	3	1:3
7 vs. 10	8.57E+06	7	2	7:2
8 vs. 1	5.90E-09	2	7	2:7
8 vs. 2	2.62E+05	4	3	4:3
8 vs. 3	1.05E-05	1	10	1:10
8 vs. 4	1.28E+03	3	3	3:3
8 vs. 5	4.97E+22	4	0	4:0
8 vs. 6	3.14E-02	0	6	0:6
8 vs. 7	1.17E-02	2	6	2:6
8 vs. 9	4.36E-03	3	7	3:7
8 vs. 10	1.25E+06	4	1	4:1
9 vs. 1	4.69E-05	3	2	3:2
9 vs. 2	4.75E+08	9	1	9:1
9 vs. 3	5.61E-04	0	5	0:5
9 vs. 4	1.01E+03	4	2	4:2
9 vs. 5	1.07E+22	6	0	6:0
9 vs. 6	6.11E-02	2	6	2:6
9 vs. 7	4.91E+01	3	1	3:1
9 vs. 8	1.62E+03	7	3	7:3
9 vs. 10	3.97E+08	9	1	9:1
10 vs. 1	1.03E-14	1	9	1:9
10 vs. 2	1.10E+00	3	2	3:2
10 vs. 3	1.43E-11	0	12	0:12
10 vs. 4	1.90E-02	3	5	3:5
10 vs. 5	9.68E+15	4	3	4:3
10 vs. 6	3.84E-06	1	7	1:7
10 vs. 7	1.08E-07	2	7	2:7
10 vs. 8	8.01E-07	1	4	1:4
10 vs. 9	2.51E-09	1	9	1:9

It has been established that the primary motor area (M1) in the precentral gyrus (PCG) and the supplementary motor area (SMA) in the medial dorsal wall are involved in movement preparation and execution of motor action. While M1 and SMA are known to be responsible in triggering and initiating motor related movements, SMA has a special function of being able to co-ordinate interlimb movements spatially and temporaly especially during bilateral execution (Aramaki *et al*. 2006). It is evident from Figure 2 that both areas are also involved even in unilateral types of movement suggesting the existence of interhemispheric connectivity between these areas.

In the present study, we only investigated the intrinsic couplings between M1 and SMA of the right and left hemisphere. The pre-motor cortex (PMC), another important area in motor co-ordination was not included in the present study due to the inconsistency of activation in the respective area for all subjects, even at a lower significance level, resulting in lack of activation in group results. This could be due to the nature of the tasks done by the subjects that does not involve the integration of sensory information which is one of the functions of PMC.

Biophysically plausible time-series models that reasonably represent interacting cortical regions can be constructed based on Equation 1. The models may consist of all of the three intrinsic couplings, modulatory and extrinsic input or may consist of only the intrinsic couplings and extrinsic input, depending on the experimental design (Friston *et al*. 2003). In this study, we used only the extrinsic inputs and intrinsic couplings. Due to experimental limitations, contextual or modulatory input was not included to be estimated by DCM in the present

paper 7.indd 164 1/20/2011 11:33:58 AM

Table 1(b). Group Bayes factor and positive evidence ratio for all model comparisons for UNI_{left}.

Model	GBF	$k: BF_{ij}^{k} > 3$	$k: BF_{ij}^{k} > 3$	PER_{ij}
1 vs. 2	6.08E+12	13	2	13:2
1 vs. 3	8.35E-07	2	6	2:6
1 vs. 4	3.60E-02	5	2	5:2
1 vs. 5	4.18E+05	9	2	9:2
1 vs. 6	6.53E-07	1	5	1:5
1 vs. 7	1.43E-01	7	2	7:2
1 vs. 8	6.69E-07	3	4	3:4
1 vs. 9	1.52E-01	7	2	7:2
1 vs. 10	9.79E+02	2	0	2:0
2 vs. 1	5.04E-10	3	12	3:12
2 vs. 3	2.47E-14	0	11	0:11
2 vs. 4	6.74E-04	0	4	0:4
2 vs. 5	4.80E-02	1	3	1:3
2 vs. 6	3.95E-15	0	13	0:13
2 vs. 7	1.65E-13	0	8	0:8
2 vs. 8	8.67E-18	1	13	1:13
2 vs. 9	2.65E-14	0	10	0:10
2 vs. 10	5.08E-09	2	12	2:12
3 vs. 1	4.02E+06	6	2	6:2
3 vs. 2	2.40E+18	11	0	11:0
3 vs. 4	3.31E+11	10	1	10:1
3 vs. 5	1.20E+17	12	0	12:0
3 vs. 6	1.55E-03	3	8	3:8
3 vs. 7	4.76E+02	4	0	4:0
3 vs. 8	1.36E+02	7	3	7:3
3 vs. 9	1.82E+03	6	0	6:0
3 vs. 10	7.23E+08	7	3	7:3
4 vs. 1	1.29E-03	2	5	2:5
4 vs. 2	8.08E+04	4	0	4:0
4 vs. 3	3.06E-12	1	10	1:10
4 vs. 5	1.53E+04	6	2	6:2
4 vs. 6	3.81E-15	0	14	0:14
4 vs. 7	6.67E-05	0	2	0:2
4 vs. 8	1.44E-12	1	6	1:6
4 vs. 9	1.05E-05	0	2	0:2
4 vs. 10	3.65E-01	1	5	1:5
5 vs. 1	3.09E-14	2	9	2:9
5 vs. 2	3.74E+01	3	1	3:1
5 vs. 3	8.32E-18	0	12	0:12
5 vs. 4	6.56E-05	2	6	2:6
5 vs. 6	5.89E-21	0	13	0:13
5 vs. 7	1.60E-09	1	5	1:5
5 vs. 8	7.67E-20	2	9	2:9
5 vs. 9	1.52E-12	0	5	0:5
5 vs. 10	1.38E-10	3	8	3:8
6 vs. 1	2.24E+07	5	1	5:1
6 vs. 2	3.50E+21	13	0	13:0
6 vs. 3	2.92E+04	8	3	8:3
6 vs. 4	1.12E+16	14	0	14:0
6 vs. 5	6.03E+21	13	0	13:0
6 vs. 7	6.71E+08	11	1	11:1
6 vs. 8	7.10E+03	6	0	6:0
6 vs. 9	3.19E+07	9	1	9:1
6 vs. 10	1.03E+10	5	0	5:0

paper 7.indd 165 1/20/2011 11:33:58 AM

Table 1(b) (cont.). Group Bayes factor and positive evidence ratio for all model comparisons for UNI_{left}.

Model	GBF	$k: BF_{ij}^{k} > 3$	$k: BF_{ij}^{k} > 3$	PER_{ij}
7 vs. 1	1.91E+02	2	7	2:7
7 vs. 2	5.99E+12	8	0	8:0
7 vs. 3	1.46E-01	0	4	0:4
7 vs. 4	1.12E+03	2	0	2:0
7 vs. 5	1.18E+05	4	1	4:1
7 vs. 6	6.86E-03	1	11	1:11
7 vs. 8	7.50E-02	3	8	3:8
7 vs. 9	6.52E-02	0	2	0:2
7 vs. 10	9.24E+04	4	8	4:8
8 vs. 1	1.45E+06	4	3	4:3
8 vs. 2	6.91E+17	13	1	13:1
8 vs. 3	6.14E-03	3	7	3:7
8 vs. 4	1.00E+05	7	1	7:1
8 vs. 5	4.44E+10	9	2	9:2
8 vs. 6	9.03E-02	0	5	0:5
8 vs. 7	5.18E+04	8	3	8:3
8 vs. 9	3.07E+04	8	4	8:4
8 vs. 10	3.08E+09	4	0	4:0
9 vs. 1	1.68E+02	2	7	2:7
9 vs. 2	3.70E+13	10	0	10:0
9 vs. 3	2.22E-01	0	6	0:6
9 vs. 4	8.08E+02	2	0	2:0
9 vs. 5	3.87E+06	5	0	5:0
9 vs. 6	5.19E-04	1	10	1:10
9 vs. 7	1.53E+01	2	1	2:1
9 vs. 8	6.56E-02	5	7	5:7
9 vs. 10	8.74E+05	5	7	5:7
10 vs. 1	1.03E-03	0	2	0:2
10 vs. 2	3.84E+09	12	2	12:2
10 vs. 3	1.17E-09	3	7	3:7
10 vs. 4	8.68E-04	5	1	5:1
10 vs. 5	7.00E+02	8	3	8:3
10 vs. 6	1.42E-08	0	5	0:5
10 vs. 7	2.89E-04	8	4	8:4
10 vs. 8	9.61E-13	0	4	0:4
10 vs. 9	2.53E-05	7	5	7:5

study since no such stimulus was given to the subject so that there was at least one area in the brain that would be influenced by contextual input.

Based on Equation 1 and the activation obtained in Figure 2, we constructed ten biologically and physically plausible models that consisted of M1 and SMA in both hemispheres as shown in Figure 1. We hypothesised that the input would be through M1 or SMA or through both. To determine which region would most probably act as the input, our assumption was that any one region was fully connected to any other regions. Therefore, one may see that there are many other alternative models that can be constructed using the right and left M1 and SMA as processing centres, with a large number of mathematically possible connections. However, we limited this study to the ten biologically physically plausible models that we believed would be able to explain the intrinsic couplings between M1 and SMA in both hemispheres.

DCM uses a fully Bayesian approach in estimating and selecting the most probable model among the competing models. According to Bayes' rule, the posterior distribution is equal to the likelihood multiplied by the prior and divided by the evidence (Penny *et al*. 2004) or $p(\theta|y,m) = [p(y|\theta,m)\ p(\theta|m)]/p(y|m)$. Taking logs for both sides: $\log\ p(\theta|y,m) = \log\ p(y|\theta,m).\ \log\ p(\theta|m) - \log\ p(y|m)$. The expression $p(y|m)$ is the probability of obtaining observed data y given a particular model m, also named as model evidence while $p(\theta|m)$ is the probability of obtaining DCM parameters θ given a particular model m which is named as prior. The expression $p(y|\theta,m)$ is the probability of obtaining observed

paper 7.indd 166 1/20/2011 11:33:58 AM

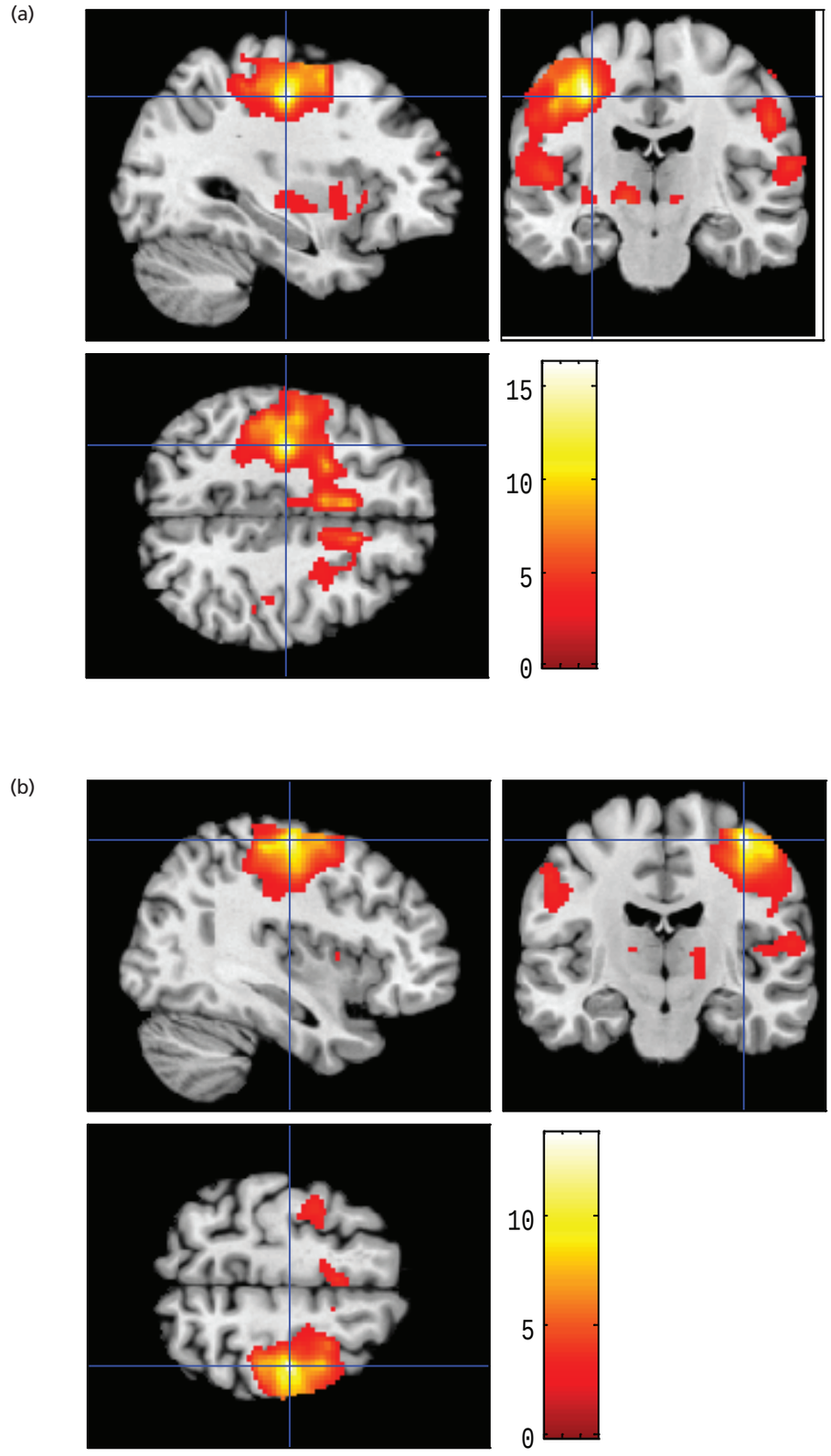

Figure 2. Statistical parametric maps (SPMs) obtained from random-effects (RFX) analysis (n = 16, t > 2.60, p < 0.01 uncorrected) showing brain activation due to (a) UNI_{right} and (b) UNI_{left} overlaid onto structural brain images. Colour codes represent increasing t value from red to white.

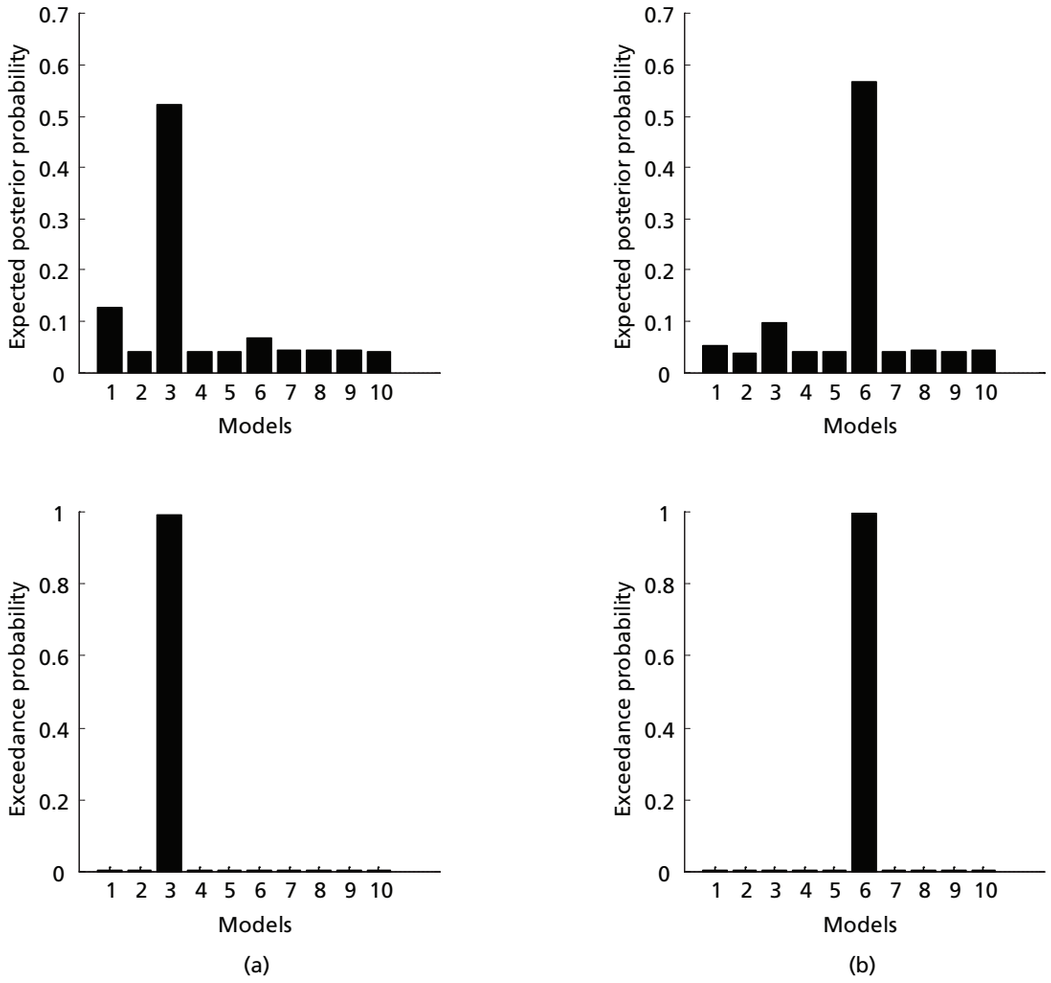

Figure 3. Bayesian model selection results for group studies indicating strong evidence of (a) Model 3 and (b) Model 6 for UNI_{right} and UNI_{left}, respectively.

data *y* given DCM parameters θ and a particular model m also named as likelihood and $p(\theta|y,m)$ is the probability of obtaining DCM parameters θ given data *y* and a particular model *m* also named as posterior distribution.

Based on the results of GBF tabulated in Table 1(a) and (b), it could be concluded that UNI_{right} prefered Model 3 while UNI_{left} prefered Model 6. Model 3 and Model 6 were similar in terms of their intrinsic input and connections between the regions of interest. Model 3 had the intrinsic input in the left M1 while Model 6 had it in the right M1 with all other areas fully forwardly and backwardly connected to each other. The results ruled out the possibility that the left and right SMA might act as the input for both UNIright and UNIleft. The results also discounted double input, whether in the same or different hemispheres. The high positive values of GBF for Model 3 and Model 6 as compared to all other models clearly indicated that during unilateral finger tapping, the contralateral M1 would act as the input centre which in turn triggered the propagation of signals to all other related areas. The fact that M1 acted as input centre during both UNI_{right} and UNI_{left} was in accordance with our earlier percentage of signal change (PSC) results that showed higher values for M1 as compared to SMA (Yusoff *et al.* 2009). Furthermore, M1 was known to be the primary area in the co-ordination of motor related movements, hence primary motor area.

The GBF decision that Model 3 and Model 6 were the two models that had the highest probability in representing the observed data for UNI_{right} and UNI_{left} was supported by PER results [Tables 1(a) and 1(b)]. To obtain PER, the number of subjects with positive or stronger evidence for one model was simply divided by the number of subjects with positive or stronger evidence for another competing model (Stephan *et al*. 2007). Model 3 for UNI_{right} and Model 6 for UNI_{left} were favoured by more subjects when

paper 7.indd 168 1/20/2011 11:33:59 AM

compared to any other competing models. With 12 out of 16 subjects in favour for Model 3 against Model 5 and with no subject in favour of Model 5 and with GBF = 1.11×10^{33} clearly showed strong evidence of Model 3. The ratio 12:0 or 12/0 is infinite which meant that the probability of having Model 3 to be the winning model against Model 5 in this group of subjects was very high in PER perspective. With reference to Table 1(b), the same argument could be applied to Model 6 for UNI_{left}. The highest GBF value is 6.03×10^{21} which was for a comparison between model 6 and model 5. The PER value is 13:0 which meant that the model was agreed by 13 out of 16 subjects.

Another convincing result was that obtained from BMS for group studies, as shown in Tables 2(a) and 2(b). The constant values of the sum of negative free energy (ΣF) for both UNI_{right} and UNI_{left} indicated a perfect balance between accuracy and complexity (Stephan *et al*. 2009) for all models shown in Figure 1. The fact that the values were almost the same for both types of movement also reflected a good fitting of the models to the observed data regardless of the side of movement. The related equation is $F = \langle \log p(y|\theta, m) \rangle q - KL[q(\theta), p(\theta|m)]$ (Stephan *et al.* 2009). Accuracy or the log likelihood is the first term on the right side of the equation which explains the probability of obtaining observed data y given DCM parameters θ and a particular model *m*. Complexity is reflected in the second term which contains the amount of information that can be obtained from the data with regards to the parameters of a model.

The Dirichlet parameter estimates (α_d), the expected posterior probability (<*r*>) and the exceedance probability (φ) are all the parameters used in BMS analyses to rank models at group level. The Dirichlet parameter estimates is a measure of effective number of subjects in which a given model generated the observed data. The sum of all α_d is equal to the number of subjects plus the number of compared models. The exceedance probability φ_k is the probability that a given model *k* is more likely than any other model to give the observed experimental data. If φ_k obtained for model *k* from *K* models is 0.95 (or 95%), one can be 95% sure that the favoured model has a greater posterior probability <r> than any other tested models. As can be seen, the sum of φ is unity. The histograms in Figure 3 graphically indicate the expected posterior probability and the exceedance probability for all models. Both two quantities for Model 3 and Model 6 are markedly higher than any other models. From Table 2, it can be seen that all the values of α_d, φ and <*r*> agree very well that both the UNI_{right} and UNI_{left} are best represented by Model 3 and Model 6, respectively. More importantly, the results obtained from group BMS studies, while being able to reproduce results of GBF and PER as obtained earlier are reported (Stephan *et al.* 2009), was able to take into consideration the presence of outliers that could have arisen in any subject under study. Since GBF is very sensitive to outliers (magnitude of differences across subjects) and PER can only describe the qualitative reproducibility of model comparison over subjects, BMS analysis is the preferred approach in model comparison involving multiple subjects.

Model 3 and Model 6 which were proven to be the winning models among the ten competing models for UNI_{right} and UNI_{left} had four ROIs that were fully connected to any other ROI. The values depicted in Tables 3(a) and 3(b) represent the average extrinsic input and intrinsic couplings between all ROIs for Model 3 and Model 6. As mentioned previously, this study excluded contextual or modulatory input. Therefore, the intrinsic coupling values in Tables 3(a) and 3(b) are basically the element of **A** matrix in Equation 1, while the values in the input column are the element of matrix **C**. Also shown in the tables are the statistics obtained from the one-sample *t*-test to test whether the average values for all connections over the

Table 2(a). The sum of negative free energy (ΣF), Dirichlet parameter estimates (α_d), expected posterior probability <r> and exceedance probability (φ) for all models shown in Figure 1 for UNI_{right}.

Variable	Model 1	Model 2	Model 3	Model 4	Model 5	Model 6	Model 7	Model 8	Model 9	Model 10
-ΣF (× 104)	1.4126	1.4223	1.4123	1.4197	1.4227	1.4161	1.4159	1.4185	1.4159	1.4189
α_d	3.2620	1.0118	13.5752	1.0271	1.0444	1.7479	1.0867	1.0927	1.1096	1.0426
<*r*>	0.1255	0.0389	0.5221	0.0395	0.0402	0.0672	0.0418	0.0420	0.0427	0.0401
φ	0.0036	0.0001	0.9953	0.0001	0.0001	0.0004	0.0001	0.0001	0.0001	0.0001

Table 2(b). The sum of negative free energy (ΣF), Dirichlet parameter estimates (α_d), expected posterior probability <r> and exceedance probability (φ) for all models shown in Figure 1 for UNI_{left}.

Variable	Model 1	Model 2	Model 3	Model 4	Model 5	Model 6	Model 7	Model 8	Model 9	Model 10
-ΣF (× 104)	1.4461	1.4541	1.4474	1.4519	1.4527	1.4438	1.4504	1.4471	1.4504	1.4476
αd	1.3189	1.0055	2.5173	1.0261	1.0312	14.7778	1.0460	1.1091	1.0538	1.1143
<*r*>	0.0507	0.0387	0.0968	0.0395	0.0397	0.5684	0.0402	0.0427	0.0405	0.0429
φ	0.0001	0.0000	0.0007	0.0000	0.0000	0.9990	0.0000	0.0001	0.0000	0.0000

paper 7.indd 169 1/20/2011 11:33:59 AM

Table 3(a). The average values of the intrinsic input at M1 and couplings between M1→SMA, SMA→M1, M1→M1 and SMA→SMA and their statistics based on Model 3 for UNI_{right}.

Variable	Intrinsic input	Intrinsic couplings											
	M1(L)	M1(L) to M1(R)	M1(L) to SMA(L)	M1(L) to SMA(R)	M1(R) to M1(L)	M1(R) to SMA(L)	M1(R) to SMA(R)	SMA(L) to M1(L)	SMA(L) to M1(R)	SMA(L) to SMA(R)	SMA(R) to M1(L)	SMA(R) to M1(R)	SMA(R) to SMA(L)
Ave	0.2656	0.3506	0.2797	0.2045	0.2162	0.1761	0.1284	0.1947	0.1676	0.1147	0.1515	0.1315	0.1197
SD	(0.0922)	(0.1127)	(0.1063)	(0.0931)	(0.1694)	(0.1179)	(0.0785)	(0.1525)	(0.1170)	(0.0805)	(0.1248)	(0.0805)	(0.0853)
p	7.55E-9	2.64E-9	2.55E-8	2.68E-7	1.30E-4	2.55E-5	9.25E-6	1.29E-4	3.99E-5	4.24E-5	2.10E-4	9.46E-6	4.92E-5
t	11.518	12.438	10.520	8.783	5.104	5.975	6.547	5.108	5.729	5.696	4.856	6.534	5.616

Ave = average, SD = standard deviation

Table 3(b). The average values of the intrinsic input at M1 and couplings between M1→SMA, SMA→M1, M1→M1 and SMA→SMA and their statistics based on Model 6 for $UNI_{left.}$

Variable	Intrinsic input	Intrinsic couplings											
	M1(L)	M1(L) to M1(R)	M1(L) to SMA(L)	M1(L) to SMA(R)	M1(R) to M1(L)	M1(R) to SMA(L)	M1(R) to SMA(R)	SMA(L) to M1(L)	SMA(L) to M1(R)	SMA(L) to SMA(R)	SMA(R) to M1(L)	SMA(R) to M1(R)	SMA(R) to SMA(L)
Ave	0.2665	0.2239	0.1436	0.1626	0.2950	0.2243	0.2106	0.1505	0.1748	0.1349	0.1492	0.1912	0.1188
SD	0.1428	0.1691	0.1235	0.1120	0.1396	0.0968	0.1334	0.1327	0.1294	0.1020	0.1065	0.1530	0.0984
p	2.00E-6	8.964E-5	3.13E-4	3.47E-5	4.35E-7	1.35E-7	1.39E-5	3.94E-4	7.33E-5	9.08E-5	5.03E-5	1.59E-5	2.20E-4
t	7.463	5.297	4.651	5.806	8.451	9.266	6.314	4.536	5.403	5.290	5.603	4.997	4.831

Ave = average, SD = standard deviation

16 subjects were significant or not against the condition of no connection, i.e. '0'. The effect of size (*t* value) and *p* values indicated that all inputs and connections were significant. However, an effective connectivity between any two ROIs can be accepted if its value is relatively high with a posterior probability greater than 0.9 (Friston *et al*. 2003). For UNI_{right} and UNI_{left}, not a single connection had all subjects with posterior probability larger than 0.9. However, the connections that had more than half of the number of subjects with posterior probability equal or larger than 0.9 were M1(L)→M1(R), M1(R)→M1(L), M1(L)→SMA(R) and M1(L)→SMA(L) for UNI_{right} and M1(R)→M1(L), M1(L)→M1(R), M1(R)→SMA(L) and M1(R)→SMA(R) for UNI_{left}. Therefore, only these connections were considered for the construction of the most probable model for UNI_{right} and UNI_{left}. The models are schematically shown in Figure 4 (a) and 4(b) for UNI_{right} and UNI_{left}, respectively.

From this robust finger tapping study that involved 16 healthy young male and female adults, it could be summarised that during the unilateral tapping of right hand fingers, M1(L) would act as the input centre, controlling the movement by triggering the signal to SMA contra- and ipsilateral to it unidirectionally but exchanging the signal with M1(R) on the opposite hemisphere bidirectionally. A similar transmission of signal was observed for UNI_{left} for which M1(R) was found to be the input centre. From Figure 4, the mean synaptic activity of the controlling M1 (the one contralateral to the side of movement) towards the opposite M1 for UNI_{right} seemed to be significantly higher as compared to the ipsilateral M1 to contralateral M1 (n = 16; p = 0.02; z = –2.299; 95% CI). The medians (IQR) were 0.34 (0.14) and 0.24 (0.32) for M1(L)→M1(R) and M1(R)→M1(L), respectively. For UNI_{left}, the mean synaptic activity is however not significant (n = 16; p = 0.228; z = –1.206; 95% CI) with the medians (IQR) 0.29 (0.36) and 0.31 (0.23) for M1(L)→M1(R) and M1(R)→M1(L), respectively. The values, even though not statistically significant for UNI_{left}, were in accordance with the results of the percentage of signal change (PSC) presented in our earlier publication (Yusoff *et al*. 2009) in which the controlling M1 has been found to exhibit a larger PSC as compared to the one ipsilateral to the side of movement. The results obtained from this study discounted the SMA-SMA connection and the connections between ipsilateral M1 and any SMA either on the ipsi or contralateral to the side of movement during unilateral tapping of hand fingers.

paper 7.indd 170 1/20/2011 11:33:59 AM

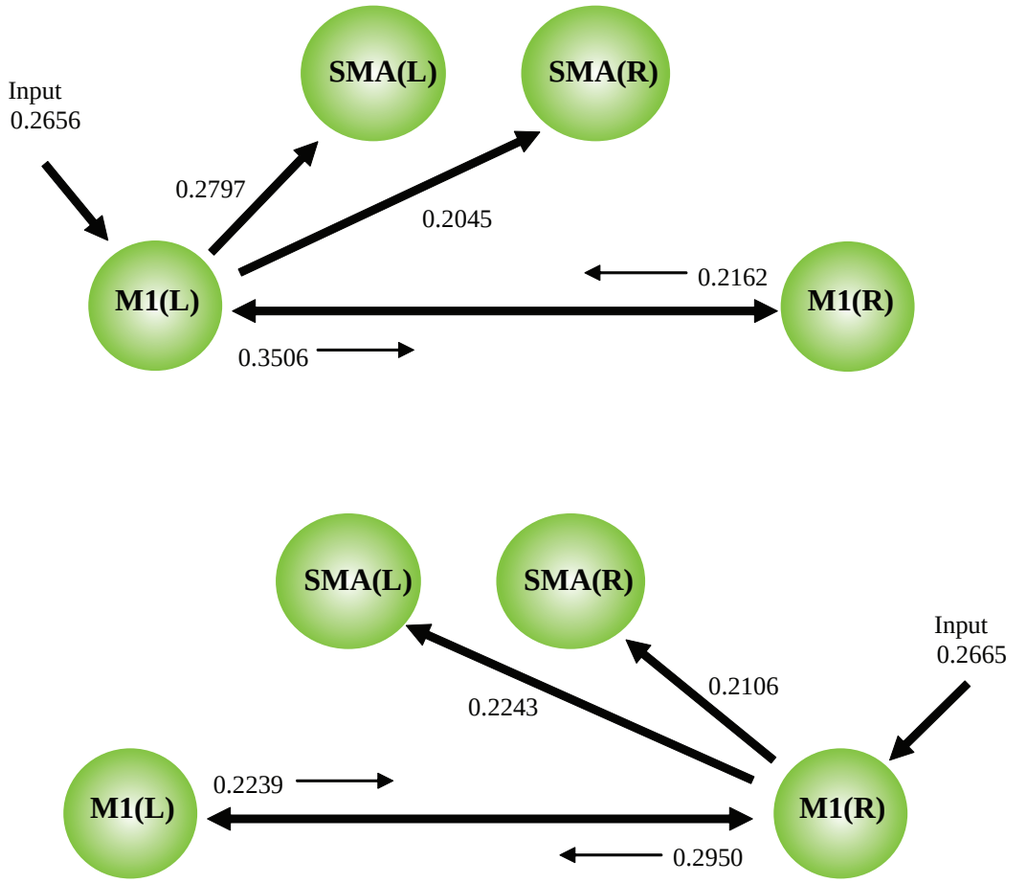

Figure 4. The most probable connectivity model for (a) UNI_{right} and (b) UNI_{left} showing the average input and coupling values in Hz.

CONCLUSION

The study of effective connectivity between activated regions in the brain evoked by experimental manipulation i.e. unilateral tapping of hand fingers (UNI_{right} and UNI_{left}), had been made possible using a noninvasive functional magnetic resonance imaging (fMRI) technique and a novel analysis of dynamic causal modeling (DCM). Ten biophysically plausible models were constructed based on specified regions of interest (ROIs), were estimated and compared in a powerful Bayesian framework. All the results of GBF, PER and BMS for group studies pointed to the same model for UNI_{left} and UNI_{right} indicating the reliability of the methods and reproducibility of the results. The primary motor area M1 in both hemispheres were determined to be the input centre during the unilateral tapping of hand fingers. Significant connections between the ROIs were M1(L)→M1(R), M1(R)→M1(L), M1(L)→SMA(R) and M1(L)→SMA(L) for UNI_{right} and M1(R)→M1(L), M1(L)→M1(R), M1(R)→SMA(L) and M1(R)→SMA(R) for UNI_{left}. The analyses implemented in this study revealed not only the specialisation of M1 and SMA in co-ordinating the unilateral movement of hand fingers but also the couplings of interaction between the two regions within and between the hemispheres. While the M1-M1 connection was found to be bidirectional for UNI_{right} and UNI_{left}, SMA-SMA coupling showed no evidence of connectivity.

ACKNOWLEDGEMENT

The authors would like to thank Sa'don Samian, the MRI Technologist of the Universiti Kebangsaan Malaysia Hospital (HUKM), for assistance in the scanning, and the Department of Radiology, Universiti Kebangsaan Malaysia Hospital for the permission to use the MRI scanner. The authors were also indebted to Prof Karl J. Friston and the functional imaging group of the University College of London for valuable discussions on experimental methods

paper 7.indd 171 1/20/2011 11:34:00 AM

and data analyses. This work is supported by IRPA research grants (09-02-02-0119EA296: the Ministry of Science, Technology and Innovation of Malaysia and, UKM-GUP-SK-07-20-205: Universiti Kebangsaan Malaysia).

Date of submission: December 2009
Date of acceptance: November 2010

REFERENCES

Aramaki, Y, Honda, M & Sadato, N 2006, 'Suppression of the non-dominant motor cortex during bimanual symmetric finger movement: a functional magnetic resonance imaging study', *Neuroscience*, vol. 141, pp. 2147–2153.

Desmond, JE & Glover, GH 2002, 'Estimating sample size in functional MRI (fMRI) neuroimaging studies: statistical power analyses', *Journal of Neuroscience Methods*, vol. 118, pp. 115–128.

Eickhoff, SB, Stephan, KE, Mohlberg, H, Grefkes, C, Fink, GR, Amunts, K & Zilles, K 2005, 'A new SPM toolbox for combining probabilistic cytoarchitectonic maps and functional imaging data', *NeuroImage*, vol. 25, pp. 1325–1335.

Friston, KJ, Harrison, L & Penny, W 2003, 'Dynamic causal modeling', *NeuroImage*, vol. 19, pp. 1273–1302.

Friston, KJ 2004, 'Experimental design and statistical parametric mapping', in Human Drain function, RSJ Frackowiak *et al*., Amsterdam, Elsevier Academic Press.

Grefkes, C, Eickhoff, SB, Nowak, DA, Dafotakis, M & Fink, GR 2008, 'Dynamic intra- and interhemispheric interactions during unilateral and bilateral hand movements assessed with fMRI and DCM', *NeuroImage*, vol. 41, pp. 1382–1394.

Maldijan, JA, Laurienti, PJ, Kraft, RA & Burdette, JH 2003, 'An automated method for neuroanatomic and cytoarchitectonic atlas-based interrogation of fMRI data sets', *Neuroimage*, vol. 19, no. 3, pp. 1233–1239.

Newton, JM, Sunderland, A & Gowland, PA 2005, 'fMRI signal decrease in ipsilateral primary motor cortex during unilateral hand movements are related to duration and side of movement', *NeuroImage*, vol. 24, pp. 1080–1087.

Penny, WD, Stephan, KE, Mechelli, A & Friston, KJ 2004, 'Comparing dynamic causal model', *NeuroImage*, vol. 22, pp. 1157–1172.

Stephan, KE, Weiskopf, N, Drysdale, PM, Robinson, PA & Friston, KJ 2007, 'Comparing hemodynamic models with DCM', *NeuroImage*, vol. 38, pp. 387–401.

Stephan, KE, Penny, WD, Daunizeau, J, Moran, RJ & Friston, KJ 2009, 'Bayesian model selection for group studies', *Neuroimage*, doi:10.1016/j. neuroimage. 2009.03.025.

Walsh, RR, Small, SL, Chen, EE & Solodkin, A 2008, 'Network activation during bimanual movements in humans' *NeuroImage*, vol. 43, pp. 540–553.

Yusoff, AN, Hashim, MH, Ayob, MM, Kassim, I, Taib, NHM & Abdullah, WAKW 2006, 'Functional specialisation and connectivity in cerebral motor cortices: a single subject study using fMRI and Statistical Parametric Mapping' *Malaysian Journal of Medicine and Health Sciences*, vol. 2, no. 2, pp. 37–60.

Yusoff, AN, Mohamad, M, Hamid, KA, Hamid, AIA, Manan, HA, & Hashim, MH 2009, 'Brain activation characteristics in M1 and SMA during unilateral finger tapping task', submitted to *Mal. J. Health Sci*.

paper 7.indd 172 1/20/2011 11:34:00 AM

Food Production from Animals in Asia: Priority for Expanding the Development Frontiers

C. Devendra[1]*

In agricultural systems, animals play a very important multifunctional role for developing communities throughout the world. This is reflected in the generation of value-added products like meat, milk and eggs for food security; socio-economic benefits like increased income, security and survival, and an infinite variety of services such as the supply of draught power and dung for soil fertility. However, and despite this importance, the situation is awesome since the projected total meat and milk consumption levels in 2020 are far in excess of anticipated supply, and projections of both meat and milk will have to be doubled by 2050 to meet human requirements. Strategies for productivity growth from animals are therefore urgent, and are discussed in the context of the scenario of waning agriculture, extreme poverty and hunger, food crisis, the current contributions from the components of the animal industries, prevailing constraints, opportunities and strategies for improved production. Current trends suggest that the non-ruminant pig and poultry industries will continue to contribute the major share of meat and all of egg production to meet projected human needs. With ruminants by comparison, overall meat production continues to come mainly from the slaughter of numbers. Strategic opportunities exist for maximising productivity in improved production systems. These include targeting rainfed areas, development of small farms, integrated crop-animal systems, intensive application of productivity-enhancing technologies, promoting intensive use of crop residues and expanding the R&D frontiers with interdisciplinarity and farming systems perspectives. The issues, together with increased investments and institutional commitment, provide for expanded animal production systems and productivity which can forcefully impact on improved human welfare in Asia in the immediate tomorrow.

Key words: animals, products and services, production systems, sustainability, integration, poverty and hunger, agro-ecological zones, technologies, strategic development, human welfare, Asia

The justification for increasing animal production is the burgeoning demand for more animal protein due to human population growth and rising incomes, and it involves two key issues. Firstly, it has to cope with circumstances where current production and available supplies are unable to meet present and projected future requirements. Secondly, it has also to contend with new challenges such as changing consumer preferences, impact of climate change on food production systems, emergence of enzootic diseases, and external factors such as rising transportation costs. At the heart of these issues is the capacity and capability of the animal industries to ensure cost-effective production, efficiency of use of production resources, ways to increase productivity to meet the spiralling demands and sustain potential contributions from the totality of the animal genetic resources (Devendra 2004). Animal agriculture strives to produce useful products and services of value to human welfare. In view of their multifunctional role, animals are often reared together with crops in farming systems for economic, ecological, social and cultural reasons that directly benefit farmers, the poor and their livelihood. Together with other natural resources such as land, crops and water, animal production is also concerned with issues of sustainability and protection of the environment.

Agricultural sustainability is important and involves environmental, socio-economic and political aspects (FAO 2003). Figure 1 illustrates a conceptual framework for sustainable ruminant production systems in Asia. Given the diversity of agro-ecological zones (AEZs), small farm systems with the the bio-physical and socio-economic environment, the major targets for development are efficiency in the management of natural resources, income growth, poverty alleviation, food security, economic viability, minimum dependence on external non-renewable input, response to changing consumer preferences, rural growth and self-reliance. The key sustainability issues are environmental protection, knowledge of traditional systems, preservation of biodiversity, maintenance of soil fertility, increased access to markets, socially acceptable improvements, wide adoption of improved technologies, farmers' organizations, co-operatives and replicability.

[1]Consulting Tropical Animal Production Systems Specialist,130A, Jalan Awan Jawa, 58200 Kuala Lumpur, Malaysia
*Corresponding author (e-mail: cdev@pc.jaring.my)

review.indd 173 1/20/2011 11:37:57 AM

This comprehensive overview focuses on the urgency to accelerate animal production to meet the demand for animal products, the use of animal production systems and trends, opportunities for productivity enhancement to include the situation in Malaysia, evolving scenarios, emerging issues and future challenges. Asia is the main focus of this paper.

THE AWESOME SETTING

Accelerating the contribution from animals is associated with several factors including the pursuit of the millennium development goals (MDGs) and the fact that two-thirds of the several millions of rural poor in developing countries are livestock keepers. It is therefore relevant to note the following concerns:

- Livestock constitutes about 30% of the agricultural gross domestic product (GDP) in the developing world, about 40% of the global GDP and is one of the fastest growing sub-sectors in agriculture (World Bank 2009a)
- About 2.6 billion farmers produce the majority of food as well as all other products and services in agriculture throughout the world on small farms of less than two hectares. More than 70% of people suffering from hunger live in rural areas (IAASTD 2008)
- Agriculture appears neglected, and the share of agriculture in GDP has declined significantly, due to low productivity, resulting in slow growth (ESCAP 2008). In East Asia and the Pacific for example, this has dropped from 3.0% in the 1980s to a mere 0.1% in 2000–2003
- Global resource depletion includes reduced arable land, irrigation water, mineral fertilisers (N, P, K and S) and financial credits
- The projected total meat and milk consumption levels in 2020 are far in excess of anticipated supplies and projections of both meat and milk will have to be doubled by 2050 (Steinfeld *et al*. 2006) to meet human requirements
- Very recent World Bank (2009b) data indicates that the number of hungry people actually increased between 1995–97 and 2004–06 and was highest in Asia and the Pacific
- 1.2 billion people live on less than USD1 per day and 800 million persons go to bed hungry every day
- In the developing countries, there are 150 million children who are underweight, 175 million whose growth is stunted, and 44 million who are wasting away; and

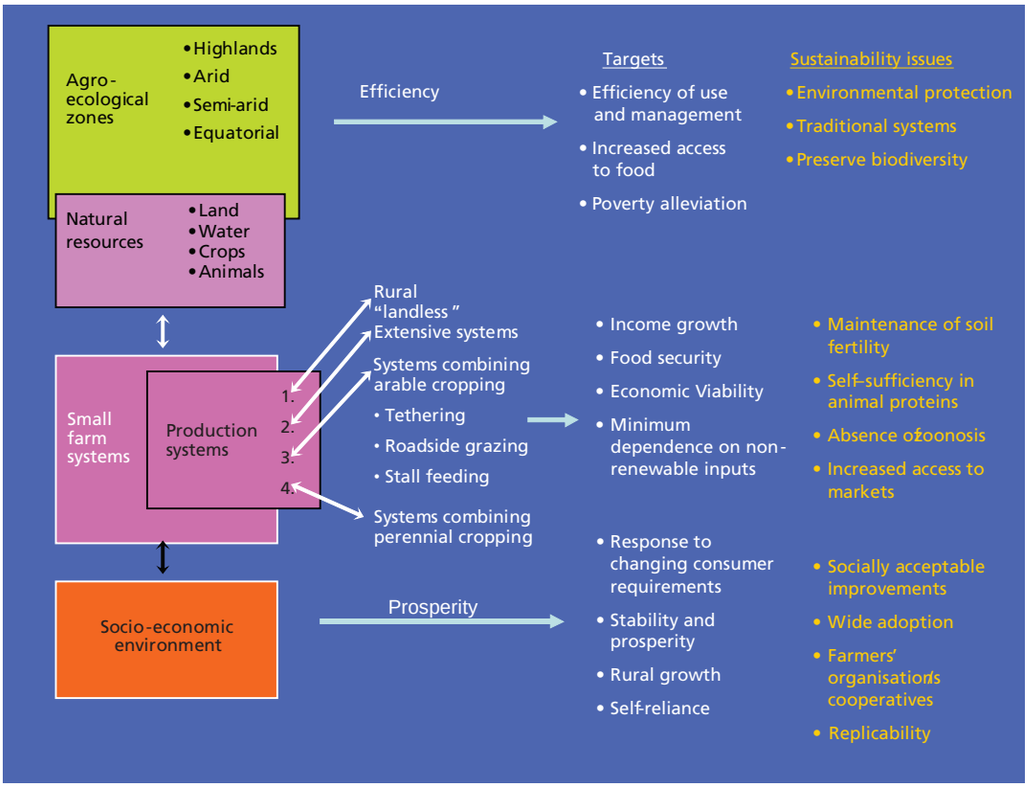

Figure 1. Sustainability of ruminant production systems.

review.indd 174 1/20/2011 11:37:58 AM

- There are between 100 and140 million children with vitamin A deficiency.

These daunting facts together pose major challenges for the future of animal production. Many of the issues are interrelated, the interactions of which have a dampening effect on animal production. The declining share of agriculture in the GDP is largely due to low productivity resulting in low growth and lower income for people dependent on agriculture. In East Asia and the Pacific for example, growth in agriculture dropped from 4% in the 1980s to mere 0.1% in 2002–2003 (ESCAP 2008).

The poverty dilemma is increasing, especially in developing communities. According to the UK Department for International Development (DFID 2008), extreme poverty and vulnerability are getting worse, initially because of the food crisis of 2008 then aggravated by high energy prices, and now because of the global financial crisis. As a result, with food prices remaining high but incomes falling, the number of people who cannot access food is increasing – by 100 million in the last year (DFID 2008). A large proportion of the poor are livestock keepers who survive because of livestock and their contribution to socio-economic well being. Improved livestock production and agricultural growth is thus an important means to reduce poverty.

Climate changes have a major impact on livestock production and also on their owners. Both risks and vulnerability are increased, in which the latter is of much greater concern. Loss in biodiversity and a higher risk of extinction are predicted. Livestock feeding systems and performance will be influenced by increased availability of more fibrous feed like straws and stovers. In rangeland situations, there is likely to be increased browse, more concentration of small ruminants, overgrazing and environmental damage.

MULTIFUNCTIONAL CONTRIBUTION OF ANIMALS

Animals are valued for their multifunctionality and the diversity of products for mankind in the developed and developing countries. Table 1 shows that the contributions refer to both food (meat, milk and eggs), and a variety of non-food products. The latter include traction and haulage activities by buffaloes and cattle, skins and hides, wealth accumulation, insurance against failure of crops, prestige in their ownership, as well as sport and recreation.

Animals occupy an important economic and ecological niche in agriculture. They serve many functions and the contributions are numerous. Their ownership provides a variety of benefits:

- Diversification in the use of production resources and reduction of socio-economic risks
- Promotion of linkages between system components (land, crops and water)
- Generation of value-added products (e.g. meat, milk, eggs and skins)
- Income generation, investment, insurance and economic security
- Supply of draught power for crop cultivation, transportation and haulage operations
- Contribution to soil fertility through nutrient recycling (dung and urine)
- Contribution to sustainable agriculture, and environmental protection
- Prestige, social and recreational values; and
- Development of stable farm households.

Table 1. Buffalo and cattle products and services in Asia.

Products	Services
Meat — raw, cooked, blood, soup and processed products	Cash income, investment and wealth
Milk — fresh, sour, yoghurt, butter, cheeses, sweets, ice cream and baby food	Security and insurance
Skin — clothes, leather, shoes, water and grain containers, tents, handicraft and thongs	Control of native herbage undergrowth in tree plantations through grazing Prestige in ownership and sport Gifts, loans and dowry
Horn	Religion e.g. harvest festivals and rituals
Bone — handicraft *Offal* — for food	Human nutrition – high quality proteins and energy, micronutrients e.g. Ca and vitamins e.g. A, B6 and B12
Draught power — e.g. cultivation	Draught and pack transport
Fertiliser — manure and urine	Soil fertility
Manure — for flooring and walls	Medicine

review.indd 175 1/20/2011 11:37:58 AM

Small animals such as chicken, ducks, goats, sheep, rabbits, quail, turkeys and geese are especially important for meeting the daily and immediate household needs for precious animal proteins. These therefore make a most important contribution to food security. Small stocks are often managed by women and children and promote the stability of farm households (Wahyuni *et al.* 1985).

Animal products such as meat, eggs and milk are important, concentrated and digestible sources of high quality proteins and energy, and they significantly contribute to good health. These sources also supply micro nutrients such as calcium, iron, zinc and vitamins A, B6 and B12, which are often deficient in cereal-based diets.

Among the red meat, goat meat has a higher lean content than beef or mutton because fat tends to be more concentrated in the viscera rather than sub-cutaneously. Goat milk also has two advantages over cow milk. One is its anti-allergic properties and the other is the presence of higher levels of six of the ten essential amino acids, and also monounsaturated, polyunsaturated, and medium chain triglycerides, all of which are known to benefit human health (Devendra 2007a).

The growth in demand for meat and milk will be greatest in Asia and Sub-Saharan Africa. Although all types of meat are consumed, the *per capita* consumption of non-ruminant meat, notably from pigs and poultry is the greatest, with increased annual rates of 4% and 7%, respectively. The demand for these two types of meat will exceed that of all other meat and this demand will come mainly from Asia. In addition, the demand for dairy products will also increase throughout the developing countries and on account of shortfall in supply, much of the demand for milk will have to be met by increasing import.

The acuteness of the demand situation also concerns Malaysia. Table 2 indicates the current and projected *per capita* consumption of individual foods of animal origin, and the corresponding levels of self-sufficiency for each species. Compared to the advances and self-sufficiency in meat produced by the non-ruminant sector, the ruminant sector lags well behind and the situation is dismal. With beef, the levels of self-sufficiency are decreasing but are projected to increase marginally by 2010. With small ruminant meat, the situation is expected to remain static. Table 2 also shows that for all meat without exception, per capita consumption is rising, and is projected to rise even further.

A recalculation of the data on dressed meat and subsequent conversion to *per capita* intake of animal proteins (Table 2) indicates that *per capita* intake is increasing. Compared to the intake in 2005, the projected consumption in 2010 of 97.1 g/day represents an increase of about 378%. Additionally, Table 2 also indicates that non-ruminants contributed 90.1%–93.7% of the protein intake, with ruminants contributing only 6.3%–9.9%. (Devendra 2006).

ANIMAL PRODUCTION SYSTEMS

Animal production involves both non-ruminants and ruminants and a variety of systems that are also integrated with crops. The systems have evolved over time and vary as functions of AEZs and the intensity of farming systems. The types of crops grown and the cropping systems determine the link with animals through the quantity, quality and distribution of animal feed resources throughout the year.

Four main livestock systems are identifiable (Devendra *et al*. 2005; Devendra 2007b):

- Landless
  > Urban and peri-urban industrial landless systems
  > Rural landless livestock production
- Mixed crop-based
- Agro-pastoral; and
- Rangeland-based.

Within the non-ruminant sector two categories are identifiable:

- Modern, demand-driven and capital-intensive non-ruminant sector that produces poultry meat, eggs and pork. Some milk is also produced from dairy

Table 2. *Per capita* consumption and percentage self-sufficiency levels of individual livestock commodities in Malaysia (1990–2010, kg/yr.)

Commodity	1990	1995	2000	2005[a]	2010[a]
Poultry	18.9 (115.2)	29.6 (112.4)	27.3 (112.5)	27.3 (112.5)	36.8 (125.2)
Pork	10.1 (126.3)	10.1 (135.2)	6.9 (99.5)	9.3 (91.5)	9.2 (102.3)
Beef	3. 2 (23.9)	4.2 (19.7)	4.8 (15.8)	6.7 (23.2)	8.5 (28.3)
Goat meat and mutton	0.4 (8.8) [b]	0.6 (5.9)	0.6 (5.9)	0.7 (8.9)	0.7 (10.2)

Source: Department of Veterinary Services, Malaysia (2003)
[a] Refer to self-sufficiency data (%)
[b] These are projections

review.indd 176 1/20/2011 11:37:58 AM

cattle and buffaloes. These are mainly industrial and peri-urban systems, which are very efficient and have good market access. The systems are very intensive, involve large concentrations of animals, have increasing pollution problems and disease risks to humans. The collection and disposal of animal manure is of increasing concern, with very limited evidence of recycling the material for crop production; and

- Traditional, resource-driven and labour intensive ruminant sector, which produces a multitude of services to subsistence farms. Low technology uptake, insufficient market facilities and infrastructure, and small economies of scale are common.

Within the ruminant production systems, there are three categories:

- Extensive systems
- Systems combining arable cropping (roadside, communal and arable grazing systems, tethering, and cut-and-carry feeding); and
- Systems integrated with tree cropping.

These production systems are unlikely to change in the foreseeable future (Mahadevan & Devendra 1986). New proposed systems and returns from them would have to be demonstrably superior and supported by massive capital and other resources. Overall, current trends suggest that the non-ruminant pig and poultry industries will continue to contribute the major share of meat and all of egg production to meet projected human needs. This is linked with the application of major advances in non-ruminant nutrition which enable maximum performance per animal and high efficiency of feed conversion. With ruminants by comparison, overall meat production continues to come mainly from the slaughter of numbers rather than improved animals having good growth rates, optimum slaughter weights and short duration to slaughter.

STRATEGIC OPPORTUNITIES FOR INCREASING PRODUCTIVITY

Strategic opportunities exist for increasing productivity, especially in the ruminant sector, in tandem with the need to increase food from animals in the future. These opportunities relate directly to overcoming the constraints and the use of animals as an entry point for development.

Targetting Development of Rainfed Areas

The justification for targeting the rainfed areas in Asia relates to the twin reasons of inadequate availability of arable land and the need to increase productivity from animals to match the projected human needs. Inadequacy of arable land is associated with the following reasons:

- Demand for agricultural land to meet human needs e.g. housing, recreation and industrialisation
- Expansion of crop production to ceiling levels
- Increasing and very high animal densities
- Increased urbanisation and use of arable land; and
- Growing environmental concerns due to very intensive crop production e.g. acidification and salinisation with rice cultivation, and human health risks due to expanding peri-urban poultry and pig production.

Consideration must therefore be given to improved use of rainfed areas and the management of natural resources therein. The priority AEZs are the rainfed humid/sub-humid tropical systems and rainfed arid/semi-arid sub-systems. Within these, two broad areas are recognised: rainfed lowlands and rainfed uplands. The characteristics of the lowlands and uplands have been reported (Devendra *et al.* 1997).The lowlands have larger areas of arable and permanent cropland which account for the greater crop production in these areas.

The real justification for focusing attention on the development of rainfed areas is reflected in the following facts:

- Emphasis in the past has been mainly in the irrigated areas through the 'Green Revolution', which were overused
- Available rainfed area account for about 82% of the land area in Asia, found mainly in the arid/semi-arid zones and also sub-humid and humid zones (TAC 1992)
- Within the rainfed areas, in the lowlands and uplands, there exists 51%–55% of the total population of cattle and small ruminants in Asia
- 86% of the total human population in Asia is found in these areas; poverty and the poorest of the poor are also found here; and
- Natural resource degradation is evident and major challenges exist for their integration and efficient use.

Table 3 provides information on the extent of the rainfed areas (CGIAR/TAC 2000). In Asia, rainfed areas (marginal/less favoured + arid lands + forests and woodlands) accounted for 83.1% of agricultural lands compared to 16.6% of favoured land. Marginal and arid lands alone constituted 48.5% of the total area. Additionally, about 63% of the rural population was found in the former, compared to only 37% in the favoured areas. It is of interest to note in this context that in 1993 in India, 42% of the rural poor lived in low potential rainfed areas, 16% in irrigated areas, and 42% in high potential rainfed areas (Fan & Hazell 2000).

review.indd 177 1/20/2011 11:37:58 AM

Table 3. Distribution of land types by region (CGIAR/TAC 2000).

Region	Land type (% of total land)				
	Favoured	Marginal	Sparsely populated arid lands	Forest and woodlands	Rural population living in favoured lands (%)
Asia	16.6	30.0	18.5	34.6	37.0
Latin America and Caribbean	9.6	20.3	8.1	61.9	34.0
Sub-Saharan Africa	8.5	23.1	24.6	43.7	27.0
Near East and N. America	7.8	22.6	65.8	3.9	24.0
Total (105 countries)	10.7	24.0	25.9	39.4	35.0

The rainfed AEZ`s of relevance are as follows:

- Rainfed temperate and tropical highlands — mainly the Hindu-Kush/Himalayan region
- Rainfed humid/ sub-humid tropical systems — mainly countries in Indo-China, South East and East Asia, and the Pacific Islands, parts of South Asia to include Bangladesh and Sri Lanka; and
- Rainfed arid/semi-arid tropical systems — mainly countries in South Asia excluding Nepal and Bangladesh.

The rainfed humid/sub-humid and rainfed arid/semi-arid tropical systems were priority AEZs. The average annual rainfall was between 1500 mm – 2300 mm, rice-based cropping systems were common but also included other annual crops and tree crops. Both ruminants and non-ruminant were reared, and the presence of both animal and crop diversity provided a variety of crop-animal interactions (Devendra & Thomas 2002). These effects of which provide major opportunities for research and development activities on productivity, livelihood of people and sustainable agriculture. The overriding major constraint was the 5–7 months of dry period. There was a 10%–25% level of contribution by animals to total farm income (Devendra 2005).

A few countries such as China, India and Indonesia have given priority to the development of these rainfed areas. In China for example, the northwestern region is given priority for the intensification of agricultural production and creation of 'climate-free' agriculture in the grasslands through irrigation from underground sources. However, population pressures on these grasslands have been increasing, with resultant increased poverty rates, degradation and dust storms (MEA 2005).

Development of Small Farms

Central to the priority development of rainfed areas is the need to concurrently focus on the small farms in Asia. Based on land area of less than two hectares, an overwhelming majority of 87% of the 470 million small farms worldwide are found in Asia (Nagayets 2005) of which China alone accounted for about 40.2% of the farms, followed by India (23%). Relevant issues associated with these farms are their significant current contribution, the considerable size of the rural populations and livestock keepers therein, the presence of continuing poverty and hunger, the threats of economies of scale, globalisation and commercialisation.

Small farms have been consistently resilient, and were able to withstand the Asian economic crisis, unlike the larger farms with higher capital requirements, input and risks. Improving small farm productivity is the most effective way to achieve mass poverty alleviation and agricultural growth and productivity in rural areas, backed by investment in infrastructure, market reform, credit facilities and risk management strategies. Recently there have been concerted references for urgent development attention by several international agencies (IAASTD 2008; ESCAP 2008; IFAD 2009; UNEP 2009; Koning & van Iffersum 2009) and by the Food and Agriculture Organisation at the recently concluded World Food Security Summit. For Asia, the characteristics of these farms, potential importance and their relevance for food production in the future has been reported (Devendra 2010).

Intergrated Crop-animal Systems: The Potential of the Oil Palm

There are two major advantages of integrated animal-crop systems involving both annual and perennial crops synonymous with mixed farming, which is characteristic of Asian farming systems. Firstly, the interactions of the individual components result in the overall productivity being significantly increased due to additive effects. Secondly, the integration enables increased efficiency in the use of production resources and also enhances the sustainability of the system.

Of the two, the latter is very underestimated, especially in situations where there is emphasis on perennial tree crop cultivation such as with citrus, coconut, oil palm and rubber.

review.indd 178 1/20/2011 11:37:58 AM

It is unfortunate that this system is being overlooked in the natonal development agenda. The oil palm is a particularly important 'golden crop' and Asia has about 84% of the total world land area under oil palm of about 10.6 million ha. The largest land areas under oil palm of 8.4 million ha are found in Malaysia and Indonesia, who together own over 79% of the world planted area and produce about 87% of the total world output of palm oil, followed by much smaller areas being found in Thailand, Philippines, India and Papua New Guinea. The integration model with oil palm offers extension of the principles involved with other tree crops like coconuts in the Philippines, Sri Lanka and South Asia, rubber in Indonesia, and citrus in Thailand and Vietnam.

Types of ruminants-oil palm interactions. Associated with the oil palm environment are the many benefits of crop-animal- soil interactions as follows:

(a) Beneficial effects of shade and available feed on animals, especially exotic stock
(b) With large ruminants, draught animal power on land preparation and crop growth
(c) Dung and urine on soil fertility and crop growth
(d) Use of AIBP from trees *in situ*; and
(e) Use of native vegetation and effects on cost of weed control, crop management and crop growth.

Economic impact. A review of the economic impact involving 21 case studies, including five using goats from seven countries over the period (1984–2007), gave the following conclusions (Devendra 2007c):

- Improved soil fertility was evident
- Distinct economic benefits were apparent e.g. improved crop yields and savings on weeding cost with concurrent increased profits
- Very few studies were concerned with quantitative animal productivity
- Decreased carbon atmospheric emission due to improved forage management; and
- Integrating goats was advantageous.

Theoretical calculations done by Basir (2005) on the economic return from four hectares of land under oil palm, inter- cropping as well as fodder cultivation for a seven year period using average and realistic field data showed that RM14,562 was the income generated from oil palm after seven years. The beneficial income generated as percentage of total income in favour of integration for cattle, sheep and goats were 44.4%, 86.6% and 91.5%, respectively. The beneficiaries of increased productivity and income were the small farmers, labourers who owned animals and the larger plantations.

Stratification and production options. The oil palm environment and the potential economic impact offers a number of production options that can significantly contribute to improve NRM, increased productivity and enhanced food security in Malaysia. Unfortunately, the wider adoption of the system is slow, and may require government intervention with appropriate incentives.

The production options include the following (Devendra 2009):

- Increase breeding of goat numbers and productivity
- More intensive utilisation of the available forage biomass and AIBP *in situ*
- Development of intensive zero grazing systems
- Improved NRM
- Increase institutional support for integrated resource utilisation
- Encourage interdisciplinarity and a focus on holistic oil palm-based production, and
- Encourage a 'market pull', access to markets and marketing.

Currently, less than about three per cent of the land is used for integration with ruminants in Malaysia. An expansion of the oil palm area for integration by a small 10% can make a substantial quantum jump in increased meat production from ruminants.

Intensification of Productivity-enhancing Technology Application

The use of a number of proven and potentially important productivity-enhancing technologies can significantly increase productivity in animals. These include *inter alia*:

(a) Three-strata forage systems
(b) Food-feed inter-cropping
(c) Integration of ruminants with tree crops
(d) Effective utilisation of crop by- products and non-conventional feed resources
(e) Strategic supplementation
(f) Rice-vegetable-ducks-fish integration
(g) Sloping agriculture land technology; and
(h) Effective use of local feed resources: large-scale beef production using ammoniated rice straw and cottonseed cake.

The food-feed systems for example has much relevance in cropping systems for both irrigated and lowland areas. An ideal food-feed system is one that maintains and increases the yield of the food crop, sustains soil fertility and provides dietary nutrients for animals (Devendra *et al.* 2001). The concept is an important strategy that is associated with the development of all year round feeding systems.

Good examples of food-feed systems in Asia are as follows:

review.indd 179 1/20/2011 11:37:58 AM

- *Bangladesh* — Lathyrus setivus has been introduced into rice cropping systems which has resulted in increased forage yield and improved soil conditions
- *India* — Fodders grown in the summer include pearl millet, maize, sorghum and cowpea, and in winter berseem and lucerne
- *Pakistan* — Inter-cropping maize with cowpea has increased both crude protein and dry matter yields; and
- *Thailand* — Cowpea has been successfully inter-cropped with cassava to increase forage yield for ruminants in the semi-arid environment in the North East region.

In the lowland areas of Pangasinan, Philippines, rice-mungbean rotation has replaced rice-fallow. Over a six-year rice cropping period, in which Siratro was introduced for the last two years, rice yield increased to 4.5 tons/ha, compared to 3.7 tons/ha on rice – mungbean – rice system and 3.0 tons/ha on rice – fallow – rice. In addition, cattle that were normally fed on rice straw now had access to increased availability of Siratro forage (Carangal & Sevilla 1993). The siratro forage together with rice bran and urea stimulated live weight gain and reduced body weight losses during the dry season, with ultimate increased benefits to poor farmers.

Promoting intensive use of crop residues. Increasing productivity from ruminants in the future implies a need for more intensive utilisation of crop residue. Straw has a number of uses, and current feeding practices to ruminants do not encourage production responses that can be achieved with treatment and supplementation. Cereal straws need targeting to implement the known advances in ammonia treatment to improve nutritive value, as well as supplementary strategies to increase straw use by ruminants. The scientific basis of feeding supplements to ruminants fed on poor quality forage has been discussed in a number of papers (Leng 2004) and the efficient use of such feed is a major way to increase animal proteins for human consumption in the future. There is no reason why these technologies cannot be put to more intensive use and adopted more widely in Asia.

The justification for this priority focus rests directly with the potential multifunctional contribution in general, especially the capacity for meat and milk production as well as draught power. The need for concerted development is also associated with the weak development of the ruminant sector in most countries. More importantly, the fact that with the exception of the buffalo, the concentration of cattle, goats and sheep are very high in the neglected rainfed areas, where there also exists the poorest of the poor people. Rainfed areas are sizeable in Asia and account for 83% of the total land area and 63% of the total rural population (CGIAR/TAC 2000). For these reasons, improved ruminant production is the entry point for the development, increased animal protein production and food security of these areas (Devendra 2000, 2010) and adequate dietary nutrients can significantly increase animal performance and productivity.

Interdisciplinary research and farming systems perspectives. A vigorous agenda for strategic and sustainable animal production in the future will require an increased commitment to interdisciplinary research and farming system perspectives that can focus on whole-farm situations and priority AEZs. The evolving scenarios will simultaneously need to address several major issues such as nutrient flow, waste disposal, overgrazing, all year round feeding systems, zoonosis and policy. These and other aspects across livestock systems and priority production systems are highlighted in Table 4.

Strengthening research–extension–farmer linkages and technology transfer. Research – extension – farmer linkages are synonymous with technology transfer. It is the traditional model that is used for the technology delivery pathway. Public sector extension services and their efficiency vary between countries and the program focus. At present the subject constitutes a dilemma. The dilemma stems from concerns about its scope and effectiveness, especially at the present time when agriculture is waning, there are problems of globalisation and there is a need for more innovative strategies to deal with the changing environment, NRM and food insecurity issues. All of these are of grave concern to the productivity of small farms and livelihood of farmers.

Throughout Asia, there is diversity in the meaning and use of the term extension, as well as the systems and structures that deal with it. The basic perception is a unified public sector service in technology transfer which is consistent with the keywords 'talking' and 'persuasion'. Variations to the approaches exist to deal with farmers and rural communities. Currently, extension is viewed in numerous ways, from approaches to help farmers to increase production, to marketing arrangements. In recent years, extension orientation is being expanded to include innovative structural, funding and managerial arrangements (Rivera & Sulaiman 2009). Additional to all these aspects is the technical capacity, commitment and skills of the extension agent, understanding of the various constraints to development and the methods that were used for diffusion in producing the desired change.

These issues together suggest that the demands on, and orientation of, extension are many and far reaching. Of particular concern is the fact that extension appears to be detracted and moving away from the primary function and focus of diffusing technology in participatory ways to spur development and to produce the desired change. There is increasing risk that the primary task of technology

review.indd 180 1/20/2011 11:37:58 AM

Table 4. Summary of livestock systems, priority production systems and major issues across regions.

Type of livestock systems	Priority production system	Regions					Major issues
		Asia	SSA	CA	WANA	LAC	
Landless	• Peri-urban/urban dairy production	×	×		×	×	• Surface water contamination
	• Peri-urban / urban poultry and	×	×	×	×	×	• Zoonosis
	• Pig production						• Waste disposal
	• Feedlot (cattle or small ruminants)	×	×	×	×	×	• Nutrient flows
	• Goat and sheep production	×	×	×	×	×	• Overgrazing
Crop-based mixed	• Integrated systems with annual crops	×	×	×	×	×	• Food-feed systems
	(ruminants and non-ruminants plus fish)	×	×			×	• All year round feeding systems • Nutrient flows / soil fertility
	• Integrated systems with perennial crops (ruminants)	×				×	• Stratification • Impact of crop animal soil interactions
	• Beef and dairy production	×	×	×	×	×	• Productivity enhancement
	• Goat and sheep production	×	×	×	×	×	• Intensification and specialization • Overgrazing
Agro-pastoralist	• Cattle		×	×	×		• Feed supplies / drought strategies
	• Goat and sheep production		×	×	×		• Property regimes • Overgrazing • Trypanosomiasis
Range-based	• Sheep and goat production	×	×	×	×	×	• Drought strategies • Overgrazing • Property regimes • Marketing

Source: Devendra *et al*. 2005

Notes:

(i) SSA — Sub-Saharan Africa, CA-Central Asia, WANA — West Asia and North Africa, LAC — Latin America and the Caribbean

(ii) × Indicates that both the production systems and animal species are most important within the region.

(iii) Major issues *inter alia* are those that currently merit R&D attention. Across regions, the issues are broadly similar as is the case with dairying.

Dairy production includes buffaloes and cattle, especially in Asia; dairy goat production across regions.

transfer to meet the needs of farmers is weak and is being neglected.

The many foregoing concerns emphasise the need for a shift and transformation from the traditional methods to more adaptive farm –oriented participatory approaches. In this context, it is now widely acknowledged that systems perspectives and systems approaches are fundamental to enhance NRM, poverty, food insecurity and issues of the environment. While strong formal disciplinary training is essential, more detailed training on agricultural systems, integrated NRM and systems perspectives must be essential components of the curriculum in colleges and universities to ensure a more rounded view of addressing animal agriculture (Devendra 2011).

FUTURE DIRECTION

Expanding the development frontiers to enhance the contribution of animals necessitates urgent attention to several important issues. These issues are identified below constitute the challenges and pathways for future direction:

review.indd 181 1/20/2011 11:37:58 AM

- The multifunctional role and contributions of livestock are varied and numerous, but are currently inadequate to meet projected needs. Vigorous development strategies are needed to enhance nutritional and food security, and to improve livelihoods of developing communities.
- Prevailing livestock production systems are unlikely to change in the foreseeable future, although specialisation and intensification are inevitable. These systems have been severely hampered recently, especially in small farm systems, due to rising costs of production inputs, unpredictable markets and other externalities.
- Development policy and livestock production objectives need clearer definition, as well as institutional commitment for poverty alleviation projects.
- Predictable improvements and sustainable development that have a poverty-alleviation focus will require initial assessments and response to important prerequisites in the R&D agenda such as understanding the biophysical environment, aspirations of farming communities, constraints and real needs, gender equality and empowerment, risks and vulnerability, value chains and innovation and partnerships.
- Given the range and complexity of the issues involved, interdisciplinary R&D using systems perspectives and community-based participation are essential. These efforts need to focus directly on small farm systems, which in Asia and Africa alone account for 95 percent of the 470 million small farms worldwide that have less than 2 ha of land.
- Livestock provide an important entry point for the development of rainfed environments.
- Value chains should be seen in the broader context of the *production-post-production-consumption systems* theme.
- More aggressive and innovative efforts are necessary to improve on past efforts in projects designed to address poverty alleviation, which have now been exacerbated.
- Pro-poor poverty initiatives are threatened by climate change, which has to be incorporated into the R&D agenda.
- Creation of appropriate networks will enhance R&D capacity.
- Increased investments in livestock R&D are urgently required; and
- Promotion and development of community-based self-help groups , farmer associations and cooperatives, as well as processes of technology transfer can be enhanced through training and empowerment.

CONCLUSIONS

Major and challenging opportunities exist for accelerating productivity and the multifunctional contribution from animals in Asian agriculture in the context of improved production to consumption systems. Increased efficiency of NRM can enhance the various AEZs in their predominant position in food production. Major constraints including climate change exist, but there are also compelling opportunities and socio-economic benefits that involve rural communities. Small farms will continue to be important in the production of a high proportion of especially ruminant meat and milk, to enhance the natural resource base, and also to help alleviate poverty, hunger and food insecurity in the foreseeable future. Priority development of the rainfed areas is essential within which animal production can serve as the entry point to address food production and pro-poor initiatives. Social and effective development policies are also needed to spur agricultural development. These issues, together with increased investment (Fan, Hazell & Thorat 2000) and institutional commitment, can provide for improved animal production systems in Asia and make a forceful contribution for enhanced human welfare in the immediate tomorrow.

The challenges for livestock production in the face of current realities are therefore overwhelming and urgent. These include frontal attention to the following, *inter alia*:

- Increasing animal protein supplies to match human needs
- Increasing efficiency in natural resource management
- Increasing food and nutritional security
- Mitigating or adapting production systems to deal with climate change threats
- Identifying ways to eliminate the poverty dilemma
- Establishing more concerted poverty alleviation and pro-poor development projects
- Improving livelihoods of small scale farming communities
- Improving self-reliance of small scale farmers; and
- Investing in agricultural growth.

The resolution of these issues hangs in the balance in the developing world. Revitalising pathways to increase productivity and the multifunctional contribution from livestock for developing communities in the future is, therefore, compelling and challenging. Addressing the many interrelated issues is a collective task, emphasising :

- the enduring evolutionary links between humans and livestock,
- the continuing multifunctional contribution of animals, and
- the demonstrable capacity of animal production as one of the important sustaining industries for human welfare in the future.

review.indd 182 1/20/2011 11:37:59 AM

This vision is consistent with the *Cape Town Declaration on Principles for Animal Production* that was unanimously endorsed at the conclusion of the *10th World Conference on Animal Production* in November 2008 which states the following:

- Animal production is practiced for the well-being of the human population.
- Animal production is practiced with regard to human dignity.
- Animal production is practiced using domesticated and semi-domesticated animals or game that have been adapted to the circumstances of production.
- Animal production is practiced with regard to sentient animals in a morally justifiable manner; and
- Animal production is practiced with regard to the impact it may have on the environment.

Date of submission: November 2009
Date of acceptance: August 2010

REFERENCES

Carangal, VR & Sevilla, CC 1993, 'Crop-animal systems research in Asia', in *Proceedings V11th World Conference on Animal Production, Edmonton, Canada*, pp. 367–386.

CGIAR/TAC (Consultative Group on International Agricultural Research/ Technical Advisory Committee) 2000, 'CGIAR priorities for marginal lands', *CGIAR*, Washington, U.S.A. (Mimeograph.)

Devendra, C 2004, 'Meeting the increased demand for animal products in Asia: opportunities and challenges for research', in *Responding to the livestock revolution. British Society on Animal Sciences Publication*, no. 33, 209–228.

Devendra, C 2005, 'Improvement of crop-animal systems in rainfed agriculture in South East Asia', in Rawlinson, P., Wachirapakorn, C., Pakdee, P & Wanapat, M, eds in *Proceedings International Conference on Livestock-Crop Systems to Meet the Challenges of Globalisation,* eds Rawlinson *et al*, 14-18 Nov., Khon Kaen, Thailand, vol. 1, pp. 220–231.

Devendra, C 2006, '*Enhancing animal protein supplies in Malaysia: opportunities and challenges*', Academy of Sciences Malaysia, Kuala Lumpur, Malaysia.

Devendra, C 2007a, *Goats: biology, production and development in Asia*, Academy of Sciences Malaysia, Kuala Lumpur, Malaysia.

Devendra, C 2007b, 'Perspectives on animal production systems in Asia', *Livestock Science*, vol. 106, no. 1, 7–20.

Devendra, C 2007c, 'Integrated tree-crops ruminant systems: expanding the research and development frontiers in the oil palm', in *Proceedings: Workshop on Integrated Tree Crops-ruminant Systems (ITCRS)/Assessment of Status and Opportunities in Malaysia*, eds C Devendra, S Shanmugavelu, & HK Wong,), Kuala Lumpur, Academy of Science Malaysia.

Devendra, C 2009, 'Intensification of integrated oil palm — ruminant systems: enhancing productivity and sustainability in South East Asia', *Outlook on Agriculture*, vol. 38, no. 1, pp. 71–81.

Devendra, C 2010, *Small farms in Asia. Revitalising agricultural production, food security and rural prosperity*, Academy of Sciences Malaysia, Kuala Lumpur, Malaysia.

Devendra, C 2011, 'Agricultural education and technological change for sustaining productivity enhancement and prosperity in Asia', in *Agricultural education and training in Africa*, eds F Swanapoel & A Strobel, University of the Free State, Bloemfontein, South Africa (In press).

Devendra, C & Thomas, D 2001, 'Crop — animal interactions in mixed farming systems in Asia', *Agricultural Systems*, vol. 71, no. 1–2, pp. 27–40.

Devendra, C, Sevilla, C & Pezo, D 2001, 'Food -feed systems in Asia', *Asian-Australasian Journal of Animal Science*, vol. 14, no. 5, pp. 733–745.

Devendra, C, Thomas, D, Jabbar, MA & Kudo, H 1997, 'Improvement of livestock production in crop-animal systems in the rainfed agro-ecological zones of South East Asia', International Livestock Research Institute, Nairobi, Kenya.

Devendra, C, Morton, JF, & Rischkovsky, B 2005, 'Livestock systems', in *Livestock and Wealth Creation*, eds E Owen *et al.* Nottingham University Press, United Kingdom.

Devendra, C, Thomas, D, Jabbar, MA & Zerbini, E 2000, '*Improvement of livestock production in crop-animal systems in agro-ecological zones of South Asia*', International Livestock Research Institute, Nairobi, Kenya.

DFID 2008, Department for International Development, United Kingdom <http://www.new-ag.info/doc.php?id=705&s=t>.

Department of Veterinary Services 2004, 'Livestock statistics', Department of Veterinary Services, Kuala Lumpur, Malaysia. (Mimeograph.)

Food and Agriculture Oganisation 2003, 'World agriculture: towards 2015/2030', FAO, Rome, Italy, <//ftp.fao.org/docrep/fao/004/ y3557e/y3557e/pdf.> viewed 30th March 2009.

Fan, S & Hazel, P 2000, 'Should developing countries invest more in less-favored lands? An empirical analysis of rural India', *Economic and Political Weekly*, vol. 35, no.17, pp. 1455–1564.

Fan, S, Hazell, P & Thorat, S 2000, 'Targeting public investments by agroecological zone to achieve growth and poverty alleviation goals in rural India', *Food Policy*, vol. 20, no.4, pp. 411–428.

Basir, I 2005, *Land agricultural policy: a mismatch*, Malaysian Palm Oil Board, Kuala Lumpur, Malaysia.

IASSTD 2008, *International assessment on agricultural knowledge, science and technology for development*, United Nations Environment Programme (UNEP), Nairobi, Kenya, <http:// agassessment.watch.org>.

IFAD, 2009, *New thinking to solve old problems*, viewed 26 March 2009, <http://www.ipsnews.net/africa/nota.asp?idnews=45905>.

review.indd 183 1/20/2011 11:37:59 AM

Koning, N & van Iffersum, M 2009, 'Can the world have enough to eat?', *Environmental sustainability*, vol. 1, pp. 77–82.

Leng RA, 2004, 'Requirements for protein meals for ruminant meat production', in *Protein sources for the animal feed industry. Expert consultation and workshop*, Bangkok, Thailand, FAO, Rome, Italy, pp. 225–254.

Mahadevan, P & Devendra, C (1986), 'Present and projected ruminant production systems of South East Asia and the South Pacific', in *Forages in South East Asia and the Pacific, Australian Centre for International Agricultural Research Proceedings*, no. 12, pp. 1–6.

Millennium Ecosystem Assessment 2005, *Current state and trends*, vol 1, eds R Hassan, R Scholes & Ash, no. 1, pp. 133–134.

Nagayets, O 2005, 'Small farms: current status and key trends', in *Proceedings The Future of Small Farms*, International Food Policy Research Institute, Washington, D.C., U.S.A., pp. 355–356.

Rivera, WM & Sulaiman, VR 2009, 'Extension: object of reform, engine for innovation', *Outlook on Agriculture*. 38, no. 3, 267–274.

Steinfeld, H, Gerber, P, Wassenaar, T, Castel, V, Rosales, M & de Haan, C 2006, *Livestock's long shadow*, Food and Agriculture Organisation, Rome, Italy.

Technical Advisory Committee FAO 1992, *Review of CGIAR of priorities and strategies*, pt 1, TAC Secretariat, FAO, Rome, Italy.

United Nations Environment Programme 2009, *The environmental food crisis*, UNEP, Nairobi, Kenya.

Wahyuni, S, Gaylord, M & Knipscheer, HC 1985, `'Women's decision making role in small ruminant production: the conflicting views of husbands and wives', in *Small ruminant-coordinated research support project*, Working Paper no. 43, Bogor, Indonesia.

World Bank 2003, *Reaching the poor. A renewal strategy for rural development*, Washington, D.C., U.S.A. (Mimeograph).

World Bank 2009a, *The state of food security in the world*, Washington, D.C., U.S.A.

World Bank 2009b, *Minding the stock: bringing public policy to bear on livestock policy*, Washington, U.S.A., No. 44010-GLB.

review.indd 184 1/20/2011 11:37:59 AM

Multivariate Regression in Complex Survey Design

G.M. Oyeyemi[1,*] and A.A. Adewara[1]

Adjustment for both stratification and clustering variables in multivariate regression analysis of complex survey designs depends on whether the model variables are exogenous or endogenous. Adjustments were necessary if the variables are exogenous, furthermore adjustments for clustering were found to be more important than those as for stratification.

Key words: adjustment; complex survey; endogenous; exogenous; cluster; strata; health survey

In most demographic and health surveys, basic descriptive statistics are given by the bivariate relationship between a health variable and some health indicators known as socio-economic status (SES). More importantly, one might want to test for the existence of causal relationships between a health variable and the SES variables and to examine the nature of the causality (Fergusen & Corey 1990). These tasks require moving from bivariate to multiple or multivariate regression analysis. In this paper, we examine some issues that generally deserve consideration when undertaking multivariate analysis in health surveys, especially when dealing with a complex survey design.

COMPLEX HEALTH SURVEY DESIGN

Demographic and health surveys used for analysis of health sectors in developing countries have complex sample designs. Typically, there is simple random sampling at some level or levels but there may be separate sampling of population sub-groups known as strata. There is also the possibility of groups of observations, otherwise known as clusters which may not be sampled independently while there may be over sampling of certain groups. The combination of these different sampling schemes constitute what is known as a complex design. In the following sections we discuss the components of complex survey designs and the need for standard error adjustment of the estimates.

STRATIFICATION

Stratification is a method of using an auxiliary variable to increase the precision of the estimate of a population characteristic (Cochran 1977; Okafor 2002; Rajj & Chandhok 1999). This design method is typically employed in household surveys undertaken in developing countries. Nigeria's Demographic and Health Survey (NDHS) uses geopolitical zones (regions) as the stratification variable in most of its surveys. A random sample, of predetermined size, is then selected independently from each of these strata. The sample accounted for by each stratum may or may not correspond to population proportion. There is equal allocation, proportional allocation and optimum allocation among others depending on the design and situation.

In the case when the sample proportions do not correspond to population proportions, the overall sample is not representative of the population and the issue of sample weight arises. If the population means differ across the strata, predetermination of strata sample sizes reduces the sampling variance of the estimators of the means (Fergusen & Corey 1990). Consequently, the standard errors of estimates of population means and other statistics should be adjusted. Adjustment is not necessary in regression analysis and in a wide variety of other multivariate modeling approaches, the provided stratification variable is exogenous within the model (Wooldridge 2001, 2005). Ordinary Least Square (OLS) estimation is found to be consistent and efficient and the usual standard errors are valid in such cases. Only if the stratification is based on an endogenous variable then the standard errors should be adjusted (Wooldridge 2001).

Therefore, the need to adjust standard errors for stratification is situation specific. In practice, adjusting for stratification may inflate the standard errors. Standard errors robust to heteroscedasiticity and clustering will be required for survey data (Hao *et al.* 2004). The magnitude of adjustment for stratification is usually modest, and normally downwards. A conservative strategy is not to make adjustments. If the stratification variable is exogenous, then there is need for adjustment and if it is endogenous, any adjustment will normally increase the statistical significance.

[1] Department of Statistics, University of Ilorin, Ilorin, Nigeria
*Corresponding author (e-mail: gmoyeyemi@gmail.com)

science forum.indd 185 1/20/2011 11:39:34 AM

CLUSTERING

In most surveys, especially in a large and complex survey, there is no sampling frame or list of households or dwelling units from which to select a sample. Therefore it is not possible or feasible to draw a sample directly from the population. In order to overcome this problem, groups of elements called clusters are formed by pooling together elements which are physically close to each other (Cochran 1977; Okafor 2002). A sample of these cluster units is then selected from the total number of clusters by an appropriate sampling scheme. This method is known as cluster sampling and a sampling unit in this case (a cluster) contains more than one unit.

Cluster sampling in health surveys have two or more stages or sampling processes. In the first stage, groups known as clusters of households are randomly sampled from either the population or strata. Typically, these clusters are villages, hamlets or neighborhoods of towns and cities. In the second stage, households are randomly sampled from each of the selected clusters. An important distinction of cluster sampling from stratifying sampling is that strata are selected deterministically, whereas clusters are selected randomly (Owen *et al.* 2007). Another difference is that strata are typically few in number and contain many observations while clusters are large in number but contain relatively few observations.

As a result of this design, observations are expected not to be independent within clusters but may be independent across clusters. There is likely to be more homogeneity within clusters than across clusters. The adjustment in standard errors of the estimates like stratification sampling depends on whether the cluster variable has endogenous or exogenous effects on the model.

RANDOM EFFECTS MODEL

A cluster or stratification variable is exogenous in a model if it has random effects on the model. Consider the following model:

$$y_{ic} = X_{ic}\beta + \lambda_c + \varepsilon_{ic}$$
$$E[\varepsilon_{ic} / X_{ic}, \lambda_c] = [\varepsilon_{ic}] = 0 \quad (1)$$

where i and c are the household (individual) and cluster (or stratification) variables respectively; X_{ic} is a vector of regressors; λ_c is cluster (or stratification) effects; and ε_{ic} are the error terms. If we assume that the cluster (stratification) effects are independent of the regressors, $E[\lambda_c / X_c] = E[\lambda_c]$, then the composite error is $u_{ic} = \lambda_c + \varepsilon_{ic}$. This model is known as random effects model.

A conventional point estimate like OLS is consistent but inefficiency arises from the fact that the cluster (or stratification) induces correlation in the composite error, which in addition, requires adjustment of the standard errors. One option is to accept inefficiency and simply adjust the standard errors. An alternative strategy is to presume consistency by estimating the within cluster or strata correlation and taking account of this in the estimation of the model parameters. In the linear case, the analyst could use generalized least square (GLS). A Lagrange Multiplier test can be used to test the null that the cluster (or stratification) effects are not significant and that the OLS is efficient (Wooldridge 2005).

FIXED EFFECTS MODEL

Using the model in Equation (1), and if we relax the assumption of independence between the cluster effects and the regressors, $E[\lambda_c / X_c] = E[\lambda_c]$, we obtain a fixed effects model.

More importantly, Hausman test of null of independence between the cluster (or stratification) effects and regressors can be used to select between the random and fixed effects models (Wooldridge 2001).

Nigerian Demographic and Health Survey (NDHS)

The NDHS provides estimates of national health and family planning statistics. The survey is designed to provide estimates for Nigeria as a whole, for urban and rural areas and for the six geopolitical regions. The survey is always conducted on a yearly basis. The 2005 NDHS data was used in this work. The health variable used as the dependent variable was the nutritional status of children and some selected variables such as the socio-economic status indicators (regressors). A child's nutritional status was assessed by comparing height and weight measurements against an international standard. By this standard, many children are malnourished (NDHS 2005). Three categories of nutritional status were identified, and they were stunting (height-for-age), wasting (weight-for-height) and underweight (weight-for-age). The socio-economic variables used were wealth index, ideal number of children, size of the baby at birth, current age of the child, sex of the child, the birth order, parent's index of height for age, total number of children ever born, educational level and religion of the parents.

STANDARD ERROR ADJUSTMENT FOR CLUSTERING AND STRATIFICATION

A multiple regression using stunting (height-for-age) as the nutritional status of the selected independent variables using the OLS method was obtained. In addition to OLS estimates, we present analyses that give standard errors with various degrees of adjustment for stratification, cluster

science forum.indd 186 1/20/2011 11:39:34 AM

and combinations of both in the model. The stratification variable used in the model was the region, which constituted the six geopolitical zones in the country. The clustering variable was the household unit. The STATA package was used to analyze the data because of its uniqueness in handling complex survey designs.

The OLS point estimates of the independent variables (coefficients) and the standard errors are given in columns 1 and 2, respectively in Table 1. Relative to simple OLS standard errors, the adjusted standard errors for cluster, stratification, and combined stratification and cluster are shown in columns 3, 4, and 5, respectively. The overall model summary (R-Square) and sample size are also indicated.

RANDOM AND FIXED EFFECTS FOR STRATIFICATION AND CLUSTER

We also examined and compared the effects of cluster as fixed or random in relation to when it was only adjusted for clusters in the OLS model. For consistency, we used the dependent and independent variables used earlier. Table 2 gives the coefficients, fixed as well as the random effects model for OLS in columns 1, 3, and 5, respectively, while columns 2, 4, and 6 give their corresponding standard errors in that order. Table 3 gives the corresponding result for stratification. Both Hausman and Breuch-Pagan Lagrange Multiplier (B-P LM) tests of significance of the stratifying or clustering variable are indicated in the two tables.

DISCUSSION OF RESULTS

Adjusting for stratification alone (Table 1 column 4) tends to inflate the standard errors in some cases when compared with conventional OLS standard errors. In some cases, the adjustment is slightly downward. The adjustments do not change the level of significanse. Adjusting for cluster and not for stratification (Table 1 Column 3) has greater impact than stratification. In all the cases, the adjustment was upward and it actually changed the level of significance of the constant term from being significant to not significant. Meanwhile, adjusting for both stratification and cluster (Table 1 column 5) shows that there is no difference between adjusting for cluster and for both stratification and cluster. The implication is that, given the adjustment for clustering, the marginal impact of stratification adjustment is small (columns 3 and 5 of Table 1).

Tables 2 and 3 give the results of examining the fixed and random effects models for clustering and stratification variables, respectively. For the clustering variables, apart from having different coefficients for both fixed and random effects models compared with OLS, the fixed effect model indicated the two variables (ideal number of child and religion) to be insignificant while all the variables were significant in both OLS and random effects models. A similar result was obtained for the stratification variable except that only an ideal number of children was reported to be insignificant for the fixed effect model.

Table 1. Regression analysis of stunting on some socio-economic status variables.

Variable	Coefficient	Standard errors			
		Unadjusted	Cluster	Stratification	Stratification and cluster
Wealth index	0.1647***	0.0251	0.0289	0.0248	0.0289
Ideal no of children	–0.0373**	0.0113	0.0134	0.0116	0.0134
Child size at birth	–0.1279***	0.0440	0.0462	0.0438	0.0463
Current age of child	–0.3514***	0.0277	0.0315	0.0286	0.0367
Sex	–0.2293***	0.0599	0.0600	0.0600	0.0600
Birth order	–0.4960***	0.0660	0.0685	0.0680	0.0674
Parents index					
Of height for age	0.1909***	0.0296	0.0321	0.0304	0.0319
Total no. of children	0.5422***	0.0664	0.0702	0.0680	0.0689
Educational level	0.1055***	0.0254	0.0264	0.0240	0.0263
Religion	–0.0664***	0.0664	0.0753	0.0654	0.0730
Constant	–0.4334**	0.1946	0.2149	0.1924	0.2149
Sample size = 5138		$R^2 = 0.1559$	$R^2 = 0.1596$	$R^2 = 0.1596$	$R^2 = 0.1596$

* Significant at 0.10; ** Significant at 0.05; and *** Significant at 0.01

science forum.indd 187 1/20/2011 11:39:34 AM

Table 2. Regression analysis of stunting on some socio-economic status variables for cluster.

Variable	Coefficients and standard errors					
	Cluster		Random effects		Fixed effects	
	Coeff.	Adj. S.E. (OLS)	Coeff.	S.E.	Coeff.	S.E.
Wealth index	0.1647***	0.0289	0.1607***	0.0295	0.0949*	0.0451
Ideal no of children	–0.0373**	0.0134	–0.0302**	0.0115	–0.0180	0.0126
Child size at birth	–0.1279***	0.0462	–0.1663***	0.0443	–0.2014***	0.0471
Current age of child	–0.3514***	0.0315	–0.3550***	0.0274	–0.3693***	0.0287
Sex	–0.2293***	0.0600	–0.2356***	0.0588	–0.2406***	0.0609
Birth order	–0.4960***	0.0685	–0.4994***	0.0651	–0.5264***	0.0679
Parents index						
Of height for age	0.1909***	0.0321	0.1847***	0.0299	0.1792***	0.0322
Total no. of children	0.5422***	0.0702	0.5393***	0.0655	0.5555***	0.0683
Educational level	0.1055***	0.0264	0.1034***	0.0263	0.0770***	0.0296
Religion	–0.0664***	0.0753	–0.3984***	0.0737	–0.1564	0.0998
Constant	–0.4334**	0.2149	–0.4403*	0.2127	–0.5542*	0.2679
Sample size = 5138	R^2 = 0.1596		R^2 = 0.1589		R^2 = 0.1434	
					B-PLM = 81.27	p-value = 0.0000
					Hausman = 33. 02	p-value = 0.0003

* Significant at 0.10; ** Significant at 0.05; and *** Significant at 0.01

Table 3. Regression analysis of stunting on some socio-economic status variables for stratification.

Variable	Coefficients and standard errors					
	Stratification		Random effects		Fixed effects	
	Coeff.	Adj. S.E. (OLS)	Coeff.	S.E.	Coeff.	S.E.
Wealth index	0.1647***	0.0248	0.1647***	0.0251	0.1745***	0.0250
Ideal no of children	–0.0373**	0.0116	–0.0373**	0.0113	–0.0179	0.0114
Child size at birth	–0.1279***	0.0438	–0.1279**	0.0440	–0.2014***	0.0438
Current age of child	–0.3514***	0.0286	–0.3514***	0.0277	–0.3484***	0.0271
Sex	–0.2293***	0.0600	–0.2293***	0.0599	–0.2245***	0.0587
Birth order	–0.4960***	0.0680	–0.4960***	0.0660	–0.4911***	0.0647
Parents index						
Of height for age	0.1909***	0.0304	0.1909***	0.0296	0.1796***	0.0291
Total no. of children	0.5422***	0.0680	0.5422***	0.0664	0.5264***	0.0651
Educational level	0.1055***	0.0240	0.1055***	0.0254	0.0837***	0.0252
Religion	–0.0664***	0.0654	–0.4553***	0.0664	–0.1892	0.0740
Constant	–0.4334**	0.1924	–0.4334*	0.1946	–0.5542***	0.1974
Sample size = 5138	R^2 = 0.1596		R^2 = 0.1596		R^2 = 0.1493	
					B-PLM = 81.27	p-value = 0.0000
					Hausman = 33. 02	p-value = 0.0003

* Significant at 0.10; ** Significant at 0.05; and *** Significant at 0.01

science forum.indd 188 1/20/2011 11:39:34 AM

CONCLUSION

In a multivariate regression analysis of a health survey, especially in a complex survey design, there was a need for adjustment of standard errors of estimates of the regression coefficient. Adjusting for clustering was more important, since there was no significant difference between adjusting for clustering and adjusting for both stratification and clustering. The adjustments may not and in most cases, do not change the significance of regression.

Determining whether the clustering or classification variable was exogenous or endogenous was very important. A fixed effect model as seen from the analysis was significantly different from a random effect model (Hausman fixed test). In both cases (clustering and stratification), the random effects model indicated the very same variables reported to be significant by the OLS, while the fixed effects model was slightly different in the variables selected.

Date of submission: November 2008
Date of acceptance: July 2010

REFERENCES

Cochran, WG 1977, *Sampling techniques*, New York, John Wiley and Sons. 3rd edn.

Ferguson, JA & Corey, PN 1990, 'Adjusting for clustering in survey design', *The Annals of Pharmacotherapy*, vol. 24, no 3, pp. 310–313.

Ke, H, Chang, L, Carsten, R & Wing, HW 2004, 'Detect and adjust for population stratification in population-based association study using genomic control markers. An application of Affimtrix Genechip Human Mapping 10k array', *European Journal of Human Genetics*, vol. 12, pp. 1001–1006.

NDHS 2005, 'Nigerian demographic and health survey', National Population Commission (Nigeria) and ORC Macro, 11785 Beltsville Drive, Calverton, MD 20705 USA.

Okafor, CF 2002, *Sample survey theory with applications*, 1st edn, Afro-Orbis Publications Ltd, University of Nigeria, Nsukka, Nigeria.

Owen, OD, Eddy VD, ADAM, W & Magnus, L 2007, *Analysing health equity using household survey data: a guide to techniques and their implementation*, World Bank Publication, WBI Learning Resources Series.

Raj, D & Chandhok, P 1999, *Sample survey theory*, Nawsa Pub. House, London. 1st edn.

Wooldridge, JM 2001, 'On the robustness of fixed effects and related estimators in correlated random coefficients panel data models', <http://econmes.jamu.edu/workshops/economics>.

Wooldridge, JM 2005, 'Simple solutions to the initial conditions problem in dynamic, nonlinear panel data models with unobserved heterogeneity', *Journal of Applied Economics*, vol. 20, no. 1, pp. 39–54.

science forum.indd 189 1/20/2011 11:39:34 AM


C
M
Y
CM
MY
CY
CMY
K

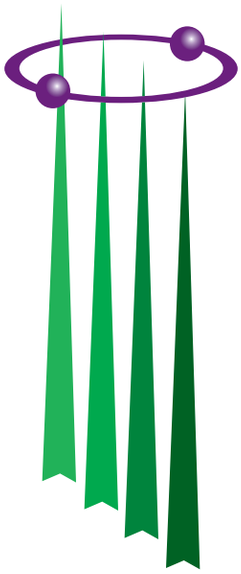

MAHATHIR SCIENCE AWARD 2011

Invitation for Nominations

The Academy of Sciences Malaysia (ASM) is a body set up with a mission that encompasses pursuit, encouragement and enhancement of excellence in the fields of science, engineering and technology for the development of the nation and the benefit of mankind. The Academy has instituted the Mahathir Science Award (formerly known as ASM Award for Scientific Excellence in honour of Tun Dr Mahathir Mohamad) in recognition of scientists/ institutions who have contributed to cutting-edge tropical research that have had an impact on society.

This Award is Malaysia's most prestigious Science Award for tropical research launched in honour of Tun Dr Mahathir Mohamad who promoted and pursued with great spirit and determination his convictions in science and scientific research in advancing the progress of mankind and nations. Tun Dr Mahathir was the major force and the man who put into place much of the enabling mechanisms for a scientific milieu in our country.

This Award will be given to researchers who have made internationally recognised breakthroughs in pioneering tropical research in the fields of Tropical Medicine, Tropical Agriculture, Tropical Architecture and Engineering, and Tropical Natural Resources.

One Award will be conferred in 2011 covering any of the above four fields. The Award carries a cash prize of RM100 000, a gold medal and a certificate.

NOMINATION CRITERIA

- Awards will be given to researchers who have made internationally recognised breakthroughs in pioneering tropical research that have brought greater positive impacts on the well-being of society.
- Nominations can be made by individuals or institutions.
- A recipient could be an individual or an institution.

Nomination forms may be downloaded from the Academy's website:
www.akademisains.gov.my

Closing date: 31 March 2011

For more information, please contact:
Academy of Sciences Malaysia
902-4, Jalan Tun Ismail, 50480 Kuala Lumpur
Tel : 603-2694 9898; Fax : 603-2694 5858
E-mail: seetha@akademisains.gov.my
admin@akademisains.gov.my

announcement.indd 191 1/20/2011 12:01:23 PM

22nd Pacific Science Congress

Asia Pacific Science in the New Millenium: Meeting the Challenges of Climate Change and Globalisation

14 –17 June 2011, Kuala Lumpur, Malaysia

The Congress will provide an inter-disciplinary platform for scientists from the region to discuss and review common concerns and priorities; bring together scientists from remote states; and serve as a catalyst for scientific and scholarly collaboration and to announce and establish new research initiatives. The Pacific Science Association (PSA) focuses on countries bordering the Pacific Ocean and the islands of the Pacific basin. PSA is a regional, non-governmental, and a scholarly organization that seeks to advance S&T in support of sustainable development in the Asia Pacific.

Sub-themes will include topics on:

- A Changing Climate: Climate Science; Physical Impacts; Ecosystem Responses; Mitigation And Adaptation Strategies; Climate Policies; Vulnerable Human Populations
- Global Change & Ecosystems: Biodiversity; Landscape Systems; Ecosystem Services; Coupled Human-Natural Systems; Invasive Species; Museum Collections and Barcoding
- Oceans: Coral Reefs; Ocean Acidification; Large Marine Ecosystems; Marine Biotechnology; Fisheries; Marine Mammals
- Earth Systems & Risk Management: Earth Science and Geophysics; Meteorology; Natural Hazards; Integrated Disaster Risk Reduction
- Globalization: Human Populations; Population Movement; Urbanization; Megacities; Gender; Economics and Trade; Governance Issues; Challenges of Small Island States; Human Security; Poverty Alleviation
- Resource Constraints & Sustainability: Millennium Development Goals; Water; Agriculture; Food; Energy; Integrated Coastal Zone Management; Ecological Economics
- Health Challenges: Persistent and Emerging Infectious Diseases; HIV/AIDS; Chronic and Lifestyle Diseases; Microbiology; Medical Tourism; Telemedicine
- Science for Policy and the Future: Science Communication; Science Education; Building Science Capacity; Science and the Media; Traditional Knowledge; Data Access and Management; Intellectual Property; Universality of Science; Frontiers of Science (Complexity Science, Materials Science, Biotechnology)

Schedule and Programme:

Both plenary and parallel sessions, invited lectures, poster sessions, with at least one session open to the public and an optional post-congress field excursion will be planned. Various symposia will also be organized around the sub-themes.

announcement.indd 192 1/20/2011 12:01:24 PM

Enquiries:

Congress Secretariat
22nd Pacific Science Congress
c/o Academy of Sciences Malaysia
902-4, Jalan Tun Ismail
50480 Kuala Lumpur
Malaysia

Tel : (603) 2694 9898
Fax : (603) 2694 5858

E-mail: nasa@akademisains.gov.my; fardy@akademisains.gov.my
Website: www.akademisains.gov.my
Website: www.22ndpsc.net

Important Dates:

31–1–2011: Deadline for Abstract Submissions
15–3–2011: Notification of Acceptance of the Abstracts
31–3–2011: Deadline for Early Registration
30–4–2011: Deadline for Submission of Speakers Presentation
18–5–2011: Close of Registration

announcement.indd 193 1/20/2011 12:01:24 PM


C
M
Y
CM
MY
CY
CMY
K

ASM Publications

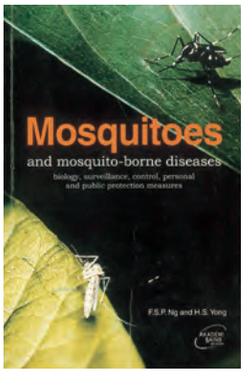

Mosquitoes and Mosquito-borne Diseases: Biology, Surveillance, Control, Personal and Public Protection Measures

F.S.P. Ng and *H.S. Yong (Editors)*
(2000)

ISBN 983-9445-05-7
Price: RM60.00 / USD20.00

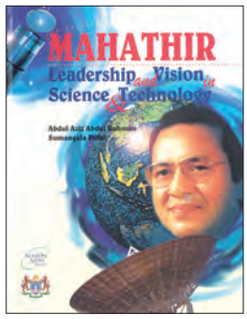

Mahathir: Leadership and Vision in Science and Technology

Abdul Aziz Abdul Rahman and *Sumangala Pillai*
(1996)

ISBN 983-9319-09-4
Price: RM100.00 / USD30.00

Budaya Kreativiti: Pameran Seratus Tahun Hadiah Nobel

Ulf Larsson (Editor)
(2004)

ISBN 983-9445-09-X
Price: RM50.00 / USD15.00

CD Kompilasi *estidotmy*

Edisi 1 – 94, 2002–2009
Price: RM40.00

Mahathir: Kepimpinan dan Wawasan dalam Sains dan Teknologi

Abdul Aziz Abdul Rahman
dan *Sumangala Pillai*
(1996)

ISBN 983-9319-09-4
Price: RM100.00 / USD30.00

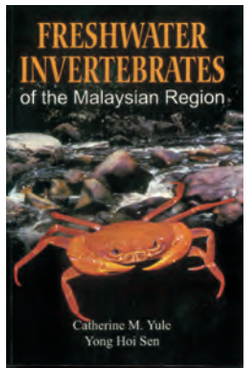

Freshwater Invertebrates of the Malaysian Region

Catherine M. Yule and *Yong Hoi Sen*
(2004)

ISBN 983-41936-0-2
Price: RM180.00 / USD52.00

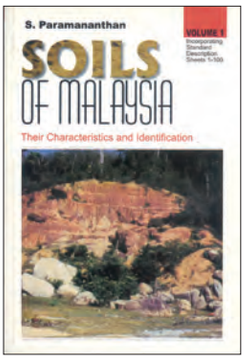

Soils of Malaysia: Their Characteristics and Identification (Vol. 1)

S. Paramananthan
(2000)

ISBN 983-9445-06-5
Price: RM100.00 / USD30.00

Bencana Tsunami 26.12.04 di Malaysia: Kajian Impak Alam Sekitar, Sosio-Ekonomi dan Kesejahteraan Masyarakat

Ibrahim Komoo (Editor)
(2005)

ISBN 983-9444-62-X
Price: RM100.00 / USD30.00

Publication.indd 195 1/20/2011 1:56:59 PM

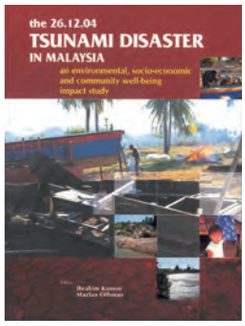

The 26.12.04 Tsunami Disaster in Malaysia: An Environmental, Socio-Economic and Community Well-being Impact Study

Ibrahim Komoo and *Mazlan Othman (Editors)*
(2006)

ISBN 983-9444-62-X
Price: RM100.00 / USD30.00

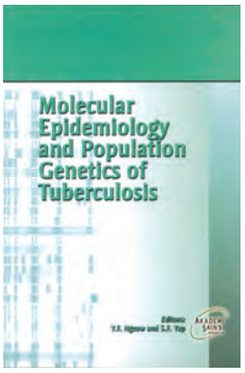

Molecular Epidemiology and Population Genetics of Tuberculosis

Y.F. Ngeow and *S.F. Yap (Editors)*
(2006)

ISBN 983-9445-14-6
Price: RM40.00 / USD12.00

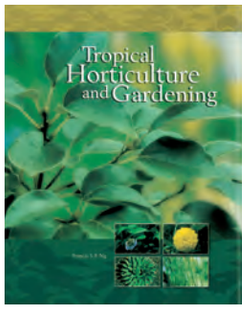

Tropical Horticulture and Gardening

Francis S.P. Ng
(2006)

ISBN 983-9445-15-4
Price: RM260.00 / USD75.00

Kecemerlangan Sains dalam Tamadun Islam: Sains Islam Mendahului Zaman
Scientific Excellence in Islamic Civilization: Islamic Science Ahead of its Time

Fuat Sezgin
(2006)

ISBN 983-9445-14-6
Price: RM40.00 / USD12.00

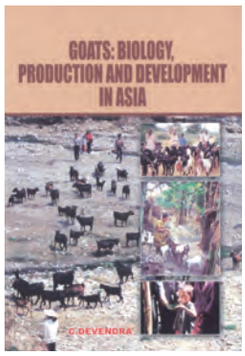

Goats: Biology, Production and Development in Asia

C. Devendra
(2007)

ISBN 978-983-9445-18-3
Price: RM180.00 / USD52.00

Proceedings: Seminar on Antarctic Research, 27–28 June 2005, University of Malaya, Kuala Lumpur, Malaysia

Irene K.P. Tan et al. *(Editors)*
(2006)

ISBN 978-983-9445-17-6
Price: RM40.00 / USD12.00

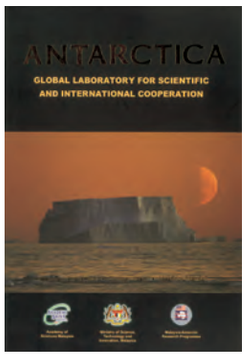

Antarctica: Global Laboratory for Scientific and International Cooperation

Aileen Tan Shau-Hwai et al. *(Editors)*
(2005)

ISBN 983-9445-13-8
Price: RM40.00 / USD12.00

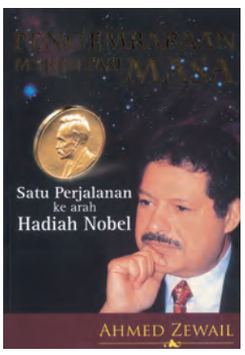

Pengembaraan Merentasi Masa: Satu Perjalanan ke Arah Hadiah Nobel

Ahmed Zewail
(2007)

ISBN 978-9445-20-6
Price: RM40.00 / USD12.00

Publication.indd 196 1/20/2011 1:56:59 PM

ASM Publications

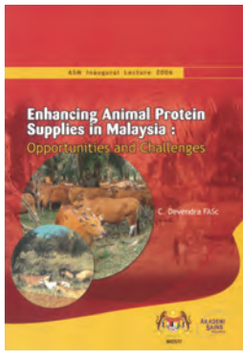

Enhancing Animal Protein Supplies in Malaysia: Opportunities and Challenges

C. Devendra
(2007)

ISBN 983-9444-62-X

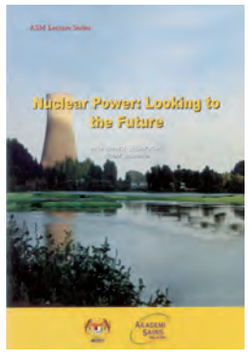

Nuclear Power: Looking to the Future

Mohamed ElBaradei
(2008)

ISBN 983-9445-14-6

Changing Forest Landscape: Impact on Rural Health
(2007)

ISBN 983-9445-15-4

Dunia Sains
Vol. 5, No. 4, Oktober – Disember 2007
(2008)

A World of Science
Vol. 5, No. 4
October – December 2007

www. akademisains.gov.my/unesco/dunia_sains/okt_dis_2007.pdf

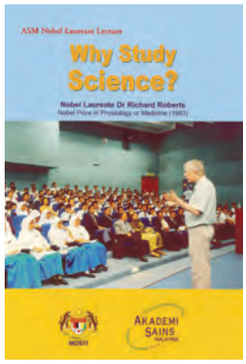

Why Study Science?

Richard Roberts
(2008)

ISBN 978-983-9445-18-3

Dunia Sains
Vol. 6, No. 1, Januari – Mac 2008
(2008)

A World of Science
Vol. 6, No. 1
January – March 2008

ASM Science Journal
Vol. 1, No. 1, June 2007

ISSN : 1823-6782

Price: RM100.00 / USD50.00 (Individual)
RM200.00 / USD100.00 (Institution)

ASM Science Journal
Vol. 1, No. 2, December 2007

ISSN : 1823-6782

Price: RM100.00 / USD50.00 (Individual)
RM200.00 / USD100.00 (Institution)

Publication.indd 197 1/20/2011 1:57:00 PM

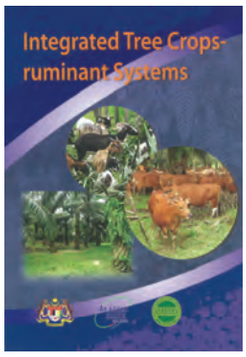

Integrated Tree Crops-ruminant Systems (Proceedings)

C. Devendra, S. Shanmugavelu and *Wong Hee Kum (Editors)*
(2008)

ISSN : 983-9445-24-3

Price: RM40.00 / USD12.00

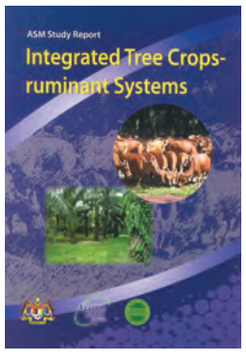

ASM Study Report: Integrated Tree Crops-ruminant Systems
(2008)

ISSN : 983-9445-24-4

Price: RM30.00 / USD9.00

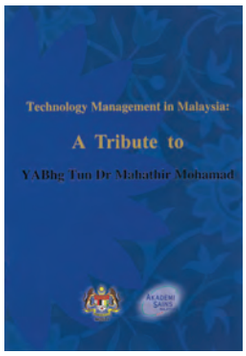

Technology Management in Malaysia: A Tribute to YABhg Tun Dr Mahathir Mohamad
(2008)

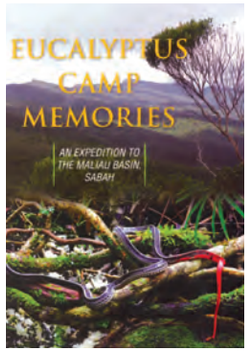

Eucalyptus Camp Memories: An Expedition to the Maliau Basin, Sabah
(2008)

ISSN : 978-983-9445-25-1

Price: RM220.00 / USD61.00 (Hard cover)
RM160.00 / USD42.00 (Soft cover)

ASM Science Journal
Vol. 2, No. 1, December 2008

ISSN : 1823-6782

Price: RM100.00 / USD50.00 (Individual)
RM200.00 / USD100.00 (Institution)

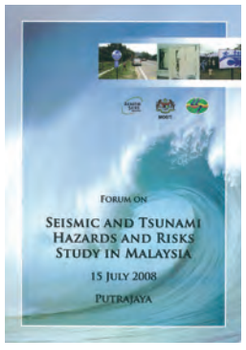

Forum on: Seismic and Tsunami Hazards and Risks Study in Malaysia 15 July 2008

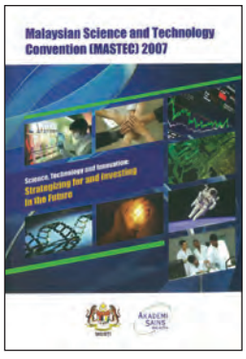

Science, Technology and Innovation: Strategizing for and Investing in the Future [Malaysian Science and Technology Convention (MASTEC) 2007]
(2009)

ISSN : 978-983-9445-27-5

Price: RM51.00 / USD22.00

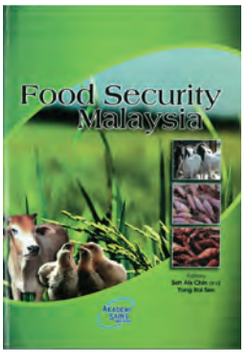

Food Security Malaysia (Proceedings)
Soh Aik Chin and Yong Hoi Sen (Editors)
(2009)

ISSN : 978-983-9445-28-2

Price: RM20.00 / USD6.00

Publication.indd 198 1/20/2011 1:57:00 PM

ASM Publications

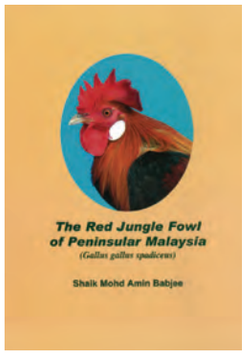

The Red Jungle Fowl of Peninsular Malaysia

Shaik Mohd Amin Babjee
(2009)

ISBN : 978-983-9445-29-9

Price: RM35.00 / USD12.00

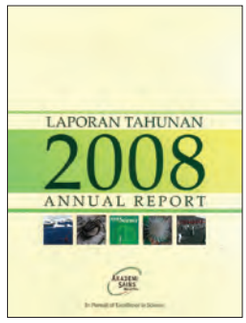

Academy of Science Malaysia

Annual Report 2008

Price: RM50.00 / USD20.00

Journal of Science & Technology in the Tropics

Vol. 4, No. 2, December 2008

ISSN:1823-5034

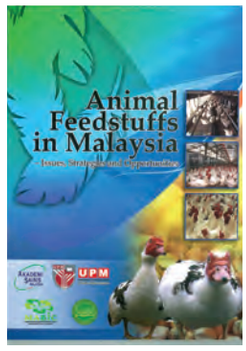

Animal Feedstuffs in Malaysia – Issues, Strategies and Opportunities
(2009)

ISBN : 978-983-9445-30-5

Price: RM35.00 / USD12.00

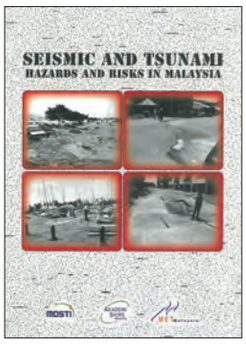

Seismic and Tsunami Hazards and Risks in Malaysia
(2009)

ISBN 978-983-9445-32-9

Price: RM45.00 / USD15.00

Groundwater Colloquium 2009 "Groundwater Management in Malaysia – Status and Challenges"

ISBN : 978-983-9445-30-5

Price: RM100.00 / USD75.00

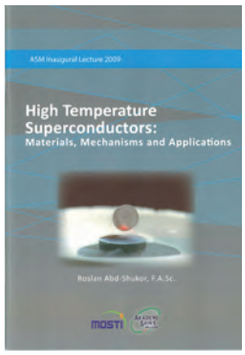

ASM Inaugural Lecture 2009
High Temperature Superconductors: Material, Mechanisms and Applications
Roslan Abd-Shukor

ISBN : 978-983-9445-30-5

Price: RM20.00 / USD8.00

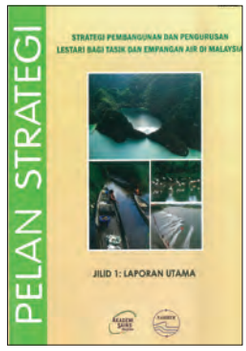

Strategi Pembangunan dan Pengurusan Lestari bagi Tasik dan Empangan Air di Malaysia

Jilid 1: Laporan Utama

Publication.indd 199 1/20/2011 1:57:01 PM

Strategies for the Sustainable Development and Management of Lakes and Reservoirs in Malaysia

Volume 1: Main Report

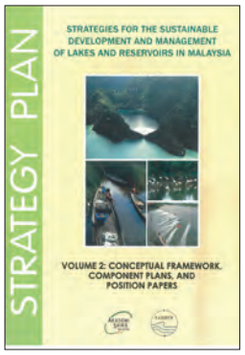

Strategies for the Sustainable Development and Management of Lakes and Reservoirs in Malaysia

Volume 2: Conceptual Framework, Component Plans, and Position Papers

Strategies for the Sustainable Development and Management of Lakes and Reservoirs in Malaysia

Volume 3: Part 1 & Part 2

ASM Science Journal
Vol. 2, No. 2, December 2008

ISSN : 1823-6782

Price: RM100.00 / USD50.00 (Individual)
RM200.00 / USD100.00 (Institution)

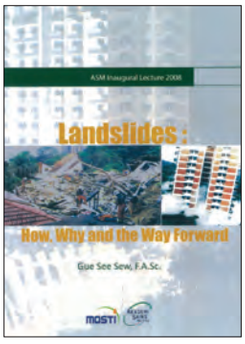

ASM Inaugural Lecture 2008
Landslides: How, Why and the Way Forward
Gue See Sew

ISBN : 978-983-9445-30-5

Price: RM20.00 / USD8.00

Journal of Science & Technology in the Tropics

Vol. 5, No. 1, June 2009

ISSN:1823-5034

Biodiversity and National Development: Achievements, Opportunities and Challenges

ISBN : 978-983-9445-30-5

Price: RM40.00 / USD15.00

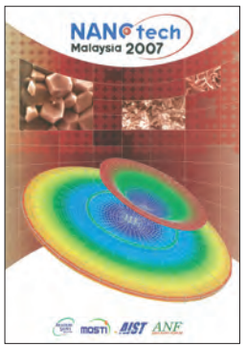

Nanotech Malaysia 2007

ISBN : 978-983-9445-30-5

Price: RM55.00 / USD20.00

Publication.indd 200 1/20/2011 1:57:01 PM

ASM Publications

Proceedings for the 3rd Malaysian International Seminar on Antarctica (MISA3) "From the Tropics to the Poles" 2007

ISBN : 978-983-9445-30-5

Price: RM40.00 / USD15.00

ASM Science Journal
Vol. 3, No. 1, December 2009

ISSN : 1823-6782

Price: RM100.00 / USD50.00 (Individual)
RM200.00 / USD100.00 (Institution)

Journal of Science & Technology in the Tropics
Vol. 5, No. 2, December 2009

ISBN : 978-983-9445-30-5

Price: RM40.00 / USD15.00

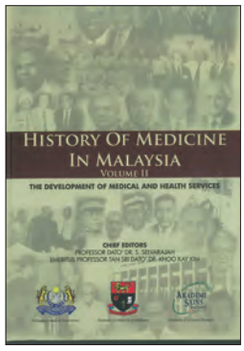

History of Medicine in Malaysia Volume II
The Development of Medical and Health Services

ISSN : 978-983-42545-1-3

Price: RM100.00 / USD50.00 (Individual)
RM200.00 / USD100.00 (Institution)

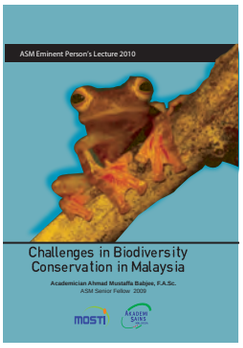

ASM Eminent Person's Lecture 2010

Challenges in Biodiversity Conservation in Malaysia
Ahmad Mustaffa Babjee

ISBN : 978-983-9445-39-8

Price: RM20.00 / USD8.00

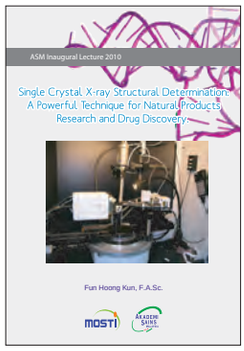

ASM Inaugural Lecture 2010

Single Crystal X-ray Structural Determination: A Powerful Technique for Natural Products Research and Drug Discovery
Fun Hoong Kun

ISBN : 978-983-9445-39-8

Price: RM30.00 / USD12.00

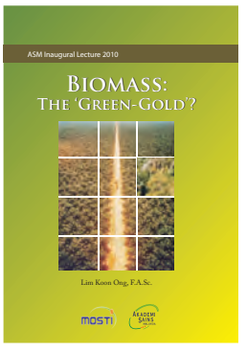

ASM Inaugural Lecture 2010

Biomass: The 'Green-gold'?
Lim Koon Ong

ISBN : 978-983-9445-38-1

Price: RM30.00 / USD12.00

ASM Science Journal
Vol. 3, No. 2, December 2009

ISSN : 1823-6782

Price: RM100.00 / USD50.00 (Individual)
RM200.00 / USD100.00 (Institution)

Publication.indd 201 1/20/2011 1:57:02 PM

Academy of Science Malaysia

Annual Report 2009

Price: RM50.00 / USD20.00

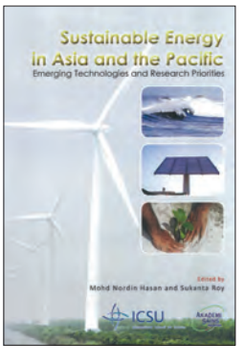

Sustainable Energy in Asia and the Pacific
Emerging Technologies and Research Priorities
Mohd Nordin Hasan and Sukanta Roy
(2010)

ISSN : 978-983-9445-43-5

Price: RM100.00 / USD50.00

25th Anniversary
A Journey Down Memory Lane:
My Times in FRIM
(2010)

Price: RM40.00 / USD15.00

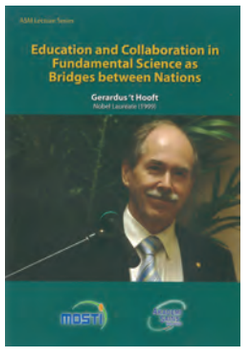

Education and Collaboration in Fundamental Science as Bridges between Nations
Gerardus't Hooft
(2010)

ISSN : 978-983-9445-44-2

Price: RM30.00 / USD12.00

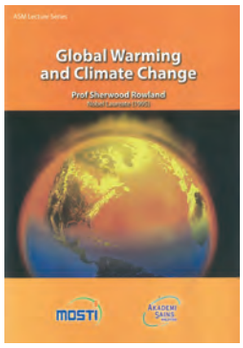

Global Warming and Climate Change

Prof Sherwood Rowland
(2010)

ISBN : 978-983-9445-46-6

Price: RM40.00 / USD12.00

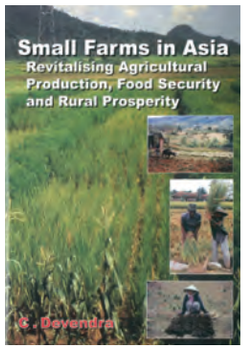

Small Farms in Asia
Revitalising Agricultural Production,
Food Security and Rural Prosperity

ISBN : 978-983-9445-40-4

Price: RM150.00 / USD50.00

The 59th Lindau Meeting of Nobel Prize Winners with Young Scientists

AND

Visits to Centres Excellence in Germany and United Kingdom
4-11 July 2009
(2010)

Sustaining Malaysia's Future
The Mega Science Agenda
(2010)

Publication.indd 202 1/20/2011 1:57:03 PM

ASM Publications

ASM Science Journal
Vol. 4, No. 1, June 2010

ISSN : 1823-6782

Price: RM100.00 / USD50.00 (Individual)
RM200.00 / USD100.00 (Institution)

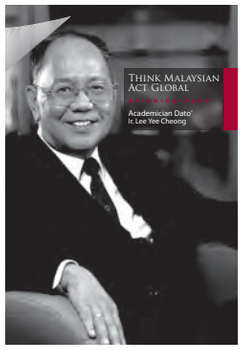

Think Malaysian Act Global
(Autobiography)

Academician Dato' Ir. Lee Yee Cheong
(2010)

ISSN : 978-983-9445-47-3

Price: RM100/USD30

Dunia Sains
Vol. 6, No. 2, April – jun 2008
(2008)

A World of Science
Vol. 6, No. 2
April – June 2008

Dunia Sains
Vol. 6, No. 3, Julai – September 2008
(2008)

A World of Science
Vol. 6, No. 3
July – September 2008

Journal of Science & Technology in the Tropics
Vol. 6, No. 1, December 2009

ISBN : 978-983-9445-30-5

Price: RM40.00 / USD15.00

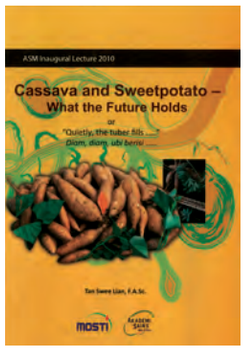

ASM Inaugural Lecture 2010
Cassava and Sweetpotato—What the Future Holds or "Quietly, the tuber fills….."
Diam, diam, ubi berisi…..
Tan Swee Lian
(2010)

ISBN: 978-983-9445-49-7

Price: RM30/USD12

ASM Inaugural Lecture 2010
The Decade of the Mind 2010 to 2020: How Malaysian Neuroscientists Can Create Knowledge, Skills and Innovative Research to Drive the 10th and 11th Malaysia Plan within the New Economic Model
J. Malin Abdullah
(2010)

ISBN: 978-983-9445-48-0

Price: RM30/USD12

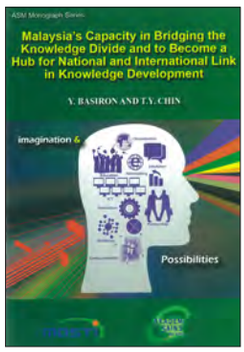

ASM Monograph Series
Malaysia's Capacity to Bridge the Knowledge Divide and to Become a Hub for National and International Link in Knowledge Development
Y. Basiron and T.C. Chin
(2010)

Publication.indd 203 1/20/2011 1:57:23 PM

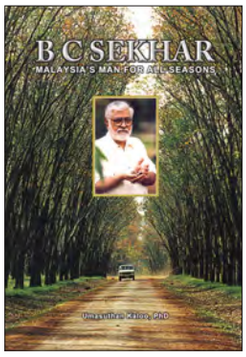

B.C. Sekhar—Malaysia's Man for All Seasons (Biography)
Umasuthan Kaloo (Editor)
(2010)

ISBN: 978-983-9445-50-3

Price: RM100/USD30

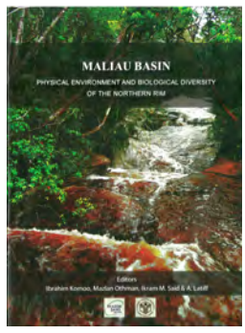

Maliau Basin
Physical Environment and Biological Diversity of the Northern Rim
Ibrahim Komoo, Mazlan Othman, Ikram M. Said and A. Latiff (Editors)
(2010)

ISBN: 978-983-9445-52-7

Price: RM55/USD30

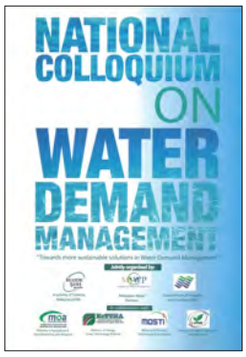

National Colloquium on Water Demand Management
Towards More Sustainable Solutions in Water Demand Management
(2010)

ISBN: 978-983-9445-56-5

Price: RM120/USD40

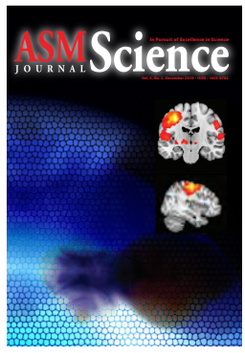

ASM Science Journal
Vol. 4, No. 2, December 2010

ISSN : 1823-6782

Price: RM100.00 / USD50.00 (Individual)
RM200.00 / USD100.00 (Institution)

For purchasing, please access:
http://www.akademisains.gov.my

Publication.indd 204 1/20/2011 1:57:40 PM

About the Journal

Mission Statement

To serve as the forum for the dissemination of significant research, S&T and R&D policy analyses, and research perspectives.

Scope

The *ASM Science Journal* publishes advancements in the broad fields of medical, engineering, earth, mathematical, physical, chemical and agricultural sciences as well as ICT. Scientific articles published will be on the basis of originality, importance and significant contribution to science, scientific research and the public.

Scientific articles published will be on the basis of originality, importance and significant contribution to science, scientific research and the public. Scientists who subscribe to the fields listed above will be the source of papers to the journal. All articles will be reviewed by at least two experts in that particular field. The journal will be published twice in a year.

The following categories of articles will be considered for publication:

Research Articles

Each issue of the journal will contain no more than 10 research articles. These are papers reporting the results of original research in the broad fields of medical, engineering, earth, mathematical, physical, chemical and life sciences as well as ICT. The articles should be limited to 6000 words in length, with not more than 100 cited references.

Short Communications

These are articles that report significant new data within narrow well-defined limits or important findings that warrant publication before broader studies are completed. These articles should be limited to 2000 words and not more that 40 cited references. Five (5) Short Communications will be accepted for publication in each issue of the journal.

Research Perspectives

These are papers that analyse recent research in a particular field, giving views on achievements, research potential, strategic direction etc. A Research Perspective should not exceed 2000 words in length with not more than 40 cited references.

Reviews/Commentaries

Each issue of the journal will also feature Reviews/ Commentaries presenting overviews on aspects such as Scientific Publications and Citation Ranking, Education in Science and Technology, Human Resources for Science and Technology, R&D in Science and Technology, Innovation and International Comparisons or Competitiveness of Science and Technology etc. Reviews/Commentaries will encompass analytical views on funding, developments, issues and concerns in relation to these fields and not exceed 5000 words in length and 40 cited references.

Science Forum

Individuals who make the news with breakthrough research or those involved in outstanding scientific endeavours or those conferred with internationally recognised awards will be featured in this section. Policy promulgations, funding, science education developments, patents from research, commercial products from research, and significant scientific events will be disseminated through this section of the journal. The following will be the categories of news:

- Newsmakers
- Significant Science Events
- Patents from Research
- Commercial Products from Research
- Scientific Conferences/Workshops/Symposia
- Technology Upgrades
- Book Reviews.

Instructions to Authors

The *ASM Science Journal* will follow the Harvard author-date style of referencing examples of which are given below.

In the text, reference to a publication is by the author's name and date of publication and page number if a quote is included, e.g. (Yusoff 2006, p. 89) or Yusoff (2006, p. 89) 'conclude.....' as the case may be. They should be cited in full if less than two names (e.g. Siva & Yusoff 2005) and if more than two authors, the work should be cited with first author followed by *et al*. (e.g. Siva *et al*. 1999).

All works referred to or cited must be listed at the end of the text, providing full details and arranged alphabetically. Where more than one work by the same author is cited, they are arranged by date, starting with the earliest. Works by the same author published in the same year are ordered with the use of letters a, b, c, (e.g. Scutt, 2003a; 2003b) after the publication date to distinguish them in the citations in the text.

General Rules

Authors' names:

- Use only the initials of the authors' given names.
- No full stops and no spaces are used between initials.

Titles of works:

- Use minimal capitalisation for the titles of books, book chapters and journal articles.
- In the titles of journals, magazines and newspapers, capital letters should be used as they appear normally.
- Use italics for the titles of books, journals and newspapers.
- Enclose titles of book chapters and journal articles in single quotation marks.

Page numbering

- Books: page numbers are not usually needed in the reference list. If they are, include them as the final item of the citation, separated from the preceding one by a comma and followed by a full stop.
- Journal articles: page numbers appear as the final item in the citation, separated from the preceding one by a comma and followed by a full stop.

  Use the abbreviations p. for a single page, and pp. for a page range, e.g. pp. 11–12.

Publication.indd 205 1/20/2011 1:57:40 PM

Whole citation

- The different details, or elements, of each citation are separated by commas.
- The whole citation finishes with a full stop.

Specific Rules

Definite rules for several categories of publications are provided below:

Journal

Kumar, P & Garde, RJ 1989, 'Potentials of water hyacinth for sewage treatment', *Research Journal of Water Pollution Control Federation*, vol. 30, no. 10, pp. 291–294.

Monograph

Hyem, T & Kvale, O (eds) 1977, *Physical, chemical and biological changes in food caused by thermal processing*, 2nd edn, Applied Science Publishers, London, UK.

Chapter in a monograph

Biale, JB 1975, 'Synthetic and degradative processes in fruit ripening', eds NF Hard & DK Salunkhe, in *Post-harvest biology and handling of fruits and vegetables*, AVI, Westport, CT, pp. 5–18.

Conference proceedings

Common, M 2001, 'The role of economics in natural heritage decision making', in *Heritage economics: challenges for heritage conservation and sustainable development in the 21st century: Proceedings of the International Society for Ecological Economics Conference, Canberra, 4th July 2000*, Australian Heritage Commission, Canberra.

Website reference

Thomas, S 1997, *Guide to personal efficiency*, Adelaide University, viewed 6 January 2004, <http://library.adelaide.edu.au/~sthomas/papers/perseff.html>.

Report

McColloch, LP, Cook, HT & Wright, WR 1968, *Market diseases of tomatoes, peppers and egg-plants*, Agriculture Handbook no. 28, United States Department of Agriculture, Washington, DC.

Thesis

Cairns, RB 1965, 'Infrared spectroscopic studies of solid oxygen', PhD thesis, University of California, Berkeley, CA.

Footnotes, spelling and measurement units

If footnotes are used, they should be numbered in the text, indicated by superscript numbers and kept as brief as possible. The journal follows the spelling and hyphenation of standard British English. SI units of measurement are to be used at all times.

Submission of Articles

General. Manuscripts should be submitted (electronically) in *MS Word* format. If submitted as hard copy, two copies of the manuscript are required, double-spaced throughout on one side only of A4 (21.0 × 29.5 cm) paper and conform to the style and format of the *ASM Science Journal*. Intending contributors will be given, on request, a copy of the journal specifications for submission of papers.

Title. The title should be concise and descriptive and preferably not exceed fifteen words. Unless absolutely necessary, scientific names and formulae should be excluded in the title.

Address. The author's name, academic or professional affiliation, e-mail address, and full address should be included on the first page. All correspondence will be only with the corresponding author (should be indicated), including any on editorial decisions.

Abstract. The abstract should precede the article and in approximately 150–200 words outline briefly the objectives and main conclusions of the paper.

Introduction. The introduction should describe briefly the area of study and may give an outline of previous studies with supporting references and indicate clearly the objectives of the paper.

Materials and Methods. The materials used, the procedures followed with special reference to experimental design and analysis of data should be included.

Results. Data of significant interest should be included.

Figures. If submitted as a hard copy, line drawings (including graphs) should be in black on white paper. Alternatively sharp photoprints may be provided. The lettering should be clear. Halftone illustrations may be included. They should be submitted as clear black and white prints on glossy paper. The figures should be individually identified lightly in pencil on the back. All legends should be brief and typed on a separate sheet.

Tables. These should have short descriptive titles, be self explanatory and typed on separate sheets. They should be as concise as possible and not larger than a Journal page. Values in tables should include as few digits as possible. In most cases, more than two digits after the decimal point are unnecessary. Units of measurements should be SI units. Unnecessary abbreviations should be avoided. Information given in tables should not be repeated in graphs and vice versa.

Discussion. The contribution of the work to the overall knowledge of the subject could be shown. Relevant conclusions should be drawn, and the potential for further work indicated where appropriate.

Acknowledgements. Appropriate acknowledgements may be included.

Reprints. Twenty copies of reprints will be given free to all the authors. Authors who require more reprints may obtain them at cost provided the Editorial Committee is informed at the time of submission of the manuscript.

Correspondence

All enquiries regarding the *ASM Science Journal*, submission of articles, including subscriptions to it should be addressed to:

The Editor-in-Chief
ASM Science Journal
Academy of Sciences Malaysia
902-4, Jalan Tun Ismail
50480 Kuala Lumpur, Malaysia.
Tel: 603-2694 9898; Fax: 603-2694 5858
E-mail: sciencejournal@akademisains.gov.my

Publication.indd 206 1/20/2011 1:57:40 PM

ASM SCIENCE JOURNAL
(ASM Sc. J.)

ORDER FORM

Subscription (Two issues per year)

	Malaysia	Other Countries
Individual	**RM100**	**USD50**
Institution	**RM200**	**USD100**

1. Complete form and return.

Name/Institution: .....
(Please print)
.....
.....

Street Address: .....
.....
. .

City, Region: .....

Country, Postal Code: .....

2. Payment method: Cheque/Bank Draft/Postal Order/
   Money Order No.: .....
   Payable to **"Akademi Sains Malaysia"**
   (Please include bank commission, if applicable)
   RM/USD: .....

Date: ..... Signature: .....

Please send to:
Academy of Sciences Malaysia
902-4, Jalan Tun Ismail
50480 Kuala Lumpur, Malaysia
Tel: 03-2694 9898; Fax: 03-26945858
E-mail: sciencejournal@akademisains.gov.my

Untitled-1 1 6/27/2009 5:37:35 PM

Untitled-1 1

ASM Science JOURNAL
In Pursuit of Excellence in Science

Affix
stamp
here

Academy of Sciences Malaysia
902-4, Jalan Tun Ismail
50480 Kuala Lumpur
Malaysia

6/27/2009 5:38:25 PM

RESEARCH ARTICLES

REVIEW

SCIENCE FORUM

ANNOUNCEMENTS